THE UNIVERSITY OF CALGARY

Role of the Dopaminergic Neuron (RPeD1) in the Control of Respiratory Behavior in *Lymnaea stagnalis*

by

Zara Haque

A THESIS

SUBMITTED TO THE FACULTY OF GRADUATE STUDIES

IN PARTIAL FULFILLMENT OF THE REQUIREMENTS FOR THE

DEGREE OF MASTER OF SCIENCE

DEPARTMENT CARDIOVASCULAR/RESPIRATORY SCIENCES

CALGARY, ALBERTA

August, 1999

ABSTRACT

An identified dopaminergic neuron, termed right pedal dorsal 1 (RPeD1) is an important component of the central respiratory pattern generating network in the fresh water snail *Lymnaea stagnalis*. In semi-intact, isolated brain and cell culture preparations, RPeD1 is required for respiratory rhythmogenesis. However, its precise role in the control of respiratory behavior in the intact animal has not yet been determined. In this study, utilizing a variety of behavioral, electrophysiological and morphological techniques, I systematically disrupted RPeD1's axonal projections to the periphery or selectively destroyed it. The effects of these perturbations on: 1) normal respiratory behavior, 2) respiratory patterned activity and 3) regeneration were examined. The data presented in this study provide the first direct evidence that an identified respiratory CPG neuron (RPeD1) is necessary for respiration in the intact animal.

ACKNOWLEDGEMENTS

I would like to express my most sincere thanks to my supervisor, Dr. Naweed Syed for the opportunity to enter the graduate program at the University of Calgary and having faith in me. Thank you for providing me with a fun and challenging project. May Allah (SWT) reward you for all your good deeds, intentions, willingness to share knowledge and expertise, generosity, and kindness. You've created an atmosphere in the lab that allows everyone who enters to leave feeling blessed that they were ever a part of it. Insha Allah your future research will be one filled with joy and prosperity. Peace and blessings to you and your family.

A special thanks to my supervisory committee, Dr. Ken Lukowiak and John Remmers. Your guidance, support, and constructive criticism remain invaluable. I will always be grateful to you Ken for believing in me, and all your assistance and encouragement throughout my program. I would also like to thank my external examiner Dr. George Bourne for participating in my examination.

I would like to thank everyone in Dr. Syed's lab and Ken's lab for creating a fabulous working environment. An amazing place in which everyone wishes for others what they wish for themselves.

Jazak Allah Khair to my family especially Nafees. May Allah (SWT) reward you for your patience and friendship.

TABLE OF CONTENTS

LIST OF FIGURES

CHAPTER ONE: INTRODUCTION

1.1. RHYTHMIC BEHAVIORS

1.1.1. Respiration

In most vertebrate species, respiration is a multi component behavior, which serves to regulate their arterial oxygen and carbon dioxide levels. This, in turn is aided by the respiratory musculature whose activities are controlled by the central nervous system (Feldman and McCrimmon, 1999). The central nervous system-derived motor activity is further regulated by peripheral feedback from various chemoreceptors (Milsom and Brill, 1986; Burleson and Smatresk, 1989) and mechanoreceptors (Milsom, 1990b), which play important roles in an animal's feedback system and maintain its internal homeostasis. Chemical homeostasis involves a balance between carbon dioxide, oxygen and pH levels; all of which vary among different species, depending upon: 1) whether the animal is a lung breather, 2) levels of cutaneous carbon dioxide excretion (frogs and some turtles), and 3) the solubility of gases in the ventilatory system .

The respiratory rhythm that underlies breathing behavior in vertebrates is generated in the absence of afferent fibers (von Euler, 1986), however the peripheral input ensures that the final motor pattern is behaviorally relevant. For example, both central and peripheral

chemoreceptors in the decerebrated animal (von Euler, 1986), central chemoreceptors in the isolated brainstem preparation (Harada et al., 1985), and other forebrain and midbrain components in the intact animal (cortex, hypothalamus, and cerebellum) have been shown to alter ventilation, but they are not necessary for this behavior (Aminoff and Sears, 1971; Tenney et al., 1977). The higher brain regions also serve to coordinate respiration with a variety of other activities such as speech (Eldridge et al., 1981; Holstege, 1989; Mitchell, 1993; Aritav et al., 1995; Waldrop and Porter, 1995). Specifically, speech involves the coordination of muscles found in the face, tongue and upper airway. Coordination between these actvities also involves feedback from many other regions of the brain (anterior limb cortex, subcallosal gyrus, gyrus rectus, midbrain periaqueductal gray, and brainstem nuclei) (Feldman and McCrimmon, 1999). It therefore, seems safe to postulate that the respiratory drive may originate in the central nervous system (specifically the brainstem which includes the medulla, pons, and spinal cord) (Ramirez and Richter, 1996) in the absence of peripheral feedback, however the later may serve to fine-tune the final patterns of this respiratory activity. Together, both central and peripheral elements allow the animal to modulate its breathing behavior in accordance with the metabolic demands (Feldman and McCrimmon, 1999).

1.1.2. Bimodal respirators

Bimodal respirators are capable of exchanging gases both through their lungs (aerial) and skin (aquatic). Among vertebrates, the bimodal respirators fall between two extremes; the air breathers (like reptiles, birds, and mammals), and the water breathers (which include most fish). Some species may either display rhythmical breathing episodes which are indicative of continuous gas exchange activity (teleost fishes, birds, and mammals), or exhibit periodic breathing patterns. The later may either be: a) episodic (fresh water turtles and crocodiles) (Vitalis and Milsom, 1986), b) a single episodic event (marine turtles, snakes, and lizards), or c) both (carp, eels, suckers, and dogfish (Shelton et al., 1986). Some animal species may also be required to utilize the latter (both patterns) during: hibernation (Milsom et al., 1986), stress, exercise or in response to an increase in the body temperature (Shelton et al., 1986). Evidence shows that despite similar rhythm generating mechanisms observed throughout various different vertebrate species, the pattern utilized by any given organism is dependent upon its metabolic state and the environment in which the animal is maintained (Milsom, 1988).

1.2. NEURONAL BASIS OF RHYTHMIC BEHAVIORS

1.2.1. Central pattern generators

Rhythmic behaviors such as feeding, locomotion, and respiration are controlled by pattern generating neurons, which are often termed as

central pattern generators (CPG) (Delcomyn, 1980; Kristan, 1980; Selverston, 1980; Getting, 1989; Harris-Warrick and Johnson, 1989; Pearson, 1993). The CPG are further classified into two main groups: 1) the intrinsic pacemakers and 2) the networks oscillators. In the pacemaker model, rhythm generation is a function of intrinsic membrane properties of individual neurons; whereas the network model relies upon synaptic interactions between the CPG neurons (Grillner and Wallen, 1985; Getting, 1986).

1.2.1.1. Intrinsic pacemaker or burster neurons

The neuronal networks based on pacemaker cells can be divided into two categories (Selverston et al., 1983): 1) "endogenous bursters" (Alving, 1968); and 2) the "conditional bursters" (Getting, 1988). Since the endogenous bursters exhibit intrinsic membrane oscillations that are a function of their inherent membrane conductances (calcium and potassium), they can therefore generate rhythmical bursts in the absence of synaptic inputs.

The conditional bursters on the other hand, require tonic inputs for their activity. These inputs may either be synaptic or humoral (eg. dopamine, serotonin, octopamine, proctlin, and muscarinic agents – see Harris-Warrick, 1988; Marder and Meyrand 1989; Harris-Warrick, 1991). The bursting neurons display voltage-dependent oscillations, where depolarization from the resting membrane potential triggers membrane

oscillations which lead to an increase in the spiking activity (Meech, 1979). Moreover, both endogenous and conditional bursters are expected to exhibit various membrane conductances which allow them to: 1) reach threshold for their bursting activity (Feldman and Smith, 1989), 2) generate a repetitive firing pattern; and 3) terminate bursting activity (Ramirez and Richter, 1996).

A variety of different conductances are active during patterned bursting activity. For instance, increased sodium, and calcium conductances found within the bursting neurons depolarize the membrane and trigger an initial burst discharge. The resulting enhancement of calcium conductance in turn increases the potassium conductance which hyperpolarizes the cell, and thus terminates the burst discharge. A decrease in calcium conductance, then reduces the drive for potassium ions and the cycle repeats (Calabrese, 1977; Smith, 1980). Since, the burst generation relies heavily upon these membrane conductances, any synaptic input that can modulate such ionic currents may easily influence the pattern of bursting activity in these oscillating neurons.

1.2.1.2. Network oscillators

In a variety of vertebrate and invertebrate species, rhythm generation is a function of emergent network properties (Selverston, 1983). These properties become apparent when synaptic and membrane

properties of neurons within a network interact. The neuronal interactions may either rely upon electrical; chemical excitatory, inhibitory or mixed excitatory and inhibitory connections (Getting, 1983; Selverston et al., 1983). Neurons that are part of any given circuit may also utilize intrinsic characteristics; such as post-inhibitory rebound, or delayed excitation and may thus auto-regulate the outcome of final patterned discharge (Getting, 1988). Both the rhythm and pattern generating properties may be difficult to separate since rhythm generating properties can alter timing and shape of the rhythmic cycles (Ramirez and Richter, 1996). Furthermore, intrinsic properties of burster neurons can amplify synaptic input, synchronize rhythmic activity, or trigger activity/termination, which together decide the pattern generated by the neural circuit (Ramirez and Richter, 1996).

1.2.1.2.1. Chemical synaptic connections

Generally, the synaptic connections found in invertebrate and vertebrate systems share a number of common features (Marder and Calabrese, 1996), however, significant differences between vertebrate and invertebrate systems arise due both to transmitter release and response properties of any given cell pair. The chemical synaptic connections between the CPG neurons may either be: 1) pure excitatory, 2) inhibitory, or 3) mixed excitatory and inhibitory, 4) monosynaptic or polysynaptic, 5) unidirectional or bidirectional 6) slow or fast etc. All these parameters

contribute significantly towards the net outcome of a patterned motor activity and are therefore, considered critical for network analysis.

1.2.1.3. Command neurons

Central pattern generators that control the crustacean forgut (Meyrand et al. 1991; Nusbaum et al., 1992), swimming in leech (Nusbaum et al., 1987) and lamprey (Grillner et al., 1991), and other rhythmic behaviors in various species are thought to be under the control of an "on and off switch" mechanism (Dean et al., 1995). In the half-center model, the switch that turns the patterns on and off is the tonic excitation that emanates either from a single neuron or a homogenous population of identical neurons (Kristan, 1980). These switches and their neuronal counterpart were earlier labeled as "command neurons" (Kupfermann and Weiss, 1978). According to Kupfermann and Weiss, for a neuron to be classified as a command cell: 1) it must fire in a manner that is appropriate for that particular behavior, 2) it must be sufficient, and 3) necessary for that behavior. Specifically, a neuron in question should fire in phase with spontaneously occurring behavior. When stimulated electrically, it should be sufficient to trigger the entire behavioral program. Finally, when silenced either by hyperpolarizing current or following its selective killing, the behavior should no longer occur. If a neuron fulfills all of the above criteria, then according to Kupferman and Weiss (1978), it can be

classified as a command cell. Since neurons fulfilling all of the above criteria have not yet been identified, the command neuron concept has now been reformulated as "command systems". In a command system configuration, various functionally and behavioral related neurons interact with one another to produce a complete behavioral program. Furthermore, since in many system examined to date, the so-called command elements have also been found to interact with other lower order CPG neurons, therefore, it seems safe to suggest that most motor programs are controlled by "polymorphic networks" (Getting and Dekin, 1985). According to this concept, the interaction between numerous CPGs underlying varies different behaviors produce behaviorally or functionally meaningful movements (Getting and Dekin, 1985).

1.2.1.4. Peripheral feedback

Evidence from a number of vertebrate and invertebrate species supports the idea that neurons embedded within a given CPG network are capable of generating rhythmical motor output in the absence of sensory input. However, peripheral feedback is important for the initiation, modulation, and termination of most rhythmic behaviors (Delcomyn, 1980). In other preparations, peripheral feedback may also act to provide important timing cues for the final motor activity (Marder and Calabrese, 1996). Rhythmic behaviors observed in both vertebrate and invertebrate models reflect the importance of interaction between

CPGs and peripheral elements in the control of rhythmic behaviors. A few examples where interactions between the central and peripheral elements have been observed are cited below. These include: limb movement in cats and coakroaches (Pearson and Duysens, 1976), swimming in dogfish (Grillner and Wallen, 1982) and tadpoles (Stehouwer and Farel, 1980), respiratory output in mammals (von Euler, 1985), wing movements in locusts (Wendler, 1978), and feeding in the gastropod (Benjamin, 1983; Benjamin and Rose, 1985). To understand the neuronal basis of rhythmic behavior, the identification and characterization of the CPG neurons, the peripheral elements, and synaptic interactions is considered essential.

1.2.1.4.1. Respiratory rhythmogenesis in vertebrates

The precise identity and the location of mammalian respiratory rhythm generating neurons has not yet been fully determined. The brainstem is believed to house a rhythm generating circuit which effects either cranial motor neurons that innervate airway resistance muscles or spinal cord motor neurons which innervate respiratory pump muscles (Feldman, and McCrimmon, 1999). A variety of activities can effect breathing such as sleep, emotional state, cardiovascular activity, temperature changes, exercise, mechanoreception and chemoreception (Feldman, and McCrimmon, 1999). During the sleep-wake cycle for example, even though breathing is a continuous phenomenon, the

underlying neural circuitry is nevertheless subjected to continuous modulation (White, 1990). Neurons innervating the thorax muscles (specifically phrenic and thoracic respiratory motor neurons) are involved in the inspiratory phase (diaphragm muscle activation) (Berger et al., 1984; Goshgarian and Rafols, 1984; Dobbins and Feldman, 1994). Expiration on the other hand, is mediated by abdominal and thoracic motor neurons which are active between phrenic discharges (internal intercostal muscle activity) (Monteau and Hilaire, 1991; Berger and Bellingham, 1995). The phrenic neurons display a variety of transmitter phenotypes including classical and non-classical neurotransmitters (Fedorko et al., 1987; Bianci et al., 1995; Feldman and Smith, 1995). Neurotransmitters may play a role in regulating respiratory rhythmogenesis over varying responses including: neural excitability over narrow and wide time ranges, cycle-cycle mediation of synaptic currents, ventilatory responses to changes in blood gas, different altitudes, during development and aging (Feldman and McCrimmon, 1999). Five respiratory phases have been implicated during respiration including: active inspiration, end-inspiratory pause, passive expiratory air flow, active expiration, and end-expiratory pause (Milsom, 1990). Premotor neurons, the most prominant of which are found in the ventrolateral medulla and are called the ventral respiratory group, provide synaptic input (excitatory and inhibitory) to the motor neuron (Feldman, 1986; Monteau and Hilaire, 1991). The premotor neurons are not involved in

the rhythm generating circuit, rather they translate this rhythm into a pattern for the motor neurons (Feldman, and McCrimmon, 1999). The Botzinger complex that innervates the ventral respiratory group and spinal cord produces reciprocal inhibition in the respiratory network, most likely during the silent periods of the cycle. Between the Botzinger complex and ventral respiratory group , is located the preBotzinger complex. The preBotzinger complex situated within the vertebrate medulla appears sufficient for the respiratory rhythm (Smith et al., 1991; Schwarzacher et al., 1995). Based on recordings from a number of semi-intact and isolated slice preparations, various models have been proposed to account for the respiratory rhythm in mammals. For instance, a three-phase network - the hybrid model has recently been proposed to account for the respiratory patterned activity. According to this model, the primary oscillator consists of two respiratory neurons, which exhibit reciprocal inhibitory connections (Richter et al., 1992). Similarly, a hybrid pacemaker-network model (Onimaru, 1995; Smith et al., 1995) whose primary oscillator consists of a group of synchronized neurons, can also generate the pacemaker respiratory activity in mammals (for review see Funk and Feldman, 1995).

Despite recent advances in our understanding of the neuronal control of respiration in vertebrates (including humans), the mechanisms underlying the generation, maintenance, and modulation of the respiratory rhythm are essentially unknown. Specifically, several

questions regarding the location, anatomical identity, and the generation of the respiratory rhythm within the medulla remain unanswered. These gaps in our knowledge are due in large measure to the complexity of the vertebrate respiratory neuronal network and to the complex nature of the respiratory behavior itself. These difficulties can however, be overcome by using a simpler invertebrate model.

1.2.1.4.2. Need for a model system

An ideal molluscan invertebrate model to investigate neural control of respiratory behavior must however, posses a number of important characteristics. In particular: 1) it should be a pulmonate whose tidal air breathing responds as a mammalian air breather does to alterations in the respiratory environment (for example increased or decreased levels of oxygen), 2) the respiratory behavior should be easily observable, 3) the central nervous system should be comprised of individually identified neurons amenable to electrophysiological studies. Dr Syed's strategy has been to develop such a model system for determining mechanisms underlying respiratory rhythmogenesis. As outlined below, the respiratory system of the pond snail *Lymnaea stagnalis* meets the above stated requirements quite well.

1.3. *LYMNAEA* AS A MODEL SYSTEM FOR STUDIES ON THE RESPIRATORY RHYTHMOGENESIS

To understand fundamental cellular and synaptic mechanisms underlying respiratory rhythmogenesis, our laboratory has opted to develop a simple invertebrate model where the neuronal basis of respiration can be investigated from the whole animal to an identified neural network level. Utilizing intact, semi-intact, and isolated brain preparations from the mollusk *Lymnaea stagnalis*, one of the main objectives of my research was to determine the involvement of an individually identified respiratory CPG neuron in the neural control of aerial breathing behavior.

1.3.1. Respiration in *Lymnaea*

The primary mode of respiration in *Lymnaea* is aerial (60%) however, if the water is well oxygenated, adequate gas exchange (40%) is achieved via the skin and lung ventilation is significantly reduced or suspended (Jones, 1961). If the water is made hypoxic (Nitrogen is bubbled through), aerial respiration increases dramatically (Lukowiak et al., 1996). Regardless of its environmental conditions, the hypoxic animal exhibits either a single (often prolonged, lasting up to one minute), or several (brief 5-10/minute) repetitive opening and closing movements of its pneumostome before submersing under water. An animal's metabolic state and the quality of its previous respiratory activity also determine the timing for subsequent visits to the water surface. In summary, *Lymnaea* is a hypoxia driven breather whose respiratory behavior is well

characterized and which can also be manipulated experimentally (Syed and Winlow, 1991a; Lukowiak et al., 1996, 1998).

1.3.2. Respiratory CPG in *Lymnaea*

Dr Winlow's laboratory was the first to describe both the respiratory behavior and motor neurons that control the respiratory musculature in *Lymnaea*. (Syed and Winlow, 1991a, b). The CPG network that underlies respiratory rhythmogenesis consists of three interneurons; input three interneuron (IP3I), visceral dorsal four (VD4), and right pedal dorsal one (RPeD1). *In vivo*, studies indicate that these three interneurons alone produce the respiratory rhythm.

The *Lymnaea* circuit resembles a classical half center model of the kind proposed by Brown in 1911. A picture therefore, emerged, which is analogous to respiratory rhythm generation in mammals. That is, the rhythmic motor output originates in two half centers (IP3I and VD4), which oscillate only when they receive input from a common excitatory drive such as RPeD1 (Syed et al., 1990). Consistent with other examples of the half center model, the *Lymnaea* respiratory CPG assures coordination of antagonistic muscles but is not inherently rhythmic.

1.3.3. Respiratory CPG in semi-intact, isolated preparations, and *in vitro* (cell culture)

During spontaneous respiratory activity recorded in the semi-intact animals, RPeD1 fires a burst of action potentials in phase with pneumostome opening movements. These bursts in RPeD1 result from IP3I activity. Similarly, in the isolated brain preparations, RPeD1 fires alternating bursts of action potentials in phase with IP3I activity. Furthermore, in an *in vitro* reconstructed network, RPeD1 has been shown to be necessary for rhythmogenesis. This pattern of excitatory activity in RPeD1 is unique to the respiratory rhythmic discharges seen in both semi-intact and isolated brain preparations (Syed and Winlow, 1991a, b). In quiescent preparations, where spontaneous respiratory activity is absent, direct intracellular stimulation of RPeD1 can trigger either a single respiratory episode, or a series of rhythmical patterns of alternating inspiratory and expiratory discharges (Syed and Winlow, 1991b). In addition to the above ascribed roles for RPeD1 in respiratory behavior, several unpublished data suggest (Inoue et al. unpublished) that RPeD1 also receives both chemosensory and mechanosensory inputs from the pneumostome area. For instance, superfusion of the pneumostome area with hypoxic saline increases the firing frequency of RPeD1. At the water interface, as the pneumostome breaks through the mechanical barrier (water tension), RPeD1 receives a strong excitatory drive. Gentle stroking of the pneumostome with a fine brush can simulate this mechanosensory input. Stronger mechanosensory inputs (noxious stimulus) on the other hand, inhibits RPeD1 activity

concomitant with pneumostome closure (Lukowiak et al., 1996, 1998). In a semi-intact animal, direct intracellular stimulation of RPeD1 was also found to induce pneumostome opening movements in the absence of IP3I activity (Inoue unpublished). This occurred only if the pneumostome was above the water interface. Under water (saline), RPeD1 stimulation failed to induce pneumostome opening, suggesting that the peripheral feedback was important.

1.4. OBJECTIVES AND HYPOTHESES

Taken together, the above studies demonstrate that both behavioral and neuronal components of the respiratory rhythm generation in *Lymnaea* are well characterized. Data from semi-intact, isolated ganglionic and cell culture studies demonstrate that RPeD1 plays an important role in the respiratory rhythm generation. However its precise involvement in respiratory behavior of intact animals has not yet been determined One of the main **objectives** of this study was to determine: What role does RPeD1 play in the control of breathing behavior in the intact animal? Utilizing, intact, semi-intact and isolated ganglion preparations, I tested the **hypothesis** that RPeD1 was necessary for respiratory behavior in an intact *Lymnaea*. To test this hypothesis directly, I selectively and systematically disrupted RPeD1's peripheral and synaptic connections by surgical procedures. The resulting perturbations in the respiratory behavior were examined

visually, whereas motor patterns were investigated electrophysiologically. RPeD1 was then allowed to re-grow its axonal processes and the effects of this regeneration on the restoration of normal respiratory behavior were examined.

CHAPTER TWO: MATERIALS AND METHODS

2.1. ANIMALS

Laboratory raised stocks of the fresh water snail *Lymnaea stagnalis* were used in all experiments. Animals were maintained in well aerated pond water at room temperature and fed lettuce. Snails with a shell length of approximately 12-15 mm were used in all experiments.

2.2. SURGICAL PROCEDURES

2.2.1. Intact animals

Prior to surgery, all animals were anesthetized by injecting 50 mmol magnesium chloride (1-3) ml directly into the foot musculature. Once injected, magnesium chloride generated an immediate response which resulted in the paralyses of the foot musculature. The animals were then placed on a dissection tray with its foot facing downwards. The tentacles were pinned down to the bottom of a dissection dish and the shell was pulled backwards. A dorsal midline incision was made to expose the central ring ganglia. Using a fine, fire-polished glass pipette, the central ring ganglia was exposed and a pair of fine forceps was used to crush the axons of interest. Specifically, 1) crushes were made either between the right pleural and parietal ganglia (ipsilateral side), or on the contralateral side; 2) the right internal and external parietal nerves or the left parietal nerve was crushed or 3) RPeD1's soma was selectively

ablated or LPeD1's soma was selectively removed using a sharp glass microelectrode. In sham operated animals, only a skin incision was made. The animals were then returned to a well-aerated tank and allowed to recover from surgery. No suture was necessary because the incision was small enough to mend itself.

2.2.2. Isolated brain preparations

To remove the central ring ganglia from the intact animals, the de-shelled snails were placed in a solution of 25% Listerine (in normal saline) for 10 minutes. Once fully anaesthetized, the animals were pinned down in a dissection dish containing standard *Lymnaea* saline (NaCl 40.0 mM, 1.7 mM KCl, 4.1 mM $CaCl_2$, 1.5 mM $MgCl_2$, HEPES) buffer to pH 7.9. A midline incision was performed to expose the central ring ganglia and this was subsequently dissected out of the animal via a pair of fine scissors (see Syed and Winlow, 1991a).

2.3. BEHAVIORAL OBSERVATIONS/ANALYSIS

Following surgery and subsequent recovery, the behavioral responses of all animals were monitored in two ways: 1) visual inspection, 2) time-lapse video recording. For visual inspections, the animals were placed in a 500-L beaker containing pond water and the pneumostome opening and closing movements were monitored over a period of one hour.

For time-lapse recordings, the respiratory movements were monitored via a RCA video recorder (Pro 8, image stabilization). Due to the reflective nature of water, the observation recorded on a recorder were difficult to discern clearly, therefore the visual inspection was preferred in most instances.

2.4. ELECTROPHYSIOLOGY

To record intracellular activity, the isolated central ring ganglia (see above) were pinned down to the bottom of a dissection dish containing normal *Lymnaea* saline. The connective tissue sheath surrounding the ganglia was removed by a pair of fine forceps, whereas the inner sheath was softened by protease (Sigma type XIV: bacterial-pronase E, P-5147). Conventional sharp electrode recording techniques were used to monitor intracellular activity (see Syed and Winlow, 1991b). Specifically, glass microelectrodes (1.5mm) were pulled on an electrode puller (Koff 700c) and these were filled with a saturated solution of potassium sulfate (resistance 30-60 Mohm). Neurons were impaled by the aid of Leitz micromanipulators. Membrane potentials were amplified using an amplifier (Neurodata IR283), displayed on an oscilloscope (Tektronix 5113) and recorded on a Astro-Med chart recorder (Dash IV).

2.5. INTRACELLULAR INJECTION OF THE DYE LUCIFER YELLOW

To visualize the morphologic profiles of both normal and regenerated RPeD1 neurons, intracellular dye injection techniques were utilized. Central ring ganglia were isolated from both normal and operated animals and maintained in normal *Lymnaea* saline. Microelectrode tips were filled with 3-5% solution of Lucifer yellow (CH-Sigma) and back-filled with lithium chloride (0.1%). Resting membrane potential and action potential parameters were used to confirm the intracellular impalement. Lucifer Yellow was injected ionophoretically by applying hyperpolarizing current pulses (MGP-I Multichannel Pulse Generator stimulator). A blue filter, mounted in front of the light source was used to determine the successful injection of the dye. The injected preparations were left overnight in the refrigerator (4°C to allow spread of the dye. These were subsequently fixed in 10% formalin (pH 7.3, PO_4 buffer) overnight in the refrigerator, and then cleared by using a series of increasing concentrations (50%,70%,90%) of ethanol (30 minutes each) leading up to 100%. Ethanol served as a dehydrating agent. Following ethanol treatment, the preparations were placed into dimethyl sulfoxide (DMSO) for 10 minutes, followed by methyl salicyate and then mounted on glass slides. The dye-injected preparations were then observed under a fluorescent microscope (Zeiss, Axioskop) and the preparations were photographed via a 35mm camera (MC 80).

2.6. CHEMICALS

Dopamine (Sigma, H8502) was dissolved in normal *Lymnaea* saline containing sodium metabisulfate (Sigma S1516) solution (ml/L) to prevent photo oxidation. The solution was diluted to obtain a 10^{-5} M concentration, (Spencer et al,. 1996). A peristaltic pump (Gilson, Minipuls 2) (total volume replaced in two minutes) was used to deliver various solutions directly to the isolated brain.

Sulpiride (Biochemicals Inc.), a dopamine antagonist was diluted in DMSO to prepare a 10^{-4} M solution.

2.7. STATISTICS

Statistical analysis was performed on data using the Student's *t* test for two groups (GB stats). The Fisher's exact test was used to indicate significant differences between data that either quantified the absence or presence of a certain phenomenon (SigmaStat; Jandel Scientific, San Rafael, CA). Differences were considered to be significant if $p < 0.05$. Data were displayed either as a percentage or mean +/- SD. Behavioral observations were performed blind. The researcher performing behavioral observations was in most instances unaware of the exact surgical procedures performed on the animals.

CHAPTER THREE: RESPIRATORY BEHAVIOR IN *LYMNAEA*: ROLE OF THE GIANT DOPAMINE CELL (RPeD1)

3.1. INTRODUCTION

3.1.1. Respiratory behavior of the mollusk *Lymnaea stagnalis*

The fresh water mollusk *Lymnaea stagnalis*, is a bimodal breather, which uses either continuous gas exchange with water, or lung exchange (aspirational lung breathing) with the atmospheric air (Jones, 1961). For atmosphere gas exchange to occur, the hypoxic animal surfaces and opens its respiratory orifice - the pneumostome. This provides an airway between the lung and the atmosphere (Figure 3.1). During pneumostome openings, the mantle cavity muscles contract and the lung gas is expired into the atmosphere (expiration). These muscles then relax, allowing a passive re-inflation of the lung by its elastic recoil. The pneumostome is then closed by the contraction of pneumostome closing muscle (inspiration) (Syed and Winlow, 1991a). Aerial respiration occurs primarily in the hypoxic environment. In well-oxygenated water, adequate gas exchange is provided via the skin and the lung ventilation is reduced significantly. In contrast, when water is made hypoxic or hypercapnic, the aerial respiratory drive increases dramatically and the animal either exhibits prolonged openings of its pneumostome or the frequency of these ventilatory movements increases dramatically (Syed

Figure 3.1 A photomicrograph of *Lymnaea stagnalis*. To fulfil its respiratory needs an hypoxic animal visits the water surface. At the water interface, the snail opens and closes its respiratory orifice, the pneumostome (P). Scale bar 5 mm. Figure taken from Syed and Winlow, 1991a.

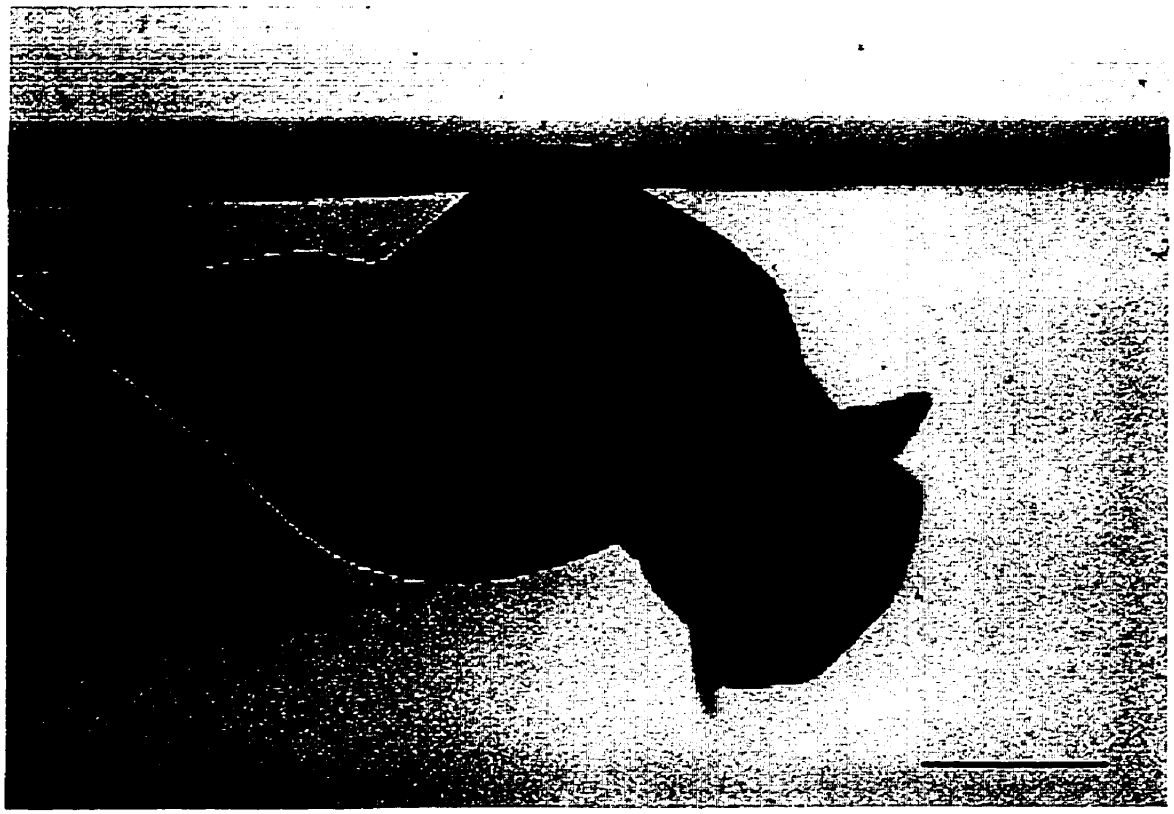

and Winlow, 1991a). This pattern of breathing in *Lymnaea* resembles that of amphibia, reptiles and diving mammals (Milsom, 1990a).

3.1.2. Neural elements of central respiratory rhythm generation

Utilizing semi-intact and isolated brain preparations, Syed and colleagues (Syed and Winlow, 1991a, b) have identified various muscle groups that control the opening and closing movements of the pneumostome, as well as motor neurons that innervate these muscles (Syed and Winlow, 1991a, b). Similarly, the central pattern generating neurons (CPG) underlying respiratory behavior in *Lymnaea* have also be identified and characterized (Syed et al., 1990). Specifically, the respiratory CPG is comprised of three interneurons: right pedal dorsal 1 (RPeD1), input 3 interneuron (IP3I) and visceral dorsal 4 (VD4). IP3I and VD4 control expiration and inspiration respectively, whereas RPeD1 initiates the respiratory behavior. Although, in semi-intact and isolated brain preparations, RPeD1 proved sufficient to trigger the respiratory rhythmogenesis (Syed and Winlow, 1991b), its precise role/s in the intact animal are yet to be determined.

3.1.3. RPeD1 is an identified neuron

RPeD1 is a well characterized neuron that is part of the neural network underlying respiratory behavior in *Lymnaea*. Preliminary evidence from the Syed laboratory shows that RPeD1 receives chemosensory information from the periphery regarding hypoxia, which

increases its spiking activity (Inoue et al., 1996b). At the water interface, as the pneumostome breaks through the water film, RPeD1 receives an additional mechanosensory input, which in turn induces a burst of spikes in this neuron (Inoue et al., 1996b) This level of excitability in RPeD1 is generally considered sufficient to trigger the respiratory episodes in both IP3I and VD4.

3.1.4. RPeD1 Morphology

Figure 3.2 shows the ganglionic location of RPeD1. Its soma is situated on the dorsal surface of the right pedal ganglia. Intracellular injections of fluorescent dye Lucifer yellow revealed that RPeD1 has a single large axon, which (after passing through right pleural, parietal and visceral ganglia) projects towards the periphery. These peripheral projections are carried via the right internal and external parietal; and the anal (visceral ganglia) nerve. In both the right parietal and visceral ganglia, RPeD1 gives off many fine branches before leaving the central ring ganglia. All of the above nerves innervate pneumostome and the mantle areas (Syed and Winlow, 1991a).

One of the main objectives of this study was to test the hypothesis that RPeD1 is necessary for respiration in the intact animal.

3.2. RESULTS

To define RPeD1's contributions in the control of respiratory behavior in the intact animal, I systematically disrupted its peripheral

Figure 3.2 A. Photomicrograph of the isolated central ring ganglia from *Lymnaea*. Photograph shows the ganglionic location of various neuronal somata that were used in the present study. RPeD1 = right pedal dorsal 1; VD4 = visceral dorsal 4; G, H,I,J,K = G, H,I,J,K cells. Scale bar 100 μm (Figure modified from Feng, 1998). B. Line drawing of the central ring ganglia of *Lymnaea stagnalis*. RPeD1 is located in the right pedal ganglia (RPeG). It's main axon (see arrow) projects towards the periphery via the right internal and external parietal nerves (1 and 2); and the anal nerve that originates from the visceral ganglia (3). LCeG, RCeG = left and right cerebral ganglia; LPeG, RPeG = left and right pedal ganglia; LPlG, RPlG = left and right pleural ganglia; LPG, RPG = left and right parietal ganglia; VG = visceral ganglia

A

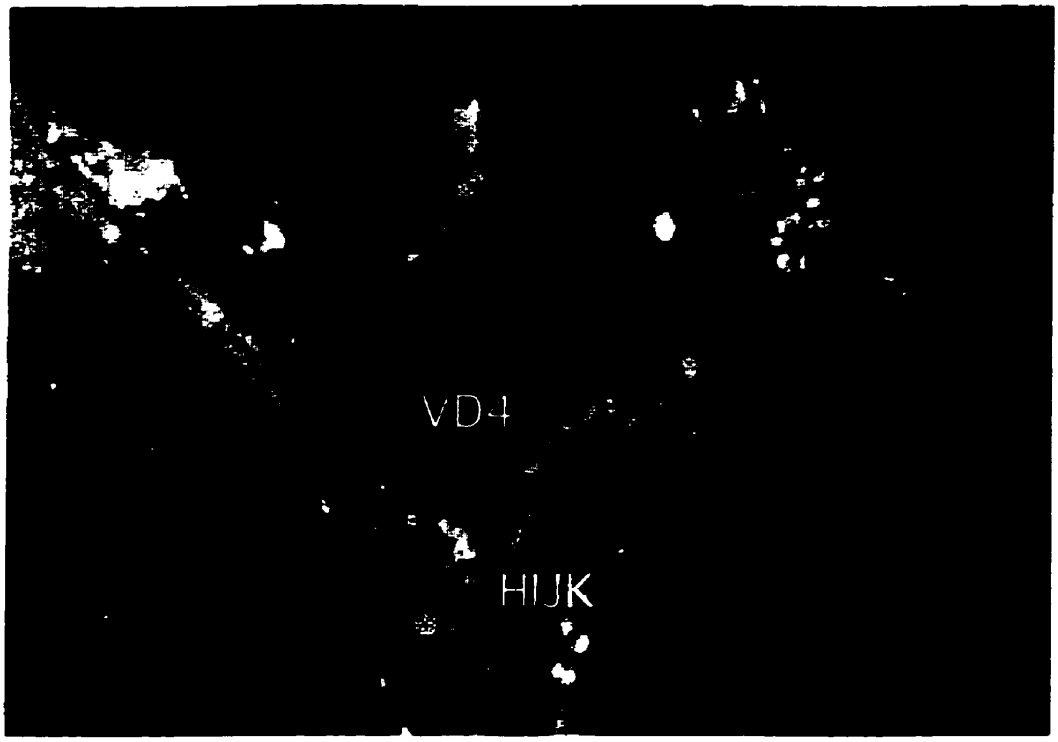

B

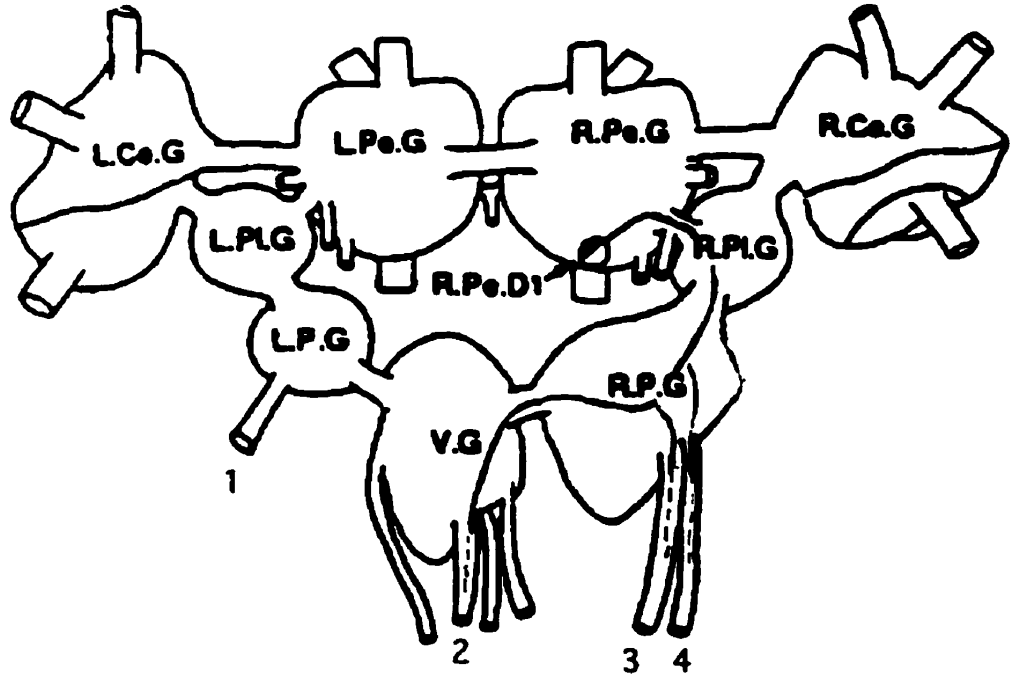

projections towards the pneumostome and mantle cavity areas. To confirm the effectiveness of my crushes, RPeD1 was axotomized in the intact animals and the central ring ganglia were isolated for dye injections. Lucifer yellow (3%) was injected ionophoretically into RPeD1's soma and the preparations were subsequently fixed and processed for fluorescent microscopy. As shown in Figure 3.3, the axotomy did indeed sever RPeD1 axon completely.

3.2.1. Axotomy of the internal and external parietal nerves disrupted normal respiratory behavior

To determine whether nerves innervating pneumostome and mantle cavity area were required for normal respiratory behavior in the intact animal, the right internal and external parietal nerves and the anal nerve were either cut or crushed (Figure 3.4), and the respiratory behavior was examined. Specifically, since the above nerves carry RPeD1's axons towards pneumostome and mantle areas, I predicted that severing these projections would disrupt the normal respiratory behavior. To test this possibility, animals were anesthetized, dissected and the above nerves were exposed. These were either cut by a pair of fine scissors or crushed via forceps. The animals were allowed to recover from surgery and their respiratory behavior was monitored either by time-lapse video recordings or via visual inspection. Since the animals receiving nerve cuts did not survive more than two days after the initial surgery (n=14), nerve crushes were performed. Specifically, in the experimental animals

Figure 3.3. Morphology of RPeD1. A) Intracellular dye injection techniques were used to reveal the morphological projections of RPeD1. EPN = external parietal nerve; IPN = internal parietal nerve; AN = anal nerve. B) Lucifer yellow was injected into RPeD1 following a connective crush between the right pleural (PLG) and parietal ganglia (PG) (see arrow). This demonstrated that the axon that passes through these connectives was indeed axotomized. Scale bar 100 μm.

Normal Morphology Of RPeD1

A

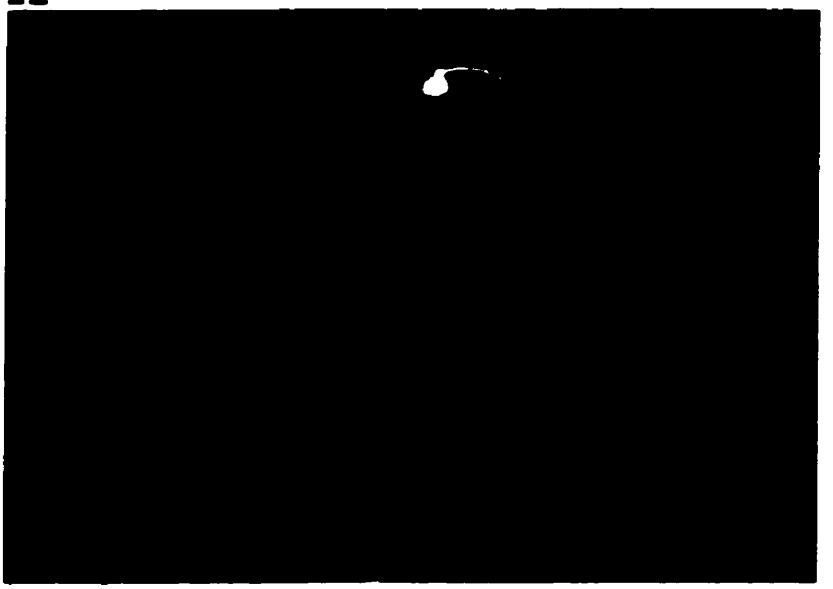

RPeD1 Morphology Following Axotomy

B

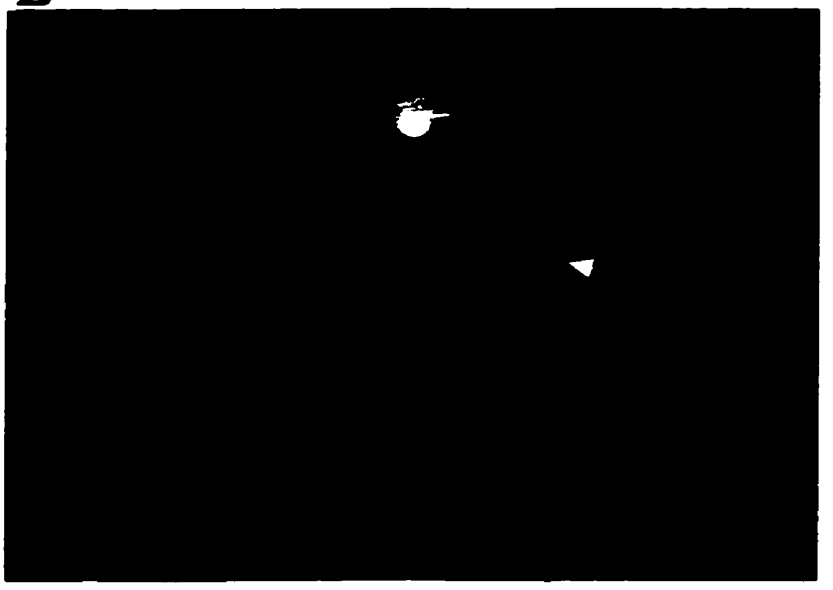

Figure 3.4. Line drawing of the central ring ganglia showing various surgical protocols that were employed in this study. Internal and external parietal nerves were crushed in the experimental animals (1), or the left parietal nerve was crushed in control animals (2). Connectives between the pleural and parietal ganglia were crushed in the experimental animals (3), or connectives between the contralateral ganglia were crushed in control animals (4). RPeD1 was selectively killed in the experimental animals (5), whereas LPeD1 was ablated in control animals (6).

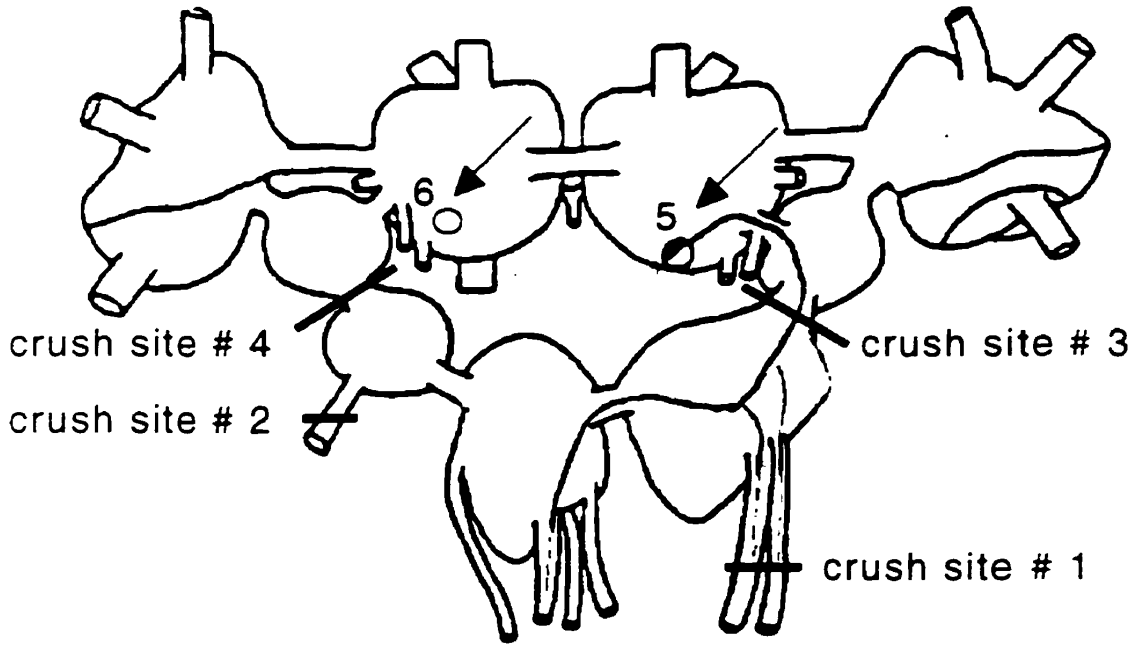
6
5
crush site # 4
crush site # 2
crush site # 3
crush site # 1

the above peripheral nerves were "crushed", whereas in the control animals the left parietal nerve (which does not contain RPeD1's axon) was crushed. The animals were allowed to recover from surgery in well-aerated tanks. Since the nerves crushed in the experimental animals contain either one or two of the RPeD1's axonal branches, I postulated that these snails would fail to breath. The respiratory movements exhibited by the experimental animals (3 ± 0.9; n = 16) were significantly fewer than the control group (8.1 ± 1.6; n = 16) ($p < 0.05$) (Figure 3.5). These differences were however not significant on days three (experimental, 3.0 ± 1.1; control, 6.3 ± 1.9) and seven (experimental, 5.6 ± 2.1; control, 5.0 ± 1.7). The data shown in Figure 3.5 demonstrate that RPeD1's peripheral projections are important for normal respiratory behavior. However, since these nerves carry both afferent and efferent projections from other neurons as well, these data do not provide unequivocal evidence that RPeD1 is indeed necessary for respiration.

3.2.2. A right side pleural-parietal crush in the intact animal disrupted the normal respiratory behavior

To further define RPeD1's role in respiratory behavior, its main axon was crushed at the connective site between the right pleural and parietal ganglia (Figure 3.4). Specifically, intact animals were anaesthetized and operated as described in Chapter Two, and their CNS exposed. Fine forceps were used to crush RPeD1's axon at the right

Figure 3.5. RPeD1's peripheral projections via right internal and external parietal nerves were required for normal breathing. Either the right internal and external parietal nerves (experimental), or the left parietal nerve (control) were crushed. The number of breaths exhibited by experimental animals on day one after surgery was significantly lower (*) than control animals ($p < 0.05$, t-test), whereas no significant differences were found on days three or seven. ($n = 14$)

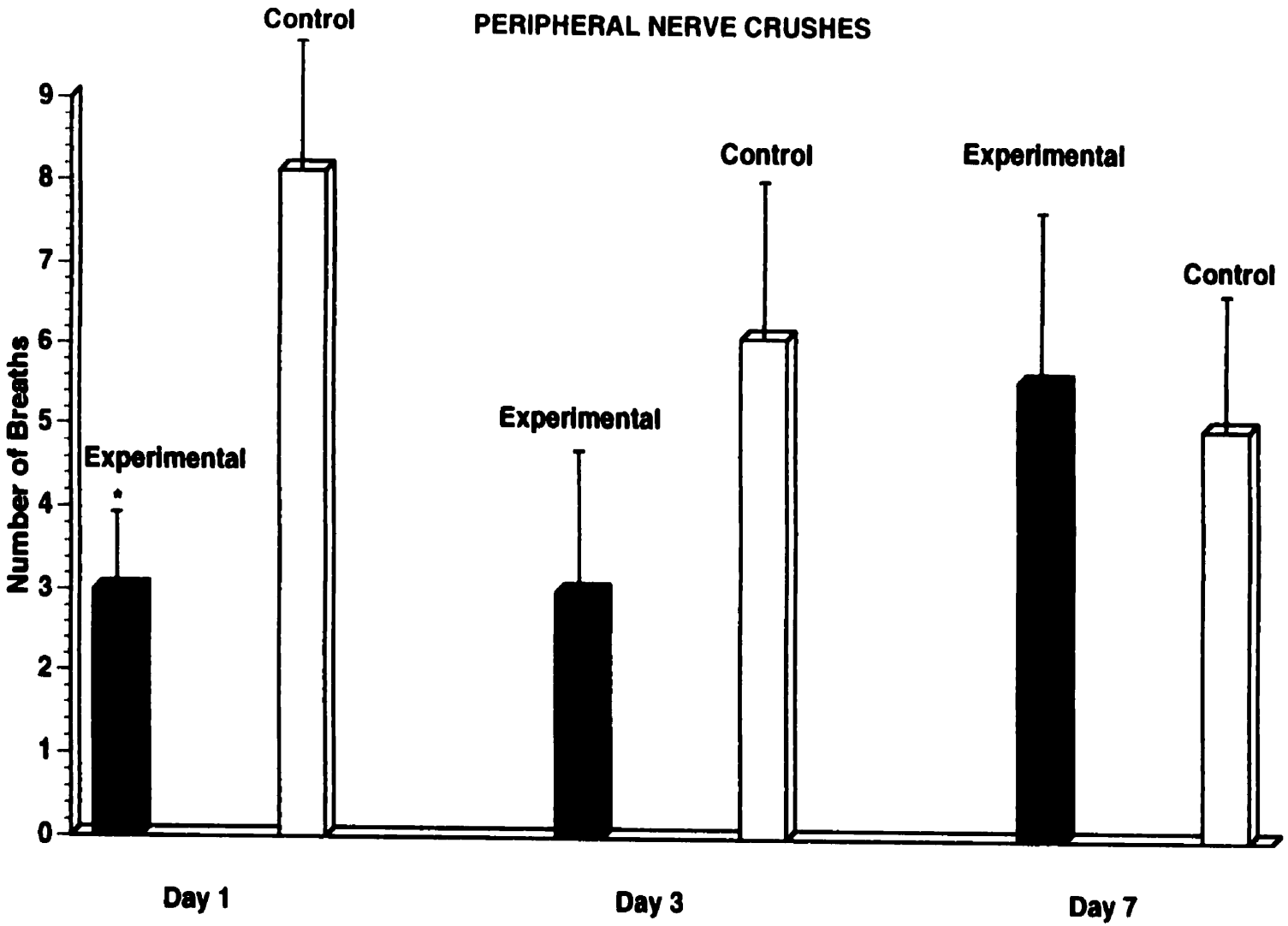
PERIPHERAL NERVE CRUSHES
Number of Breaths
0
1
2
3
4
5
6
7
8
9
Experimental
*
Control
Experimental
Control
Experimental
Control
Day 1
Day 3
Day 7

pleural-parietal connective in the experimental animals, whereas the control animals received crushes on the contralateral side (i.e. connective between left pedal and pleural ganglia). The sham operated animals on the other hand, received only a skin incision. All three groups were allowed to recover from surgery and their respiratory behavior was monitored in water. Sham (11.0 ± 1.8; n = 25) and control (10.8 ± 1.3; n = 40) groups exhibited normal respiratory behavior, while the experimental animals (0.1 ± 0.1; n = 73) failed to breathe on day three (Figure 3.6). On day seven however, significantly less respiratory movements were exhibited by experimental animals (1.5 ± 0.3) than sham (9.8 ± 1.9) or controls (13.1 ± 2.0) ($p < 0.01$). In their normal habitat (i.e. water), the experimental animals exhibited behavior that was quantitatively and qualitatively different from both control and sham groups. For example, both sham (2.7 ± 0.3; n = 18) and control (2.8 ± 0.2; n = 36) animals visited the water surface more often than the experimental animals (0.9 ± 0.1; n = 58) on day three ($p < 0.01$), and these visits were almost always accompanied by breathing movements (Figure 3.7). Experimental (1.4 ± 0.1), sham (2.3 ± 0.3), and control (2.2 ± 0.2) animals exhibited similar behavioral repretoire on day seven ($p < 0.01$). In contrast, neither did the experimental animals visit the water surface, nor were the respiratory movements performed as often.

3.2.3. A right pleural-parietal crush resulted in unusual behaviors

Figure 3.6. A right pleural-parietal crush disrupted normal respiratory behaviour in the intact animal. Data from the animals in which the connectives between the right pleural and parietal ganglia were crushed are compared with sham-operated and control animals. In control animals crushes were made between the left pleural and parietal ganglia, whereas the sham operated animals received a skin incision only. The number of breaths exhibited by experimental animals were significantly lower than sham or control groups (*) ($p < 0.01$, t-test) on days 3 and 7. However, no significant differences were observed between sham and control groups. (experimental, n = 73; sham, n = 25; control, n = 40)

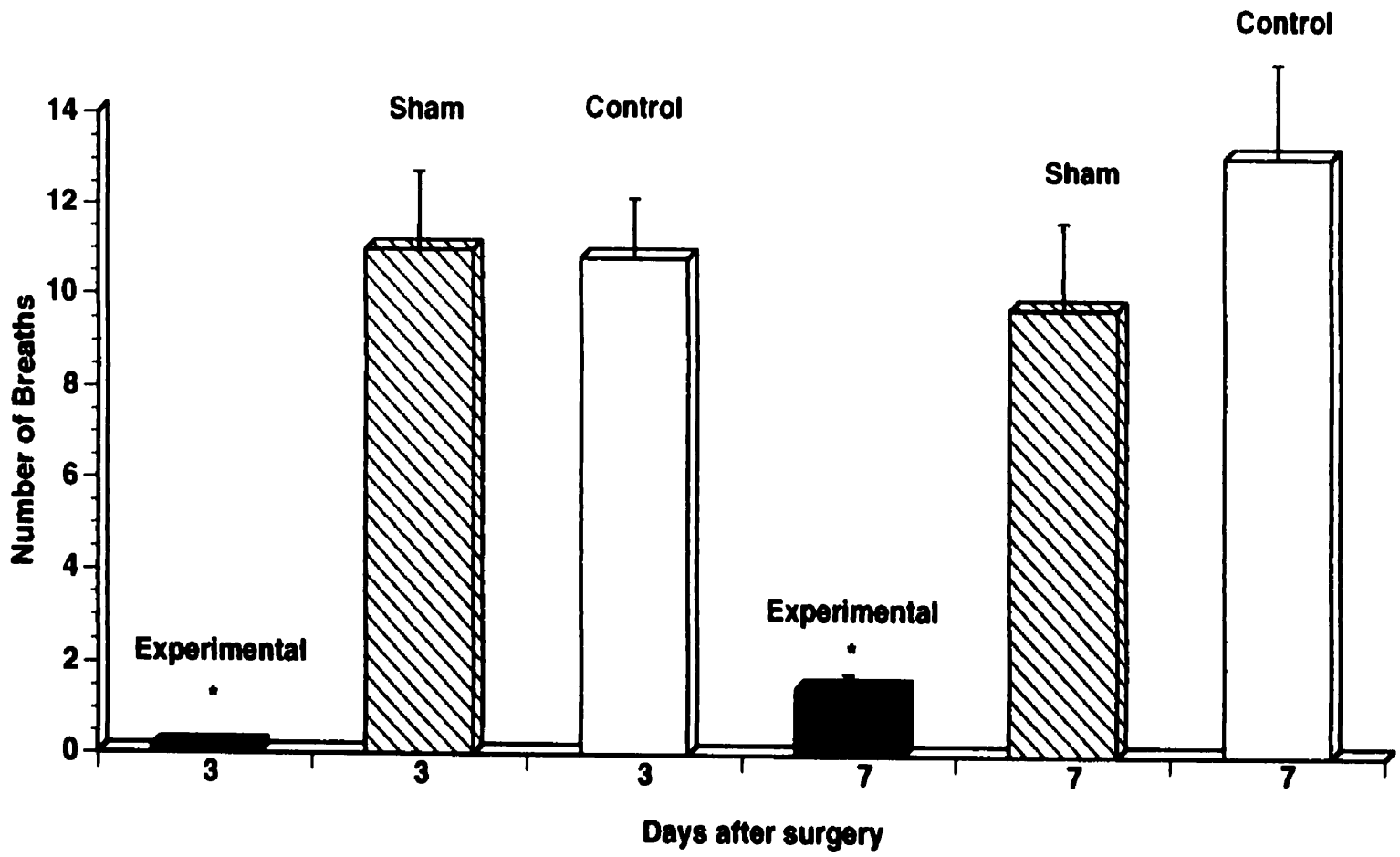
PLEURAL-PARIETALCONNECTIVE CRUSHES
Control
Sham
Control
Sham
14
12
10
8
6
4
2
0
Number of Breaths
Experimental
*
Experimental
*
3
3
3
7
7
7
Days after surgery

Figure 3.7. A right pleural-parietal crush disrupted the normal respiratory drive in the intact animal. The number of visits to the water surface by experimental animals were compared with sham and control animals, and these were found to be significantly different (*) ($p < 0.01$, t-test) on days 3 and 7. The differences between sham and control groups on these days were however not significantly different. (experimental, $n = 58$; control, $n = 36$; sham, $n = 18$)

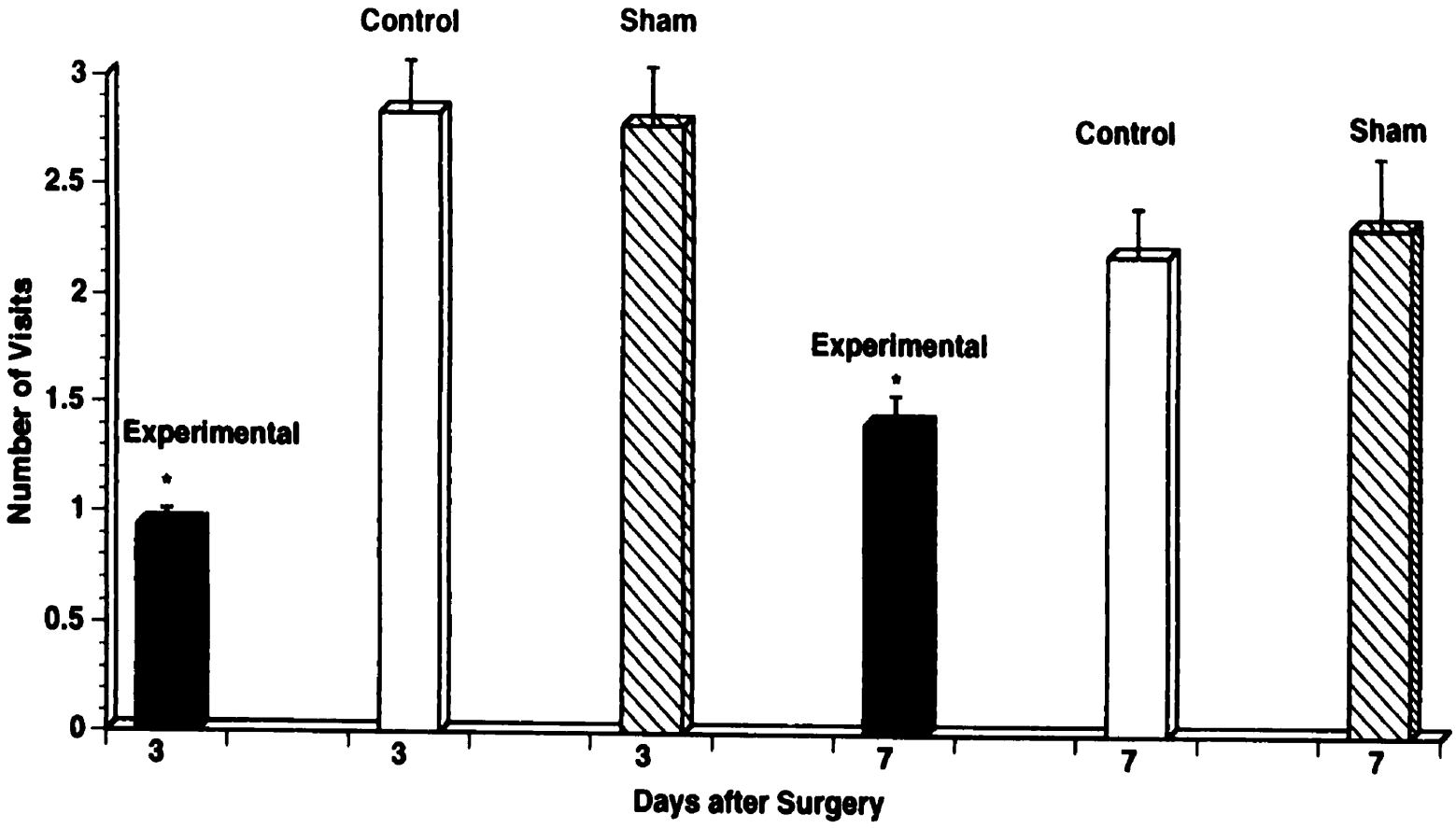
Control
Sham
Control
Sham
Experimental
Experimental
*
*
Number of Visits
3
2.5
2
1.5
1
0.5
0
3
3
3
7
7
7
Days after Surgery

In addition to the absence of normal respiratory movements, the experimental animals exhibited various behaviors that were different than the control and sham operated animals. For example, in water, a majority of the experimental animals did not feed on lettuce; they were less active and did not interact with other animals as compared with the control groups. In instances where the experimental animals did make it up to the water interface, they preferred to remain there for longer periods of time. Interestingly, on many occasions, these experimental animals completely crawled out of the water, eventually landing on the table top (Figure 3.8). The number of animals that crawled out of the water on day three (n = 30 of 76;) were not significantly different than day seven (n = 8 of 24). Of the 20 animals examined, only two attempted to crawl out of the water on day nine.

At the water surface, some of the experimental animals could not remain attached to the side wall of the tank and fell into the water, landing on the back of their shells. None of these animals were capable of reorienting themselves back onto their foot-pad. Moreover, they could not come out of their shell, and remained in that position for many hours (up to 12 hrs). Both sham and control animals on the other hand, did not display the above motor abnormalities. Interestingly, however, I noted that once out of water, the experimental animals did exhibit pneumostome opening and closing movements and these were subsequently quantified in the next series of experiments. Moreover, for

Figure 3.8. The right pleural-parietal connective crushed animals exhibited water avoidance behaviour. The percent of right side crush animals that crawled out of the water on day three was not significantly different than day seven (P = 0.0636, Fisher's exact test). However, the animals that exhibited this behaviour on day three were significantly higher than day nine (p = 0.015, fisher's exact test). (day 3, n = 30/76; day 7, n = 8/24; day 9, n = 2/20)

Note: Control and sham operated animals did not exhibit such behaviour.

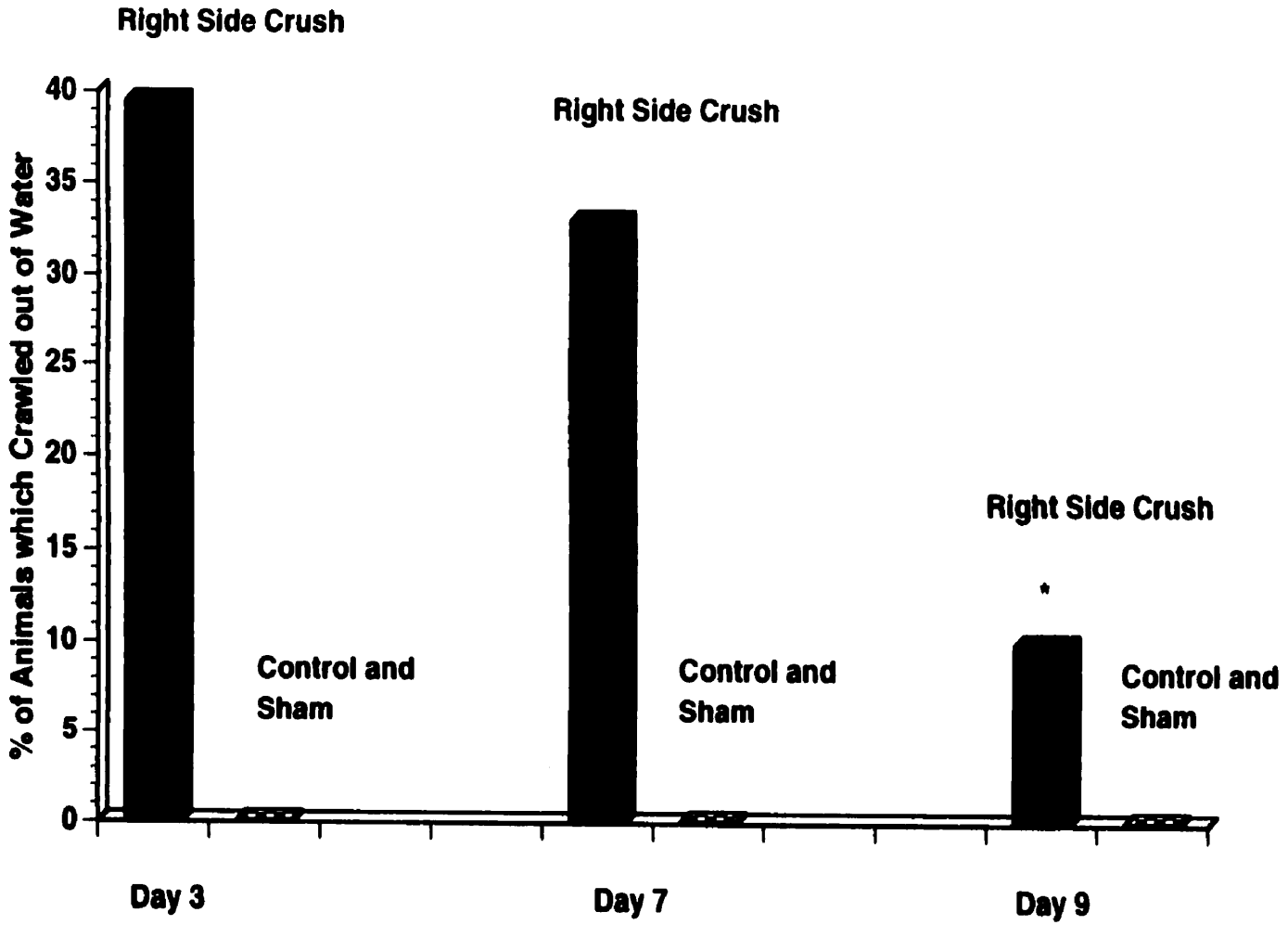
Right Side Crush
Right Side Crush
Right Side Crush
*
% of Animals which Crawled out of Water
40
35
30
25
20
15
10
5
0
Control and Sham
Control and Sham
Control and Sham
Day 3
Day 7
Day 9

comparative purposes, this "out of water" pneumostome movements were also analyzed in both control and sham animals.

I found that all three groups of animals were indeed able to open and close their respiratory orifice under these conditions (Figure 3.9). The number of opening and closing movements exhibited by the experimental animals (5.2 ± 1.3; n = 10) were however significantly less ($p < 0.01$) than that of either control (15.3 ± 1.6; n = 6), sham (24 ± 3.5; n = 6), or normal (21 ± 2.8; n = 5) group. Taken together, the above results show that in a normoxic environment, the experimental animals not only failed to exhibit normal respiratory behavior but that the right side crush induced a variety of abnormal behaviors.

3.2.4. Hypoxia did not override the effects of a crush to the right pleural-parietal connective on normal respiratory drive

The lack of respiratory drive in experimental animals kept in an aquatic environment (as compared with land), could be attributed to the fact that adequate gas exchange occurred through the skin. In the next series of experiments, all three groups were therefore, exposed to a hypoxic environment and their respiratory behavior analyzed. Specifically, instead of air, 100% nitrogen was bubbled into the water and the respiratory behavior of all groups compared. Behavioral analysis performed after three days of surgery revealed that despite the fact that all animals were maintained under acute hypoxia, the experimental animals (n = 24) did not exhibit normal respiratory movements (Figure

Figure 3.9. In a non-aquatic environment, right pleural-parietal crushed animals exhibited pneumostome opening and closing movements. The number of pneumostome openings observed in experimental animals maintained out of water for one hour were statistically significant (*) from sham, control and normal, animals ($p < 0.01$, t-test); while the number of breaths observed in sham, control, and normal groups were statistically insignificant. (experimental, n = 10; sham, n = 6; control, n = 6; normal, n = 5)

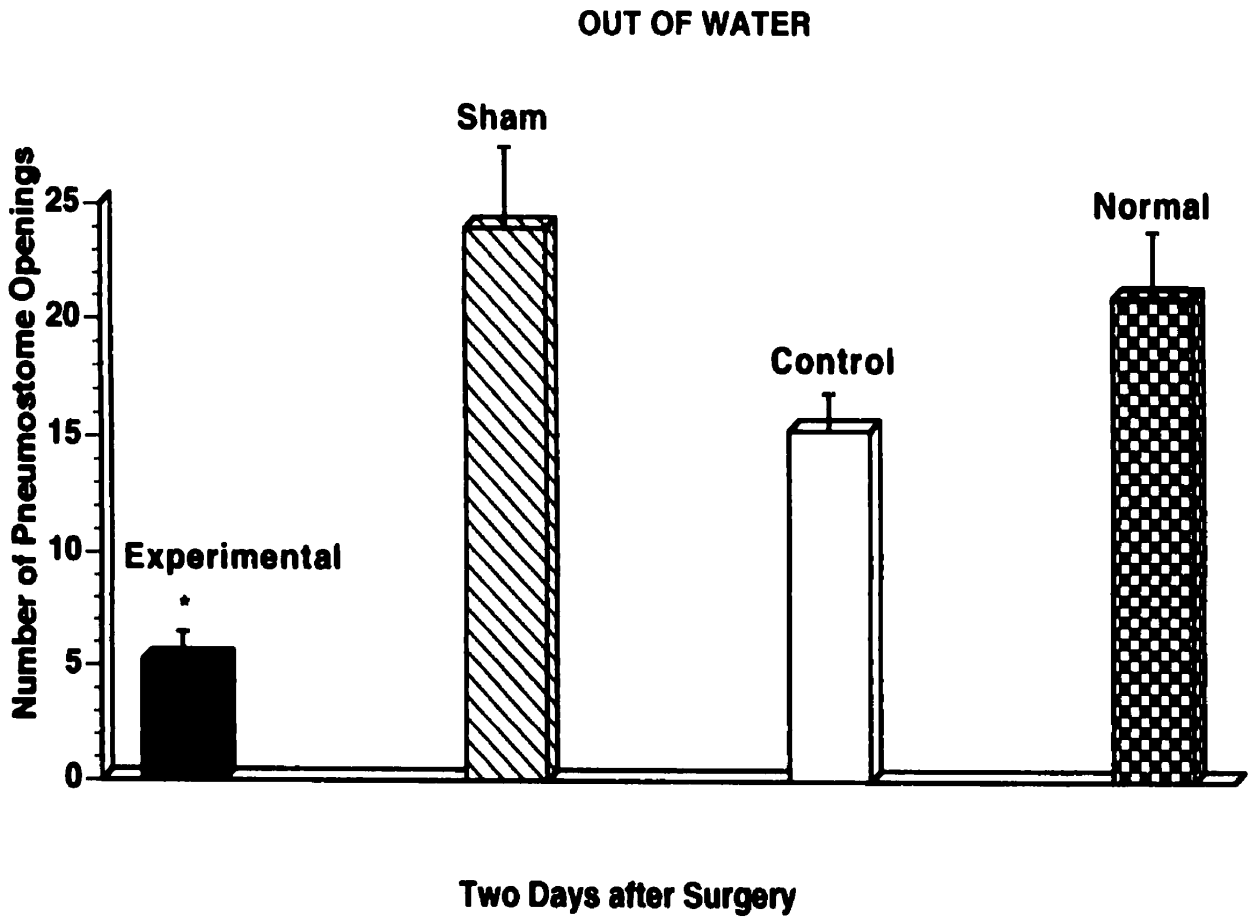
OUT OF WATER
Sham
Normal
Control
Experimental
*
Number of Pneumostome Openings
25
20
15
10
5
0
Two Days after Surgery

3.10). Control (8.3 ± 2.1; n = 22) and sham (11.8 ± 2.0; n = 21) animals on the other hand, were able to breathe at a rate that was comparable to normoxic animals. Together, these data show that regardless of their environmental conditions (normoxia or hypoxia), the experimental animals failed to exhibit normal respiratory movements.

3.2.5. A right pleural-parietal crush resulted in an increased number of deaths

Since the majority of experimental animals did not exhibit normal respiratory behavior, therefore, their mortality rate was much higher than that of the control snails. The numbers of deaths following right side crushes were therefore quantified. These data revealed that as compared with both sham (14.6%) and control (18.2%) groups, significantly larger numbers of experimental animals (62.2%) died after surgery (accumulative death percentages calculated on day seven) (Figure 3.11). These data demonstrate that in most instances, the right but not the left side crushes were generally fatal.

The above experiments suggest RPeD1's involvement in the control of normal respiratory behavior and for the perception of chemosensitivity, but they do not rule out the involvement of other, as yet unidentified neurons, whose axons were also axotomized during a right pleural-parietal crush. Therefore, an ultimate approach would have been to selectively ablate RPeD1 (Figure 3.4), and this was achieved in the next series of experiments.

Figure 3.10. Hypoxia failed to induce the respiratory drive in right pleural-parietal crushed animals. The number of breaths exhibited by experimental, sham, and control groups were compared on day 3 and 7 during nitrogen perfusion (1 hour). Breathing behaviour displayed by experimental animals was significantly different (*) from sham and control groups ($p < 0.01$), whereas no significant differences were found between sham and control groups on day 3 and 7. (experimental, $n = 24$; sham, $n = 22$; $n = 21$)

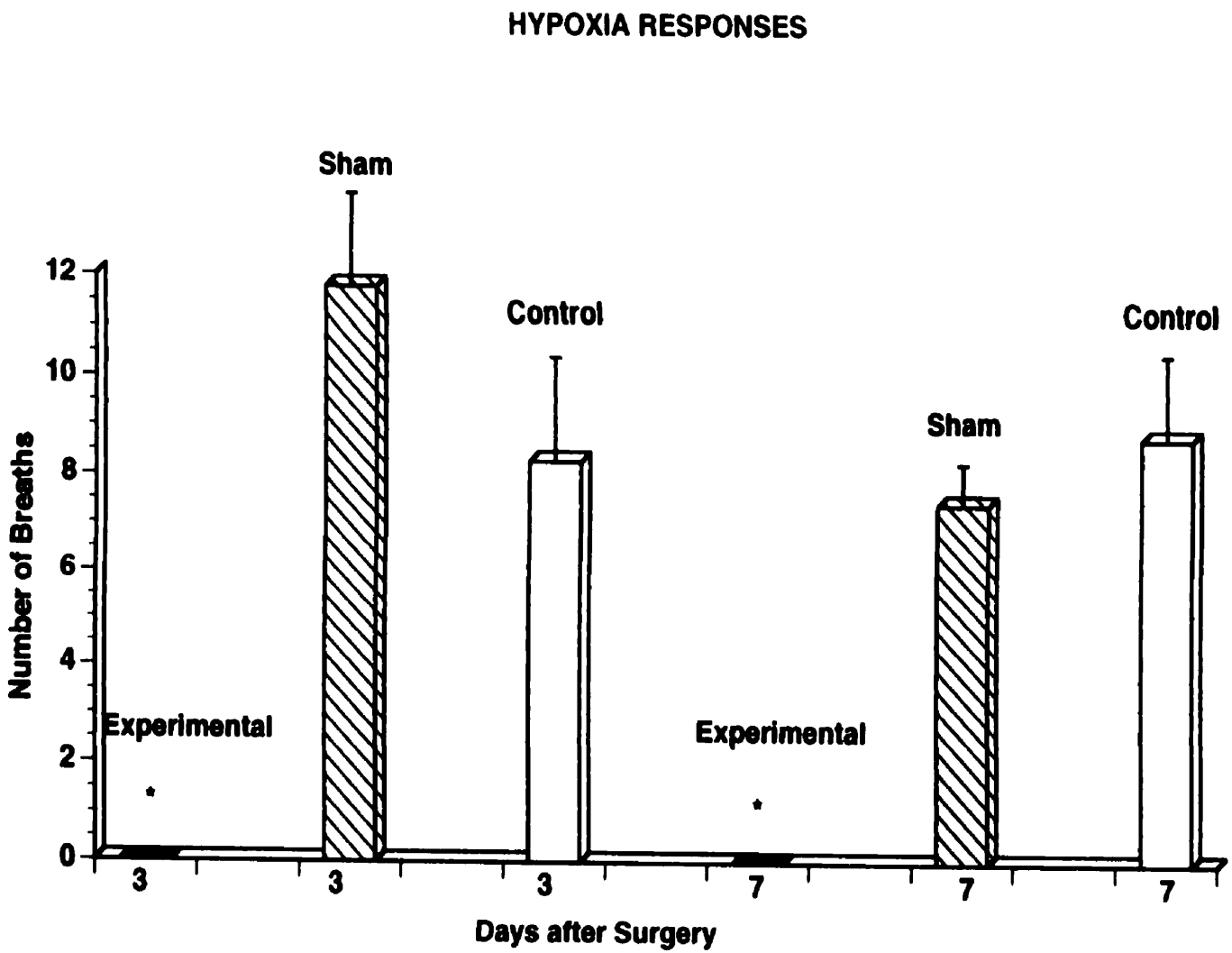
HYPOXIA RESPONSES
Sham
Control
Control
Sham
Number of Breaths
12
10
8
6
4
2
0
Experimental
Experimental
3
3
3
7
7
7
Days after Surgery

Figure 3.11. Right pleural-parietal crushed animals died more frequently than their control counterparts. Accumulative quantification of the percentage of animals that died following crushes performed on the right or left side connectives, or sham operated animals on days 1 through 7.

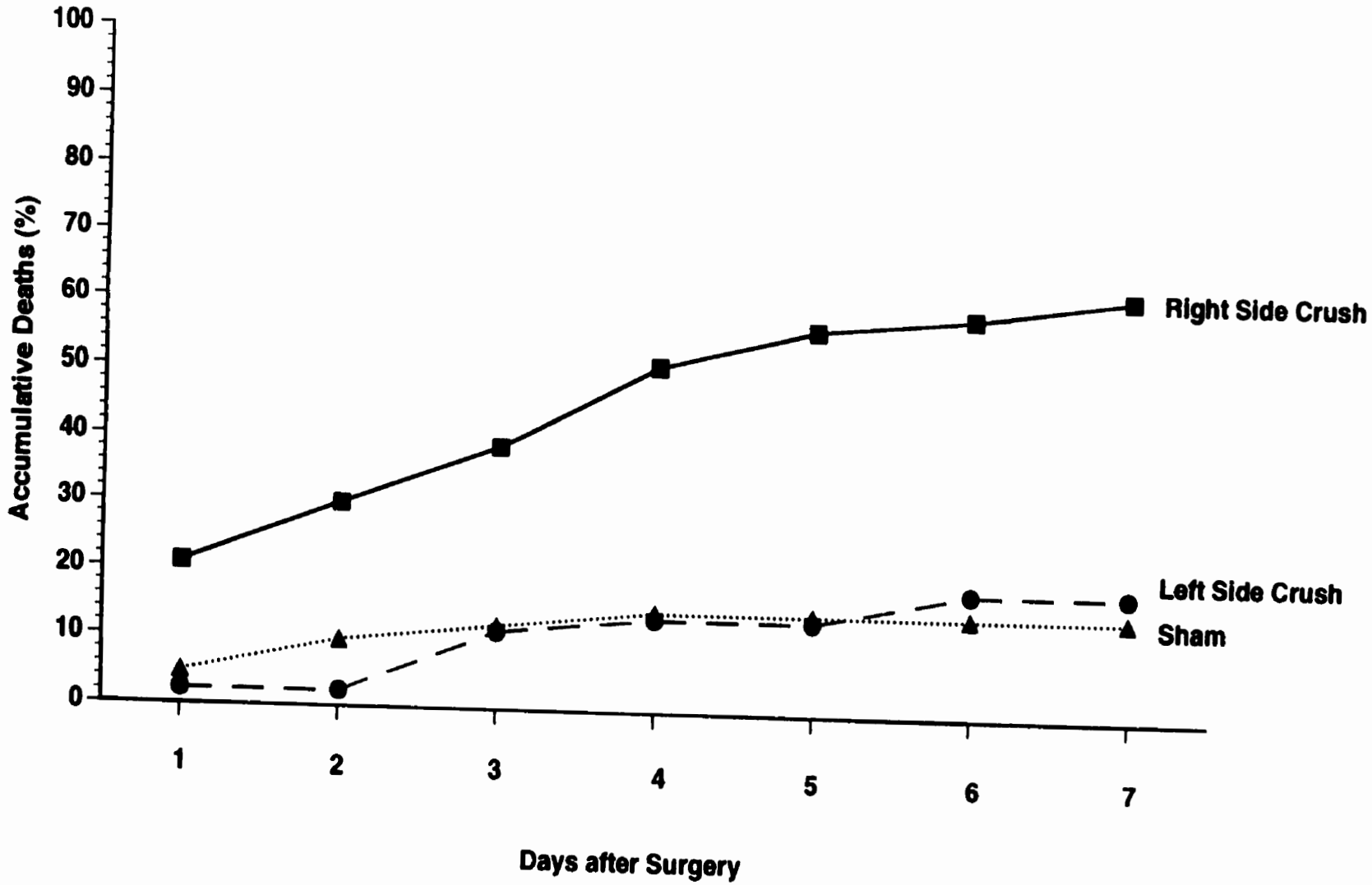
100
90
80
70
60
50
40
30
20
10
0
Accumulative Deaths (%)
1
2
3
4
5
6
7
Days after Surgery
Right Side Crush
Left Side Crush
Sham

3.2.6. RPeD1 soma ablation disrupted the normal respiratory behavior

To test directly, whether the disruption of normal respiratory behavior in the right pleural-parietal crush animals did indeed involve RPeD1, this cell was selectively ablated in the intact animal and the respiratory behavior was analyzed after recovery. Specifically, intact animals were anesthetized and operated as described above. The central ring ganglia were exposed and RPeD1's soma was selectively destroyed via a sharp glass electrode. In control animals, another identified neuron, left pedal dorsal 1 (LPeD1 - the giant serotonergic neuron) was ablated; whereas, in sham operated animals only a skin incision was made. The three groups were allowed to recover from surgery and their respiratory behavior was monitored as described above. I found that the number of breaths exhibited by the experimental animals were significantly fewer than that of sham or control group on days one (1.1 ± 0.3; n = 48), two (1.2 ± 0.4; n = 40), three (1.5 ±0.4; n = 25), and seven (2.1 ± 0.6; n = 30) ($p < 0.01$) (Figure 3.12). While the number of breaths exhibited by sham (5.4 ± 0.6; day one) and control groups (6.4 ± 0.7; day one) were indistinguishable after the first two days of surgery; differences were nevertheless observed on days three and seven. By day three, sham operated animals (11 ± 1.8; n = 25) began opening their pneumostome at a significantly higher rate ($p < 0.05$) than that of the control animals (6.1 ± 1.1; n = 25). However, the incidence of breathing exhibited by control

Figure 3.12. Ablation of RPeD1's soma disrupted the normal respiratory behaviour in the intact animal. The number of breaths exhibited by RPeD1 ablated and sham-operated or control animals were compared. RPeD1 ablated animals on days 1, 2, 3, and 7, displayed breathing that was significantly different (*) from the breathing behaviour that was exhibited by sham-operated and control animals on all days post surgery ($p < 0.01$, t-test). While sham and control groups did not show any statistical differences on days 1 and 2, significant differences were found between them on days 3 and 7 ($p < 0.05$, t-test). (At the start of the experiment: experimental, n = 48; sham, n = 25; control, n = 25)

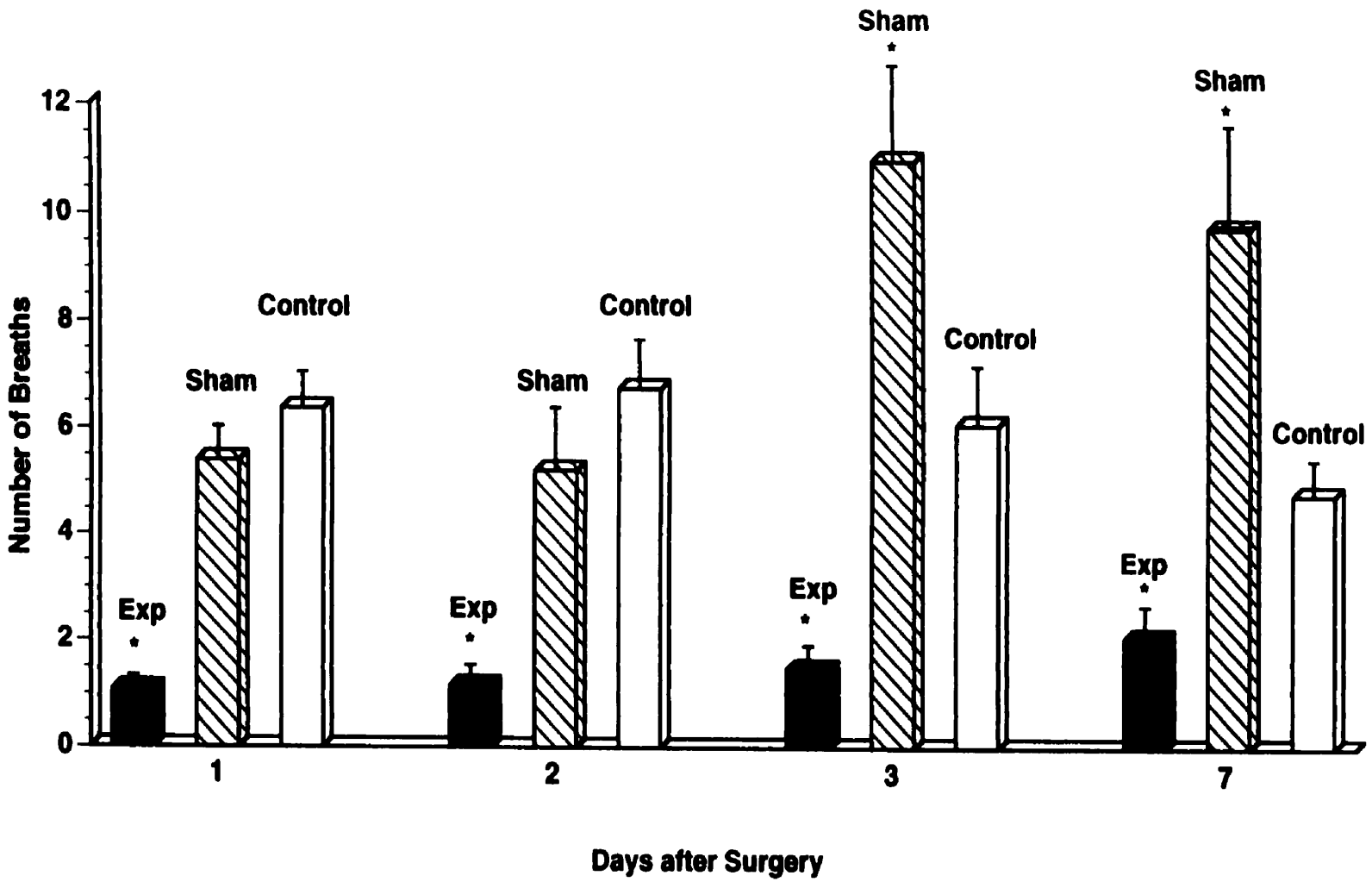
Number of Breaths
12
10
8
6
4
2
0
Exp
Sham
Control
1
2
3
7
Days after Surgery

animals, decreased to the level of 4.8 ± 0.7 (n = 23) by day seven ($p < 0.05$).

The second parameter examined was the number of visits made by each of the above groups (Figure 3.13). Specifically, in control animals (n = 23) the number of visits to the water surface were almost indistinguishable from those of sham operated animals (n = 18) on days one, three and seven. However, this parameter was reduced significantly in the experimental animals (n = 48) as compared with both control groups on days one, three and seven.

Following recovery, the death rate was also quantified in all animal groups. These data revealed that as compared with sham or control animals, a greater percentage of experimental animals died following surgery (Figure 3.14). These data show that selective ablation of RPeD1's soma disrupted the normal respiratory behavior, albeit this was not completely abolished.

The severed axons from a variety of vertebrate and invertebrate species are known to survive axotomy and maintain their functional properties (Bittner, 1988). Therefore, to rule out the possibility that in the absence of its soma, the RPeD1 axon may have still been functional, pronase was injected intracellularly.

3.2.7. RPeD1 soma ablation by pronase injection disrupted the normal respiratory behavior

Figure 3.13. RPeD1 soma ablation disrupted the normal respiratory drive. The number of visits to the water surface were monitored following RPeD1 ablation and the data were compared with sham-operated (received a skin incision only) and control (LPeD1 ablated) animals. On all days, experimental animals exhibited behaviour that was significantly different (*) from both sham and control groups ($p < 0.01$ on days 1 and 3; $p < 0.05$ on day 7, t-test). (experimental, n = 48; sham, n = 18; control, n = 23)

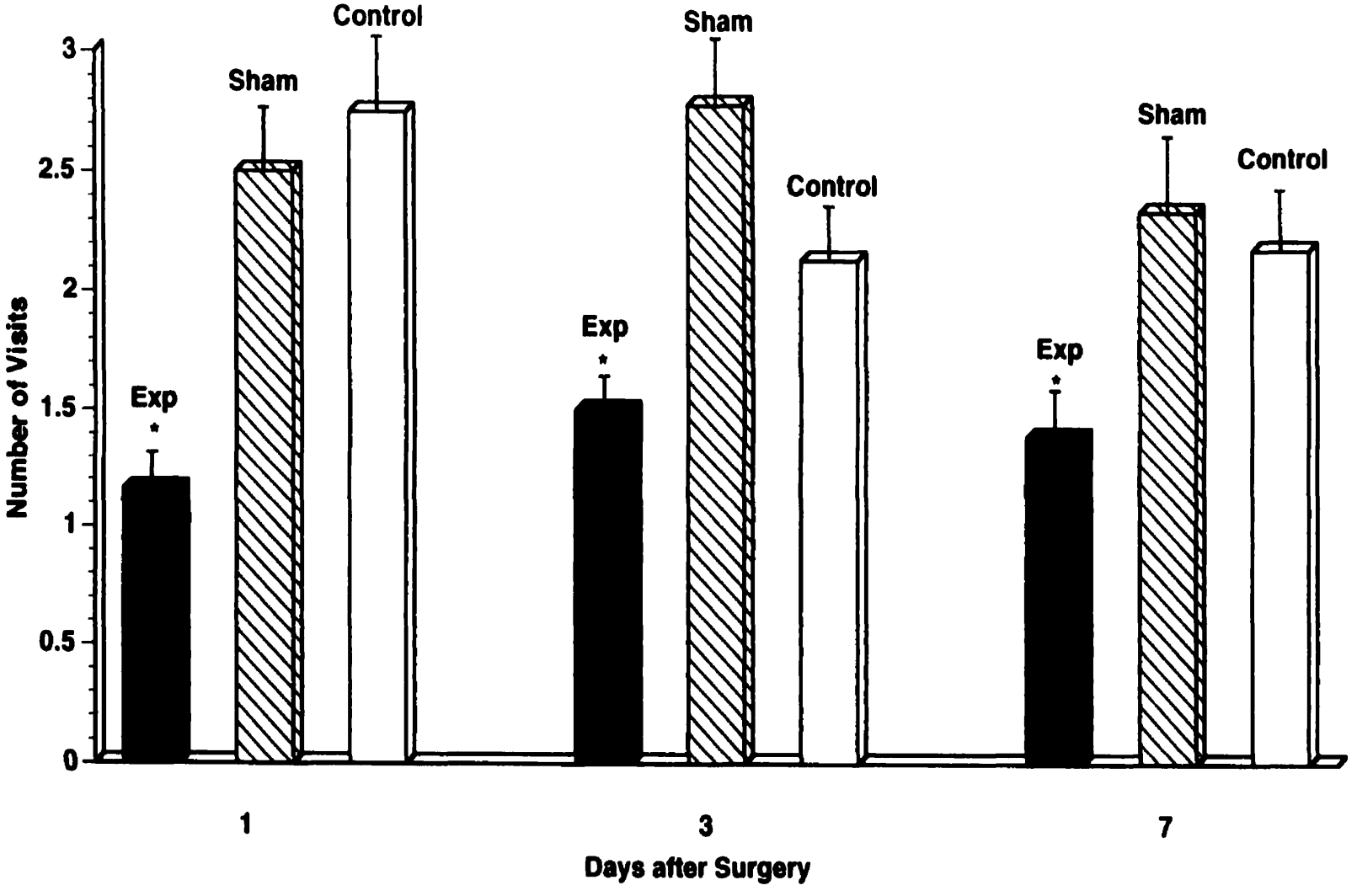
Control
Sham
Exp
Sham
Control
Exp
Sham
Control
Exp
*
*
*
3
2.5
2
1.5
1
0.5
0
Number of Visits
1
3
7
Days after Surgery

Figure 3.14. RPeD1 soma ablated animals died more frequently than their control counterparts. Number of accumulative deaths that occurred following the surgical removal of RPeD1, or LPeD1, or sham-operated animals on days 1 through 7 are shown.

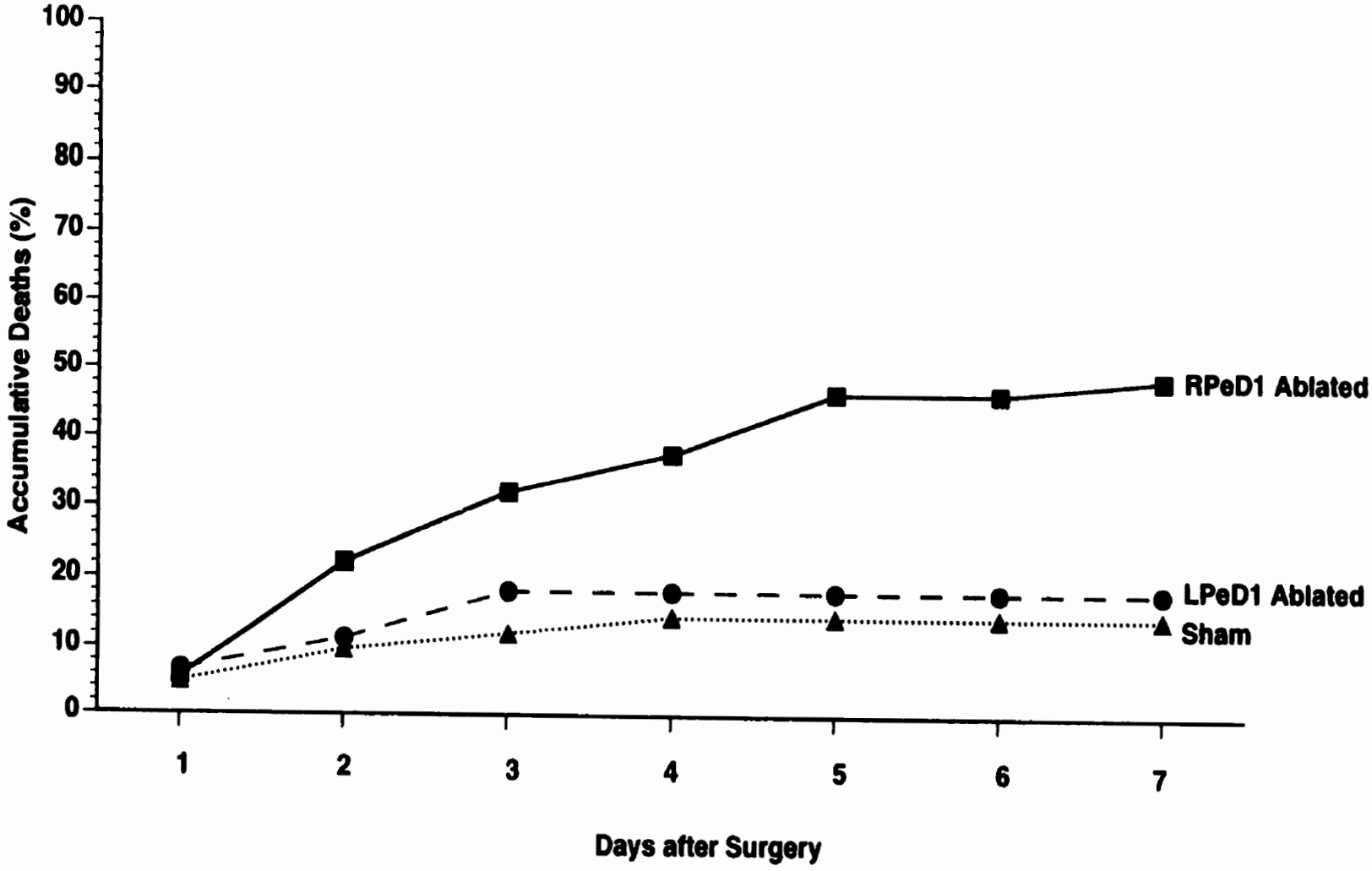
100
90
80
70
60
50
40
30
20
10
0
Accumulative Deaths (%)
1
2
3
4
5
6
7
Days after Surgery
RPeD1 Ablated
LPeD1 Ablated
Sham

Since a number of RPeD1 soma ablated animals did exhibit respiratory movements, the above data are although consistent with the hypothesis that RPeD1 is necessary for normal respiratory output, they are not conclusive. To explore this possibility further, both the soma and its axon were killed via pronase injections. Specifically, the anaesthetized animals were prepared for surgery and pronase was injected directly into RPeD1 soma. Following surgery, the animals were allowed to recover and their respiratory behavior was monitored from days 1 through 3. These data were compared with the control group where LPeD1 was injected with pronase.

I discovered that experimental animals failed to open their pneumostome (n=10). Additionally, these snails were less active (movement was very "sluggish" and they also exhibited contact avoidance behavior). At best, these animals visited the water surface only once during a one hour examination period and remained there for the entire period. At the air-water interface, the animals made very few attempts to open their pneumostome. In contrast, pronase was injected into the LPeD1 soma in control animals. These animals exhibited breathing on days 1 through 3 (n = 4). Taken together, these data provide first direct and unequivocal evidence for RPeD1's involvement in the respiratory behavior of the intact animals.

3.3. DISCUSSION

The giant dopamine cell (RPeD1) is well known for its role in the respiratory rhythmogenesis. In both the isolated ganglionic and *in vitro* cell culture preparations, RPeD1 not only initiates the respiratory activity in neurons IP3I and VD4, but it is also required for the maintenance of breathing rhythm (Syed et al., 1990). The present study is however, the first to test for RPeD1's involvement in the respiratory behavior of the intact animals. Moreover, since RPeD1 soma ablation in the intact snails also resulted in several abnormalities of other behavioral programs (water avoidance and anti-social), the data presented in this study therefore underscore the importance of this cell in many different behaviors.

To test for the involvement of any particular cell in a given behavioral repertoire, an ideal approach is to disrupt its axonal projections towards the effector organs. In this study, I systematically disrupted RPeD1 axons towards pneumostome and mantle areas by cutting and crushing various peripheral nerves that carry its axons. In instances, where internal and external parietal nerves were cut, the animals failed to exhibit normal respiratory behavior and died, suggesting that these nerves are not only required for normal breathing but that they are also vital for animal survival. Since these nerves also carry a large number of afferent and efferent projections from other neurons as well, it can be argued that the resulting effects can not be

attributed exclusively to RPeD1. These data, do at the least, demonstrate that normal respiratory drive is central in origin and that the peripheral nervous system is not sufficient for rhythmical opening and closing movements of the pneumostome.

RPeD1 axotomy at the pleural-parietal connective not only disrupted normal respiratory behavior, but many other behavioral programs were also altered. For instance, most right side crushed animals visited the water surface less frequently than their control counterparts, suggesting that RPeD1 axotomy may have also perturbed the normal chemosensory drive. This notion is consistent with other data from our laboratory where RPeD1 was found to exhibit sensitivity to hypoxia drive which originated at the periphery (Inoue et al., 1996b). Moreover, since RPeD1 axotomized animals did not open and close their pneumostomes as often as the left side crush and sham operated animals, these data demonstrate that RPeD1 may also be involved in the pneumostome opening and closing movements. Indeed, Inoue et al., 1996b have shown earlier that in the absence of IP3I activity, direct intracellular stimulation of RPeD1 can induce pneumostome opening movements. Since RPeD1 has been shown to inhibit the activities of the pneumostome opener motor neurons (VJ etc.) (Syed and Winlow, 1991b), these data suggest that RPeD1 may exert direct control over pneumostome musculature. Further experiments are however required to test this possibility directly.

To rule out the possibility that the experimental animals which exhibited motor abnormalities such as lack of feeding, absence of copulatory behavior, and a reduced drive to come to the water surface had lower metabolic demands and thus reduced O_2 consumption, these snails were challenged with hypoxic stimuli. These stimuli, however, failed to trigger respiratory episodes in the experimental animals suggesting that in the absence of RPeD1 axon, the animals not only failed to exhibit normal respiratory behavior, but also that their chemosensitivity was lost. These data also suggest the possibility that either RPeD1 is the only central chemosensory element for the respiratory drive in *Lymnaea*, or that others as yet unidentified chemoreceptors are also located on the right side. This would perhaps make sense because anatomically these structures are likely to be situated on the same side to that of the pneumostome.

An issue that requires special attention is the fact that the experimental animals (right pleural-parietal crush) were indeed capable of opening their pneumostomes out of water, a reflex shown earlier to be a component of the whole animal withdrawal behavior (Sakharov and S.-Rozsa, 1989). Specifically, during breathing-related pneumostome opening, a noxious stimuli not only induces its closure but also the termination of the respiratory activity (Syed, 1988). In contrast, a similar stimulus applied to the head-foot complex (in the absence of respiratory activity ie. pneumostome closed), induces a forceful opening of the

pneumostome both in *Lymnaea* (Sakharov and S.-Rozsa, 1989) and *Planorbis* (Arshavsky et al., 1994). The behavioral significance of these pneumostome movements was postulated to reduce body volume by expelling both air and hemolymph from the mantle cavity (Inoue et al., 1996b). This provides the animal with space in which to retract its head-foot complex (Sakharov and S.-Rozsa, 1989; Arshavsky et al., 1994b). It is therefore, plausible that the out of water pneumostome movements may reflect withdrawal behavior, for which the local peripheral nerve system (the osphradium ganglia situated near the pneumostome) should be sufficient. Consistent with this idea is the observation in which noxious stimuli applied to the pneumostome area (in the absence of CNS) can trigger its opening movements (Syed personal communications). Moreover, in *Helix* and *Planorbis*, a common motor neuronal pool has been implicated in both pneumostome opening movements and the whole body withdrawal behavior (Balaban, 1983; Vehovszky et al., 1989). In *Lymnaea*, however, Syed and Winlow (1991a) and Inoue et al., (1996a, c) have shown that both pneumostome and whole body withdrawal behaviors are controlled by a distinct group of motor neurons. However, at present the possibility of potential functional overlap between these motor neurons can not be ruled out.

Statocysts, located on the dorsal surface of both left and right pedal ganglia are sensory structures that are involved in geotaxis. They are thought to provide important orientation cues to the animal with

respect to its position in the water. Since most experimental animals failed to stop at the water interface and crawled out of the water, it is therefore, plausible that these effects may have been due to the disruption of statocyst function. Should this be the case however, then one would have expected the sham animals to exhibit a similar behavior; a scenario that was not observed in the present study. These data therefore, demonstrate that either RPeD1 itself or its association with the statocyst is critical for proper upward orientation of the pneumostome at the water interface.

A similar water avoidance behavior was observed by (Lukowiak et al., 1996) during operant conditioning of the respiratory behavior in *Lymnaea*. Specifically, a noxious stimulus delivered to the pneumostome area during its opening movements resulted in the operant conditioning of the respiratory behavior. As compared with their yoked counterparts, however, the operantly conditioned snails often crawled out of the water (Lukowiak et al., 1996). These data suggested that the animals established an association between hypoxia and water and thus to avoid this "unfavorable environment", they preferred to crawl out of the water. Alternatively, the animal may have associated the noxious stimulus with its presence in the water and thus to avoid this situation, it crawled out of the tank. Since in the present study, no noxious stimulus was delivered to the pneumostome, it therefore seems plausible that hypoxia may have served as a signal that drove the animal out of water. On the

other hand, since in both operantly conditioned (Spencer et al., 1999) and the experimental animals (Figure 5.8A) RPeD1 was found to be quiescent, it seems safe to attribute this behavior directly to the lack of RPeD1 function.

In addition to the above abnormal behavior, neither did the experimental animals feed very well, nor were they "socially active". It is tempting to attribute these "abnormalities" to the lack of RPeD1 function, however further experiments are required to determine the significance of this cell in these behaviors. These data do nevertheless, demonstrate that RPeD1 may be a multifunctional neuron whose role/s extend beyond that of respiration. Additionally, since RPeD1 ablation perturbed the normal respiratory behavior in many important ways, the data presented in this study provide strong support for the hypothesis that this cell is indeed necessary for respiratory behavior in *Lymnaea*. Moreover, this study is the first to test for the functional significance of an identified neuron in a behavioral program, and it validates further the usefulness of *Lymnaea* as a model system for studies on the respiratory rhythmogenesis.

Together with previously published studies, the data presented here show that RPeD1 indeed fulfils the criteria of a command neuron. Specifically, its appropriateness and sufficiency for the respiratory behavior has previously been demonstrated (Syed et al., 1990; Syed and Winlow, 1991b), whereas in this study, I showed that RPeD1 is indeed

necessary for respiration in the intact animals. To the best of my knowledge, RPeD1 is perhaps the only neuron to have successfully met the criteria that was set forth for a command neuron (Kupfermann and Weiss, 1978). In addition, since RPeD1 soma ablation also disrupted a number of other behaviors, it would not be surprising to find that RPeD1 is also a member of a larger "polymorphic" network that serves to regulate many different behaviors. Future studies should therefore be directed towards elucidating RPeD1's role in other behaviors as well.

Similarly, efforts should also be directed towards elucidating RPeD1's role in chemoreception. Together with preliminary data from our lab, this future research will give rise to the concept that in addition to their role in respiratory rhythm generation, the CPG neurons also exhibit chemosensitivity to hypoxia, hypercapnia, and pH changes. These studies will be consistent with those performed earlier on the land snail *Helix aspersa* where CO_2 sensitive neurons located within the CNS have been demonstrated experimentally (Erlichman and Leiter, 1993; Erlichman and Leiter, 1994; Erlichman et al., 1994). Moreover, since identified *Lymnaea* neurons can be isolated in cell culture, the cellular and molecular mechanisms underlying chemoreception can also be examined.

CHAPTER FOUR: RPeD1 SOMA ABLATION PERTURBS THE RESPIRATORY RHYTHMOGENESIS

4.1 INTRODUCTION

4.1.1. Central pattern generators

Networks of neurons, termed central pattern generators (CPG) control rhythmic behaviors such as respiration. Evidence supports the idea that CPGs are capable of generating rhythmic output, independent of peripheral feedback. However, peripheral input is important for the initiation, maintenance, modification, and termination of most rhythmic behaviors (Delcomyn, 1980). Therefore, to determine the neuronal basis of rhythmic behaviors, the identification of various CPG neurons and characterization of their synaptic interactions is considered essential.

4.1.2. Neural network mediating respiration in *Lymnaea*

The neural network underlying pulmonary ventilation in *Lymnaea stagnalis* is comprised of RPeD1, VD4 and IP3I (Figure 4.1). The synaptic connections between VD4 and IP3I are reciprocally inhibitory (Syed and Winlow, 1991b). Similar inhibitory synapses also exist between RPeD1 and VD4. RPeD1 excites IP3I biphasically (excitation followed by inhibition). Once activated, IP3I exerts excitatory effects on RPeD1. All of these synaptic connections are chemical and monosynaptic. RPeD1 stimulation in a semi-intact preparation, triggers respiratory activity in

Figure 4.1. A summary diagram depicting the neural network underlying respiratory behaviour in *Lymnaea*. RPeD1 receives chemosensory/mechanosensory input from the periphery and excites IP3I via a dual inhibitory-excitatory synaptic connection. Once activated, IP3I excites RPeD1 and the pneumostome opener motor neurons (eg. HIJK, and G). Following recovery from its inhibition by IP3I and RPeD1, VD4 fires a burst of spikes inhibiting IP3I and RPeD1, while exciting pneumostome opener motor neurons (POM). The cycle repeats several times. Open and close symbols represent excitation and inhibition respectively. All synaptic connections are monosynaptic and chemical.

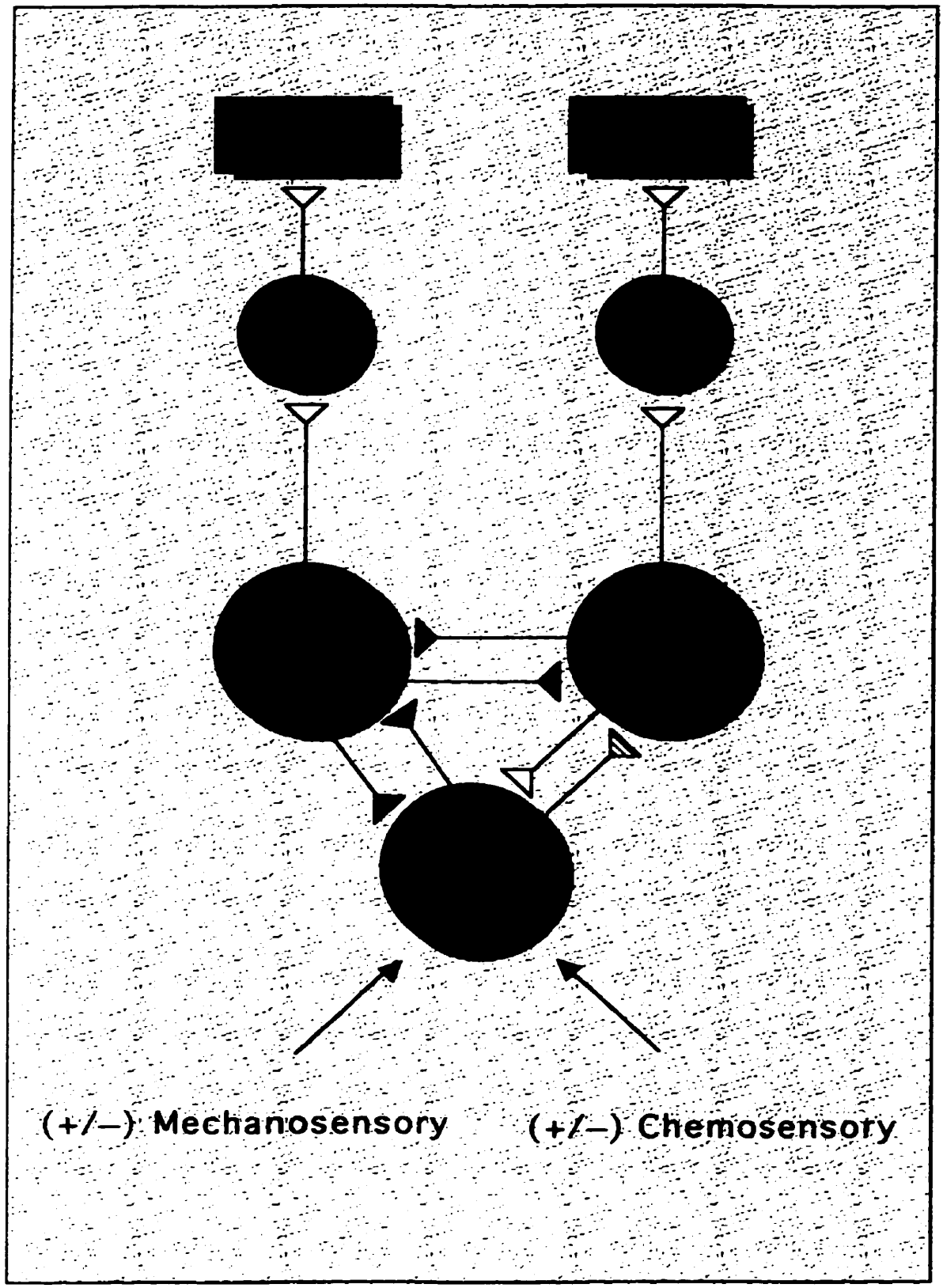
(+/–) Mechanosensory
(+/–) Chemosensory

both IP3I and VD4. In an isolated ganglionic preparation, spontaneously occurring respiratory discharges can be recorded from the motor neurons for many hours; whereas in a quiescent preparation RPeD1 can trigger this activity (Syed and Winlow, 1991b). Since IP3I is located on the ventral side of the right parietal ganglion (opposite to that of RPeD1 and VD4), the evidence for its activity is generally obtained indirectly from its target motor neurons (G and H,I,J,K cells). These cells exhibit excitatory and inhibitory discharges that are well-characterized and unique to IP3I activity (Winlow and Benjamin, 1981).

Dr. Syed's lab has experimentally demonstrated both *in vivo* and *in vitro* that the *Lymnaea* respiratory central pattern generator assures coordination of the antagonistic muscles but is not inherently rhythmic. Either alone or together, both IP3I and VD4, which are conditional bursters, do not produce rhythmical alternating oscillations. Rhythmicity requires activity in RPeD1, which allows emergent network properties to be expressed. Overall, a picture emerges that is analogous to respiratory rhythm generation in mammals, i.e., rhythmic motor output originates in two half centers which are connected via mutual inhibitory synapse. The two half centers (VD4 and IP3I) oscillate only when they receive input from a hypoxia driven RPeD1.

The CPG neurons are capable of generating the respiratory rhythm both in the semi-intact and the isolated brain preparations, but whether this simple circuit provides the necessary neural substrate for respiratory rhythmogenesis in the intact animal can only be demonstrated *in vitro*. In

1990. Syed et al., successfully reconstructed the three-cell network (RPeD1, IP3I and VD4) *in vitro*. In cell culture, these cells not only regenerated their axonal projections, but they also reformed appropriate synaptic connections when electrically stimulated. This *in vitro* reconstructed network generated the respiratory rhythm was indistinguishable from that seen *in vivo* (Syed et al., 1990).

4.1.3. Synaptic inputs to and from RPeD1

RPeD1 makes monosynaptic connections with a large number of postsynaptic follower cells (localized in the visceral and parietal ganglia) (Figure 4.1). RPeD1 is known to contain and release dopamine and its transmission with the follower cells is dopaminergic (Benjamin et al., 1981). RPeD1 is spontaneously active in semi-intact and isolated brain preparations and this regular beating activity is augmented by synaptic inputs from IP3I, which strongly excite RPeD1 (Syed and Winlow, 1991a, b). IP3I is the only excitatory input that RPeD1 is known to receive in the isolated brain preparations. In contrast, RPeD1 receives a number of inhibitory inputs from sources such as Input 2 (IP2 – source unknown), VD4 (Syed and Winlow, 1991b) and the whole body interneurons left and right pedal dorsal 11 (L/RPeD11) (Inoue et al., 1996a).

4.2. RESULTS

In chapter three, I have demonstrated that RPeD1 soma ablation in some animals in the intact animal disrupts normal respiratory

behavior. In this section, I sought to determine whether the isolated central ring ganglia from the experimental animals were able to generate respiratory rhythm in the absence of RPeD1's soma.

4.2.1. Respiratory patterned activity in RPeD1 soma ablated animals

To determine whether experimental (RPeD1 soma ablated) animals would exhibit normal respiratory rhythm (reflected by the presence of IP3I activity) in the absence of RPeD1's soma, the central ring ganglia from experimental groups and both sham and control (LPeD1 ablated) animals were isolated on day three and day seven, and prepared for intracellular recordings. Specifically, after behavioral analysis, all animals groups were anaesthetized and their CNS removed. Simultaneous intracellular recordings were made from the following neurons: pneumostome motor neurons (H, I, J, K cell cluster neurons) and RPA neurons (mantle motor neurons) in experimental animals; from RPeD1 and H, I, J, K/RPA neurons in control animals; or from RPeD1 and H, I, J, K/RPA/G neurons in sham animals. All three animal types displayed IP3I activity (Figure 4.2). The number of IP3I discharges observed in experimental animals (24.3 ± 3.4; n =14) were not significantly different ($p > 0.05$) than sham (29.6 ± 4.0; n = 11) or control animals (28.1 ± 5.5; n = 6) on day three (or on day seven). These findings were not in agreement with the hypothesis, which predicted that in experimental animals no rhythmic discharges could be discernable, whereas both control and sham animals should exhibit normal respiratory activity.

Figure 4.2. Selective removal of RPeD1's soma did not significantly alter the number of IP3I bursts in the isolated ganglia. The number of IP3I bursts exhibited by RPeD1 ablated animals were compared to LPeD1 ablated and sham operated animals over a 20 minute period. Characteristic IP3I discharges were monitored in H,I,J,K, and/or RPA group neurons by direct intracellular recordings. No significant differences were found between experimental and control groups on either day 3 or day 7 ($p < 0.05$, t-test). (experimental, n = 14; control, n = 11; sham, n = 6)

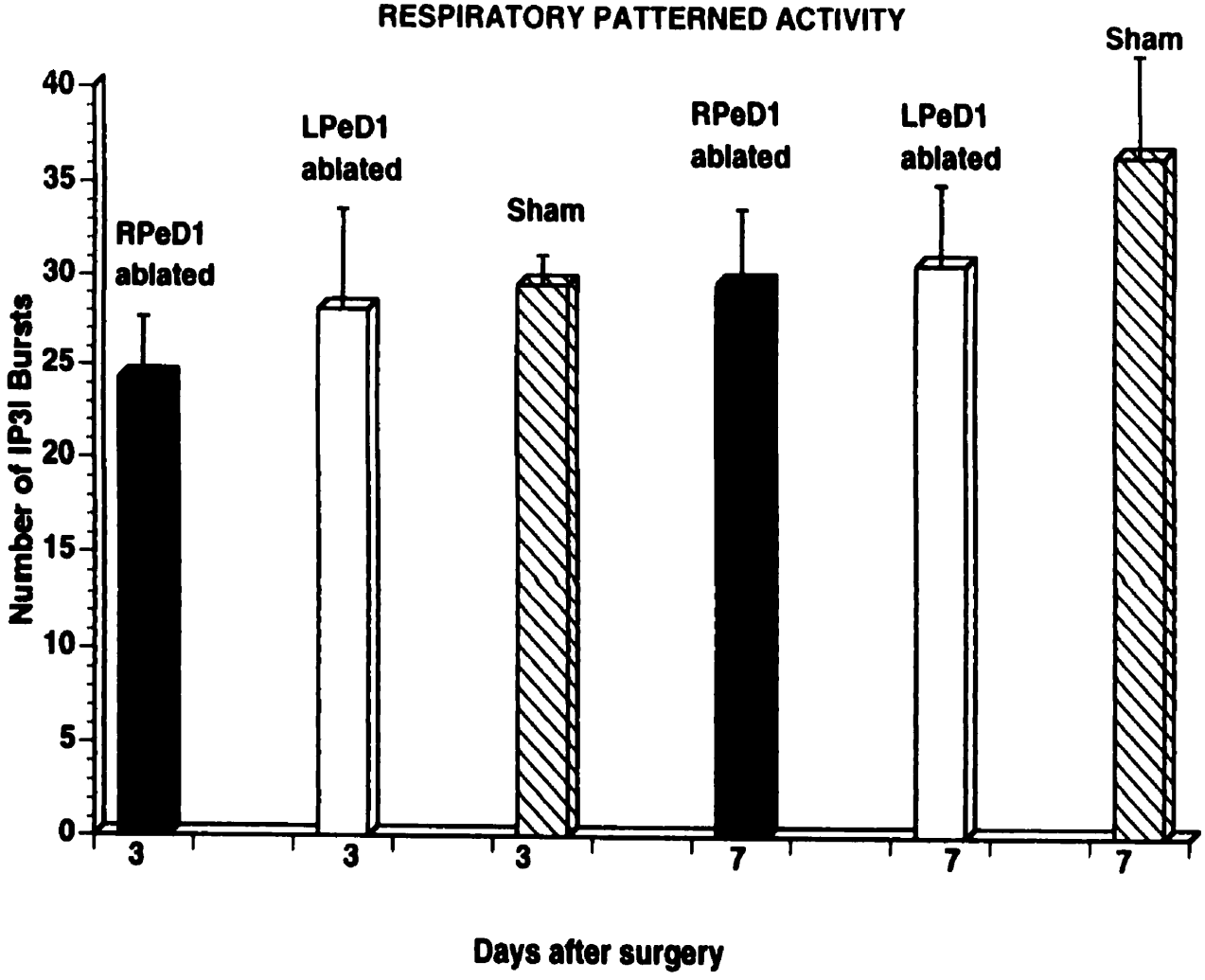
RESPIRATORY PATTERNED ACTIVITY
Number of IP3I Bursts
40
35
30
25
20
15
10
5
0
RPeD1 ablated
LPeD1 ablated
Sham
RPeD1 ablated
LPeD1 ablated
Sham
3
3
3
7
7
7
Days after surgery

4.2.2. Spontaneous respiratory discharges in RPeD1 soma ablated ganglia were abolished by a dopamine antagonist

Since in a variety of animal species, severed axons remain functional in the absence of their somata, we hypothesized that the respiratory activity recorded from RPeD1 soma ablated animals may have still involved dopamine release from the axotomized axon. Therefore, I predicted that the spontaneously occurring IP3I discharges in RPeD1 soma ablated animals would be blocked by a dopamine antagonist. To test this possibility, sulpiride (10^{-4}M) was bath applied. Specifically, simultaneous intracellular recordings were made from two follower cells in the RPeD1 soma ablated preparations and spontaneously occurring IP3I discharges were recorded on day three. Sulpiride was then bath applied during continuous recordings. I found that sulpiride application completely and reversibly blocked IP3I discharges in all of the follower cells (n = 8) (Figure 4.3). Furthermore, IP3I activity could be triggered by exogenously applied dopamine 10^{-5}M (data not shown) . Similarly, on day seven, IP3I activity continued to persist in both animal groups (Figure 4.4). This was also blocked by sulpiride in a reversible manner (n = 8) (data not shown). Together with behavioral observations, these results indicate that selective ablation of the RPeD1 somata may have although removed its cell body from the central ring ganglia, however the axon was most likely functional.

Figure 4.3. IP3I activity in RPeD1 soma ablated animals was abolished by a dopamine antagonist. Spontaneously occurring IP3I discharges were recorded from H,I,J,K cells (top panel – control). These were abolished completely when dopamine antagonist sulpiride (10^{-4}) was applied exogenously (middle panel). The IP3I activity however resumed upon wash out with normal saline (lower panel).

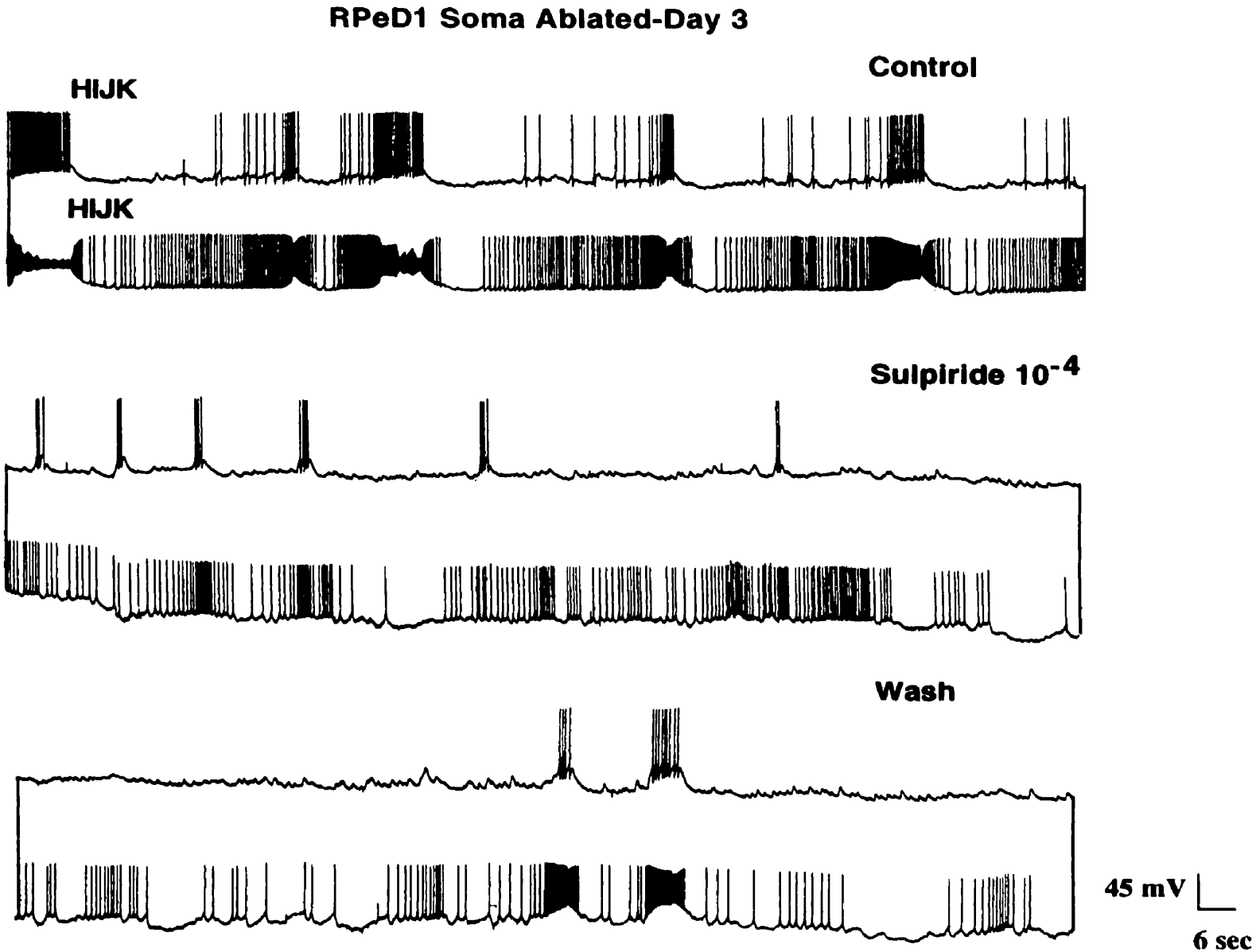
RPeD1 Soma Ablated-Day 3
Control
HIJK
HIJK
Sulpiride 10^{-4}
Wash
45 mV
6 sec

Figure 4.4. The isolated ring ganglia from both RPeD1 and LPeD1 soma ablated animals exhibited spontaneously occurring IP3I discharges on day 7. Simultaneous intracellular recordings were made from the isolated ganglia of either RPeD1 (experimental) or LPeD1 (control) soma ablated animals. IP3I discharges were recorded from the H,I,J,K cells in both LPeD1 and RPeD1 ablated animals.

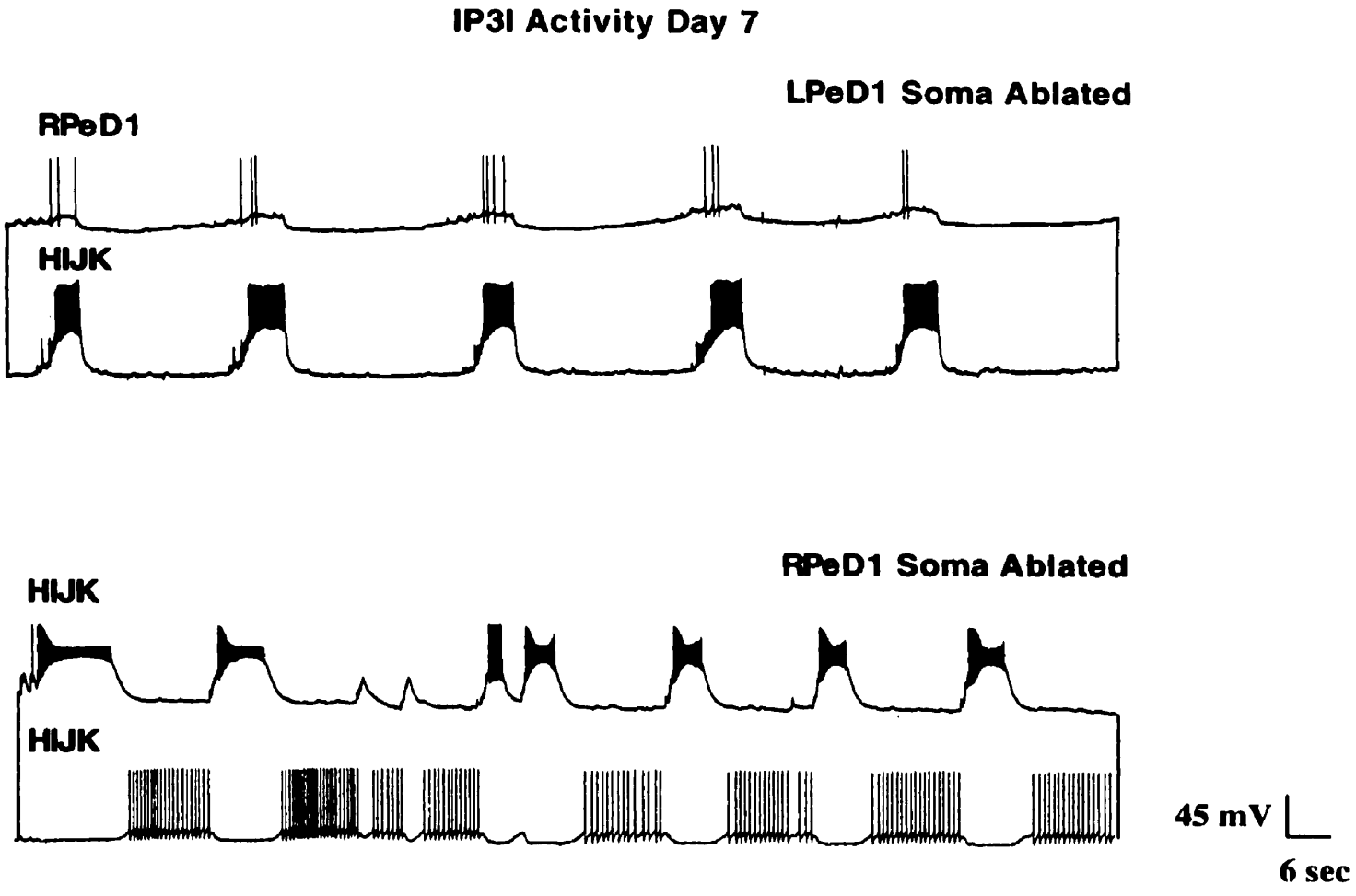
IP3I Activity Day 7
LPeD1 Soma Ablated
RPeD1
HIJK
RPeD1 Soma Ablated
HIJK
HIJK
45 mV
6 sec

4.2.3. Pronase injected preparations did not exhibit normal respiratory rhythm

To test further whether spontaneous IP3I activity seen in the RPeD1 soma ablated animals was indeed due to dopamine release from the RPeD1 axon, pronase was injected intracellularly into RPeD1's soma. Animals, which had been injected with pronase, failed to exhibit breathing on days one through three. Intracellular recordings were made from the isolated central ring ganglia of these animals, two days after the surgery. In eight out of the ten animals, no discharges indicative of IP3I activity were observed (Figure 4.5). However, in two preparations IP3I activity was observed, but this may have resulted from the unsuccessful attempts to inject pronase. In contrast, pronase injection into LPeD1 (control), did not disrupt IP3I activity (data not shown) (n = 4). Overall, pronase injection into RPeD1 eliminated IP3I activity. These data set are consistent with the hypothesis that in the absence of RPeD1 somata, the RPeD1 axon continues to function.

Figure 4.5. IP3I activity was completely abolished following pronase injection into RPeD1. Pronase (5%) was injected intracellularly into RPeD1 somata in the intact animal. Animals were allowed to recover from surgery and their behaviour was monitored. On day 2, intracellular recordings were made from the isolated ganglia of pronase (into RPeD1) injected animals. No IP3I discharges were observed.

Effects of Pronase Injection into RPeD1

Day 2

4.3. DISCUSSION

In the previous chapter, I showed that RPeD1 soma ablation in the intact animal disrupts normal respiratory behavior in some animals. From these results therefore, I predicted that the central ring ganglia isolated from these animals would not exhibit patterned respiratory activity. Contrary to this assumption however, it was surprising to see that the isolated central ring ganglia from RPeD1 soma ablated animals exhibited IP3I discharges that were characteristic of patterned respiratory activity observed in ganglionic preparations (Syed and Winlow, 1991a).

One possible interpretation for the above data is that although RPeD1's soma was selectively ablated in the intact animals, its axon may have remained functional to generate patterned respiratory activity. This notion is consistent with numerous other studies on invertebrates (flatworms, crustaceans, insects, annelids, and gastropods - see Bittner, 1988) where distal portions of severed axons not only remain alive, but also re-grow their axonal projections and synaptic connections. For instance, in both crustaceans (Hoy et al., 1967) and *Aplysia* (Ross et al., 1994), the distal axon stump has been shown to survive and conduct action potentials from weeks to months. If the severed portion of the distal axon is long enough (severed close to the cell body), it also generates action potentials which produce successful muscle contractions for up to one year (Atwood et al, 1989). The survival of the

crustacean axon stump is supported by glia and/or glia-derived factors (Viancour et al., 1988). Similarly, in *Aplysia* the severed axon utilizes pre-existing factors for their survival (Benbassat and Spira, 1993). Since in *Lymnaea*, most trophic factors are derived from the central ring ganglia (Ridgway et al., 1993), it is therefore highly likely that they may have contributed towards the survival of RPeD1 axon in the nervous system. Whether the severed RPeD1 axon also exhibits collateral sprouting remains to be determined.

The survival of severed axons may serve many advantages (Moffet, 1996). For instance, distal axon stumps are capable of neurotransmitter release and can continue to contribute towards synaptic transmission required for normal functioning of various neuronal circuits (Grossfeld, 1994). In addition, the axotomized distal axon stump from crayfish has been shown to release a protein (similar to a mammalian stress protein) which serves to attract non-neuronal cells at the site of axon crush (Xue and Grossfeld, 1993). These cells in turn help to repair the damaged tissue and accelerate the healing process. The ability to survive injury may be an inherent property of all axon stumps. This may serve to provide the nervous system with temporary relief during which the somata can regenerate to restore functional deficit. Indeed, the isolated axonal stumps from *Lymnaea* are capable of *de novo* protein synthesis (van Minnen et al., 1997) and can thus synthesize all necessary proteins

that are required for survival, synaptic function and plasticity (Spencer et al., 1999 manuscript submitted).

The support for the hypothesis that the RPeD1 axon was indeed alive and functional, stems from the data showing that the spontaneously occurring IP3I discharges were abolished by the dopamine antagonist sulpride. It can be argued, that in addition to RPeD1, other as yet unidentified neurons, may also be responsible for the patterned respiratory activity that was observed in RPeD1 soma ablated animals. This is highly unlikely, since dopaminergic neurons other than RPeD1, have not yet been identified in *Lymnaea*. Consistent with this notion is the pronase injection data (which in most preparations not only killed the RPeD1 soma but also its axon stump), in which no patterned respiratory activity was recorded in the isolated ganglia. Taken together, these data provide strong support for the hypothesis that the RPeD1 axon was indeed alive and functional.

If the conclusions drawn from the above data are acceptable, then the question arises: Why did RPeD1 soma ablated animals exhibit reduced respiratory movements? In other words, if the central ring ganglia from RPeD1 soma ablated animals were indeed capable of generating the patterned respiratory activity; why did these animals failed to exhibit normal respiratory behavior? Two possibilities are likely: 1) since RPeD1 is involved in O_2 perception, in its absence therefore, the animals were rendered incapable of chemosensitivity. If this explanation

were acceptable, then one would predict that in the semi-intact preparations made from RPeD1 ablated animals, the IP3I discharges would not be discernable. 2) The periphery may exert an inhibitory effect on the rhythm generating circuit in an intact animal. This notion is consistent with observations in the semi-intact preparation, in which the respiratory discharges in the CPG neurons are triggered immediately after the severance of peripheral projections to the pneumostome area (Spencer and Kazmi personal communications). Further experiments are however, required to test the above possibilities directly. Peripheral feedback has been shown to be an important stabilizer/modulator of rhythmic behaviors (Delcomyn, 1980). The periphery may effect motor neurons directly without altering the effects of the CPG rhythm or motor neuron activity (Delcomyn, 1980). Peripheral feedback has although been shown to drive and terminate behaviors, it is not however considered essential for normal behavioral output (eg. continuous swimming by deafferented dogfish sharks) (Lissmann, 1946). Furthermore, timing of rhythmic behavior may be driven or changed via peripheral input (eg. swimming rhythm of dogfish sharks) (Grillner and Wallen, 1977). Therefore, peripheral input together with the characteristics of the neural network mediating a certain behavior shapes the final motor output. Thus, the inhibitory effects of the periphery may explain why the intact animal exhibits significantly reduced breathing in the absence of the

RPeD1 soma, while the isolated brain preparation exhibits IP3I activity similar to that of control.

RPeD1 has previously been shown to inhibit IP3I activity. It is only after a strong depolarization of RPeD1 that a biphasic (excitation followed by inhibition) response is generated in IP3I (Syed and Winlow, 1991b). Syed (1988) has previously shown that RPeD1 stimulation does indeed terminate IP3I activity in the middle of its discharge. Moreover, in instances where RPeD1 was found to be spontaneously hyperactive, IP3I discharges were rare (Syed, 1988). Taken together, these previously published observations suggest that a tonically active RPeD1 continues to inhibit the activity of IP3I. It is only when the pneumostome breaks through the water film that RPeD1 (excited by the mechanosensory input) fires a burst of spikes, which in turn trigger a biphasic response in IP3I. Based on these observations, I speculate that the IP3I discharges seen in RPeD1 soma ablated ganglia can also be attributed to the lack of RPeD1 activity. How does this interpretation then fit with the sulpiride data? One likely explanation for this is that the dopamine receptor antagonist may also serve as an agonist (Spencer personal communication), thus mimicking the inhibitory effects of dopamine on the IP3I activity. Consistent with this notion are data from a number of vertebrate and invertebrate species where a variety of transmitter receptor antagonists have been shown to function as partial agonists as well (Cooper et al.,1978).

It is important to note that although RPeD1 soma ablated animals did exhibit normal respiratory rhythm, these rhythmical discharges did not translate into behavioral output. Caution should therefore be exercised in extrapolating patterned activity recorded in the CNS to behavioral output.

Taken together, the data presented in this section show that: 1) the rhythm generation and pattern generation are two distinct features of the CPG neurons, 2) after axotomy, the RPeD1 axon remains alive and functional for many days and 3) in the intact (RPeD1 soma ablated) animals, the periphery exerts an inhibitory effect on the respiratory rhythm generating network.

CHAPTER FIVE: NORMAL RESPIRATORY BEHAVIOR IS RESTORED AFTER RPeD1 REGENERATION

5.1. INTRODUCTION

Following injury to the nervous system, both neuronal and non-neuronal cells undergo development-like changes, which are essential for successful regeneration. In general, regeneration implies that all axonal/dendritic and synaptic connections are reestablished to restore the behavioral deficit. However, rarely is this process so simple because the regenerating tissue is often faced with many environmental obstacles, such as growth inhibitory molecules (Fitch et al., 1997). In addition, the growth permissive molecules (cell and substrate adhesion molecules, trophic factors etc.) (Xu et al. 1995; Bregman et al., 1997; Tuszynski et al., 1997; Ye et al., 1997) that are expressed during development are no longer available to regenerating neurons. Due primarily to these limitations, the regeneration and full functional recovery in higher animals is rather rare (Bregman, 1998). Most invertebrate neurons on the other hand, have a remarkable propensity to regenerate their axonal and synaptic projections with a high degree of accuracy (Moffet, 1996). For instance, a variety of invertebrate phyla (Cnidaria, Platyhelminthes, Ctenophora, Nemertea, Annelida, Arthropoda, Mollusca, Echinodermata and Chordata) have not only been show to regenerate but also to replace larger parts of their nervous system (see Moffet, 1996). Most pertinent in this context are the

regenerative capabilities of gastropod mollusks, these are therefore discussed below in some detail.

Neurons from a variety of molluscan species (*Helisoma*, *Aplysia*, *Lymnaea* etc.) have been shown to regrow their axonal projections both *in vivo*, organ culture and *in vitro* (Moffet, 1995, 1996). In *Lymnaea*, RPeD1 has previously been shown to regenerate its axonal projections and synaptic connections *in vivo* (Allison and Benjamin 1985; Benjamin and Allison, 1985), *in situ* (organ culture) and *in vitro* (Syed et al., 1990). Specifically, Benjamin and Allison (1985) showed that following axotomy, RPeD1 not only regenerated its neurites *in vivo* but also established appropriate synaptic connections with its follower cells. These synapses were in most instances similar to those seen in the normal animals. However, neither the functional consequences of RPeD1 axotomy examined, nor was the significance of this regeneration investigated. One of the main objectives of this study, therefore, was to determine if: 1) RPeD1 regenerates its axonal projections in the intact animal and 2) if this regeneration results in the restoration of normal respiratory behavior.

5.2. RESULTS.

5.2.1. RPeD1 regeneration restored the normal respiratory behavior in the intact animals

As described in chapter three, RPeD1 was axotomized between right pedal and pleural ganglia and following recovery, the respiratory behavior was monitored. Between day ten (2.9 ± 0.8) and day fourteen (2.8 ± 0.7), a significantly greater number of axotomized animals began exhibiting normal respiratory movements (Figure 5.1A, B). Qualitative differences were however observed between right (experimental) and left side crushes (control) or sham animals. Right side crush animals did not breathe as frequently as their control groups. Additionally, both the duration and the size of pneumostome openings in the experimental animals on day seven were significantly reduced compared with both control groups. In most experimental animals, the duration of pneumostome openings on days 10-14 was no longer than three seconds; whereas, in both sham and control animals the pneumostome remained opened for greater than three seconds. Together, these data show that between days 10-14 the experimental animals began to exhibit respiratory movements, characteristic of the control group.

5.2.2. Respiratory patterned activity in right pleural-parietal crushed animals was absent three days after surgery

Electrophysiological techniques coupled with the behavioral analysis were used to determine whether the behavioral restoration involved RPeD1 regeneration. Specifically, simultaneous intracellular recordings were made to determine whether regeneration and subsequent behavioral recovery were due to RPeD1 reconnecting with its target cells

Figure 5.1A. Normal respiratory behaviour was restored in right pleural-parietal crushed animals after 10 days post surgery. Connectives between the right pleural and parietal ganglia were crushed and the respiratory behaviour was monitored over a period of 2 weeks. Breathing behaviour exhibited by experimental animals on days 1, 5, and 7, was statistically significant from days 10 and 14 ($p < 0.01$ on days 1, 5, and $p < 0.05$ on day 7, t-test); but not significantly different among days 1, 5, and 7 or between days 10 and 14. (experimental, n = 19 for all days)

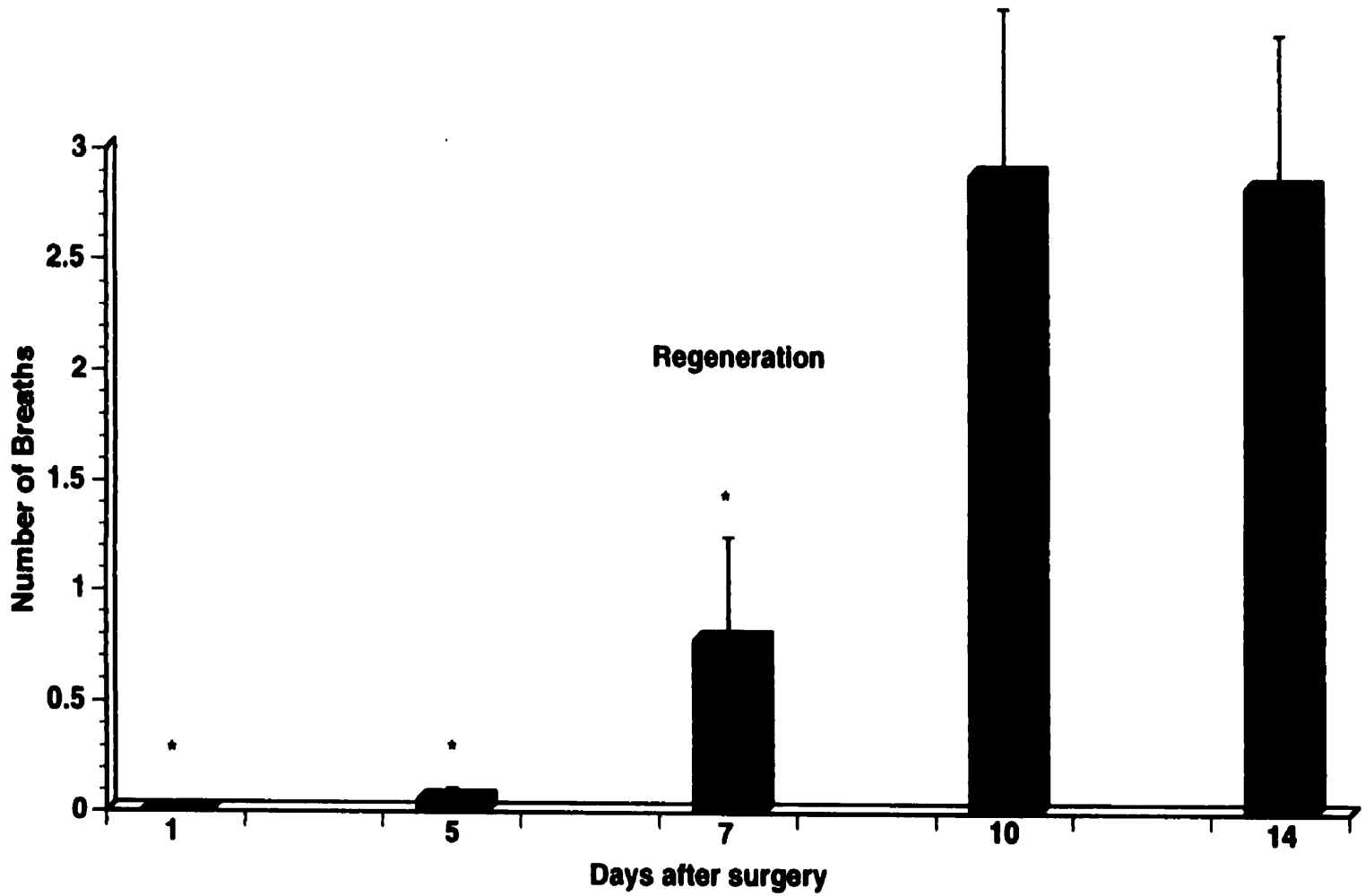
Number of Breaths
3
2.5
2
1.5
1
0.5
0
Regeneration
*
*
1
5
7
10
14
Days after surgery

Figure 5.1B. Percent of animals that exhibited breathing following a right pleural-parietal connective crush. The percent of animals that breathed on days 10 and 14 were significantly greater than on days 5 and 7. (Fisher's exact test, $p < 0.0001$) (experimental, $n = 19$ for all days)

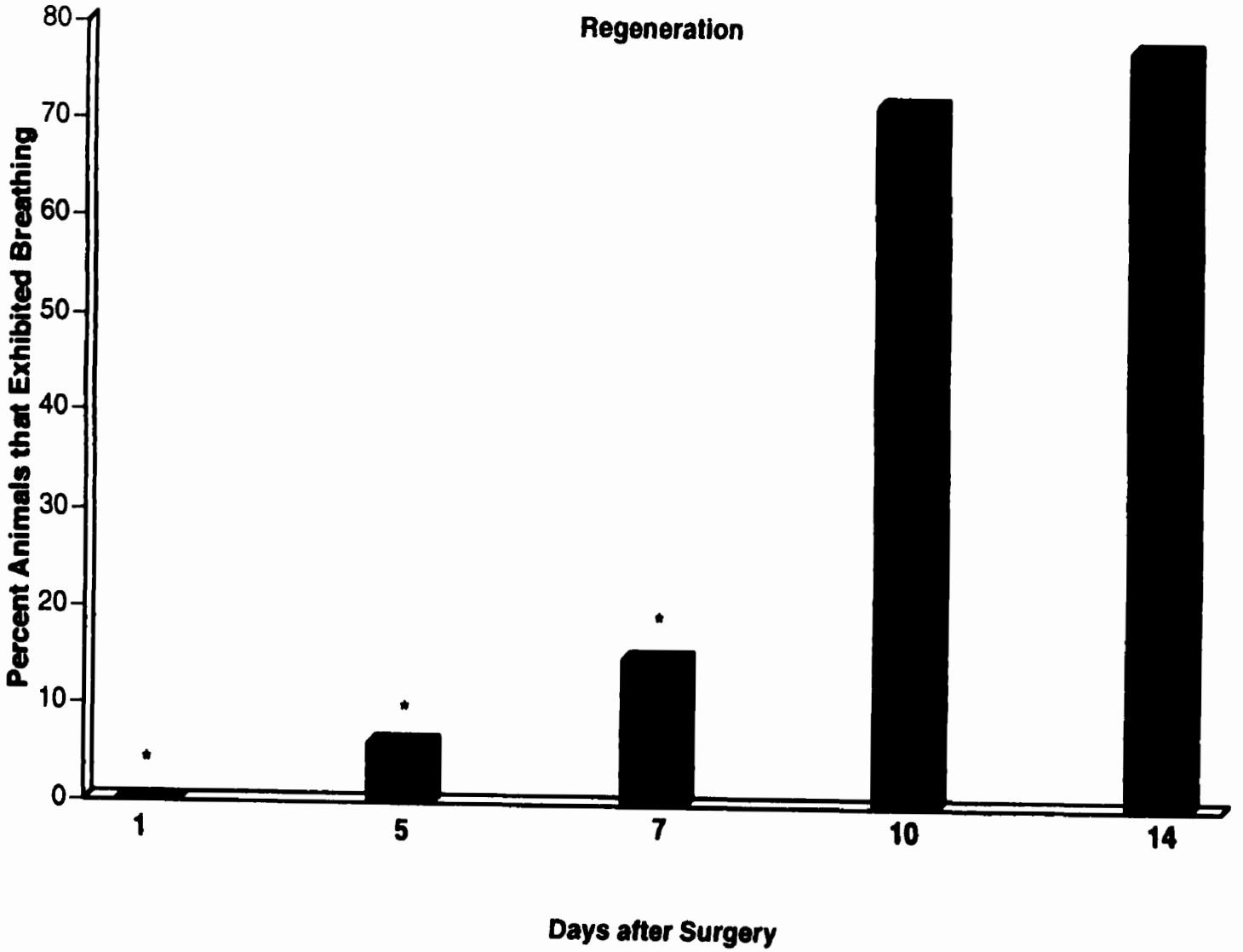
Regeneration
Percent Animals that Exhibited Breathing
80
70
60
50
40
30
20
10
0
1
5
7
10
14
Days after Surgery

within the CNS and/ or peripheral projections. Simultaneous recordings were made from RPeD1, H, I, J, K, RPA, or G neurons. Three days after surgery, control animals exhibited IP3I activity (n = 14) (Figure 5.2). In contrast, IP3I activity was absent in most right side crush animals (n = 16) (Figure 5.3). This provided strong evidence that RPeD1 axotomy did indeed disrupt synaptic interaction with its follower cells. The absence of IP3I activity on day 3 indicated that the regenerated processes from RPeD1 may not have reached the follower cells.

5.2.3. Respiratory patterned activity in right pleural-parietal crushed animals returned on day seven

Qualitative and quantitative differences were observed in the patterned respiratory activity between experimental, control, and regenerated animals. On day three, either prior to behavioral recovery or the return of respiratory rhythmogenesis, experimental animals displayed significantly lower number of IP3I discharges (4.6 ± 3.1; n = 16) ($p < 0.01$) than sham (29.5 ± 1.6; n = 6), control (19.3 ± 3.8; n = 14) or regenerated animals (21.7 ± 4.3) (Figure 5.4). By day seven however, even though most experimental animals failed to open their pneumostome, IP3I activity was restored (Figure 5.5). IP3I activity exhibited by these experimental animals on day seven (21.8 ± 5.0) was not statistically different than control (27 ± 6.0), sham (36.5 ± 5.4), or regenerated animals (21.7 ± 4.3; n = 12) (Figure 5.5).

Figure 5.2. Left side crushes did not disrupt IP3I discharge activity in the isolated brain preparation. Simultaneous intracellular recordings were made from RPeD1 and H,I,J,K cells in left side crushed animals. Spontaneous IP3I discharges were recorded in both instances.

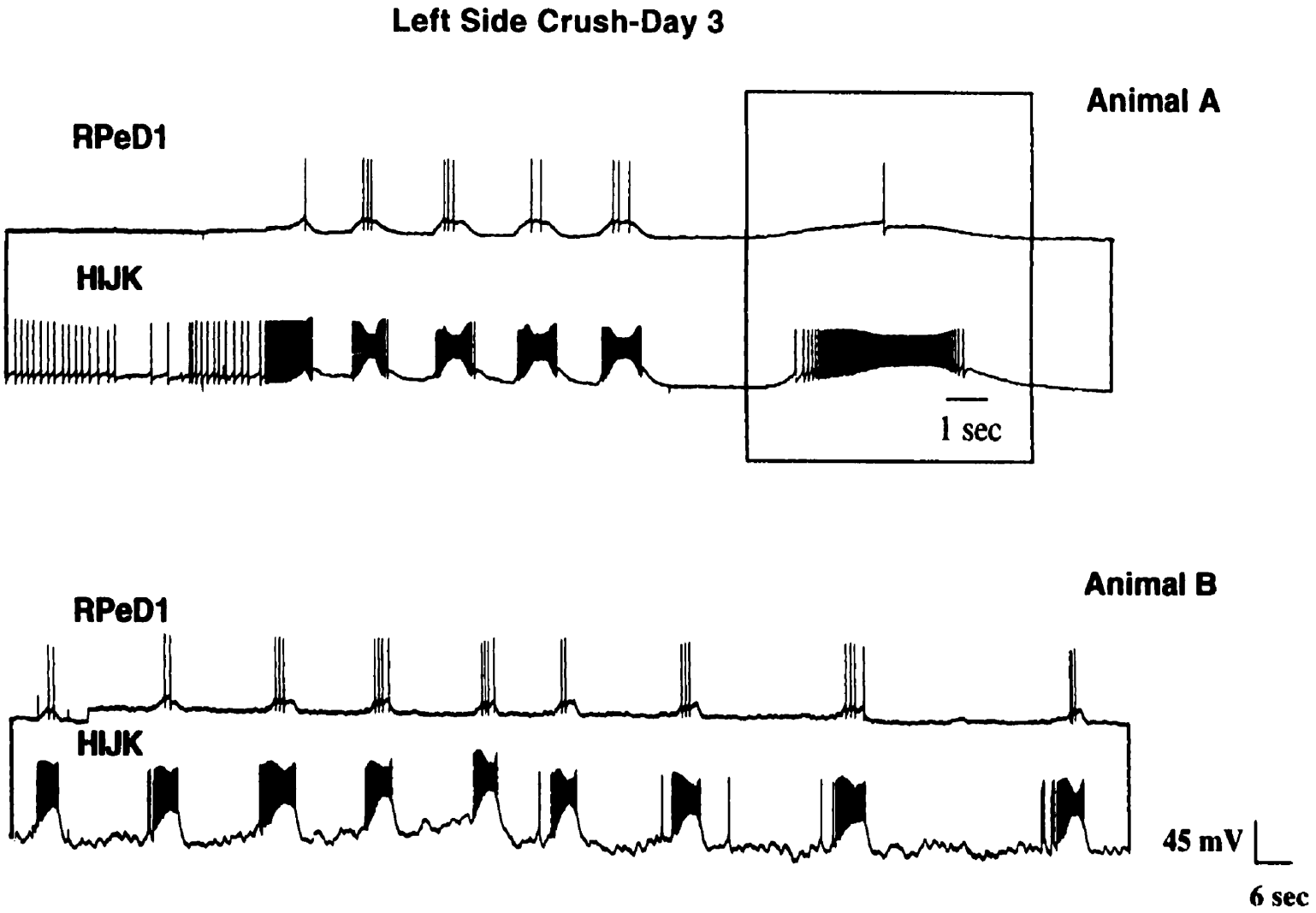
Left Side Crush-Day 3
Animal A
RPeD1
HIJK
1 sec
Animal B
RPeD1
HIJK
45 mV
6 sec

Figure 5.3. Right side crush animals did not exhibit IP3I discharges on day 3 post surgery. Simultaneous intracellular recordings from RPeD1 (top) and a H,I,J,K cell (bottom) in animal A; or from H,I,J,K cells in animal B were made. No IP3I discharges were recorded in either animal.

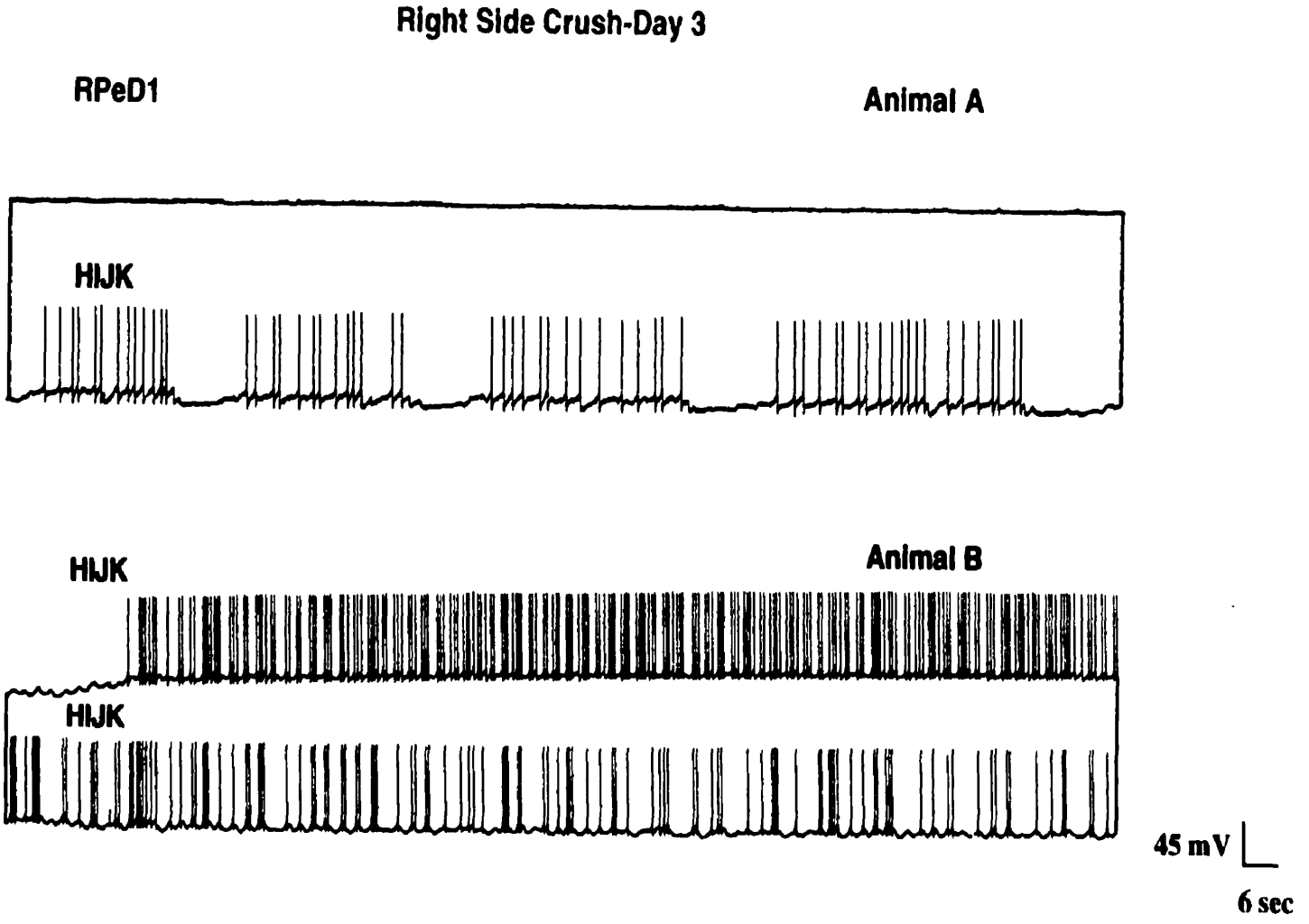
Right Side Crush-Day 3
RPeD1
Animal A
HIJK
HIJK
Animal B
HIJK
45 mV
6 sec

Figure 5.4. A right pleural-parietal connective crush altered the pattern of IP3I activity. Number of IP3I bursts that occurred in right side crush, left side crush, and sham operated animals are compared on 3 and 7 days after surgery. The number of bursts were analysed from two simultaneous intracellular recordings made from RPeD1, H,I,J,K, or RPA neurons over a 20 minute period. The number of IP3I bursts that occurred in right side crush animals were not significantly different (*) from left side crush and sham animals on day 7 (but were significantly different on day 3; $p < 0.01$, t-test). Left side crush and sham operated animals did not display any significant differences on either day. Furthermore, the number of IP3I bursts that occurred in regenerated animals were significantly different than day 3 right side crush animals only ($p < 0.01$, t-test). (experimental, n = 16; control, n = 14; sham, n = 6)

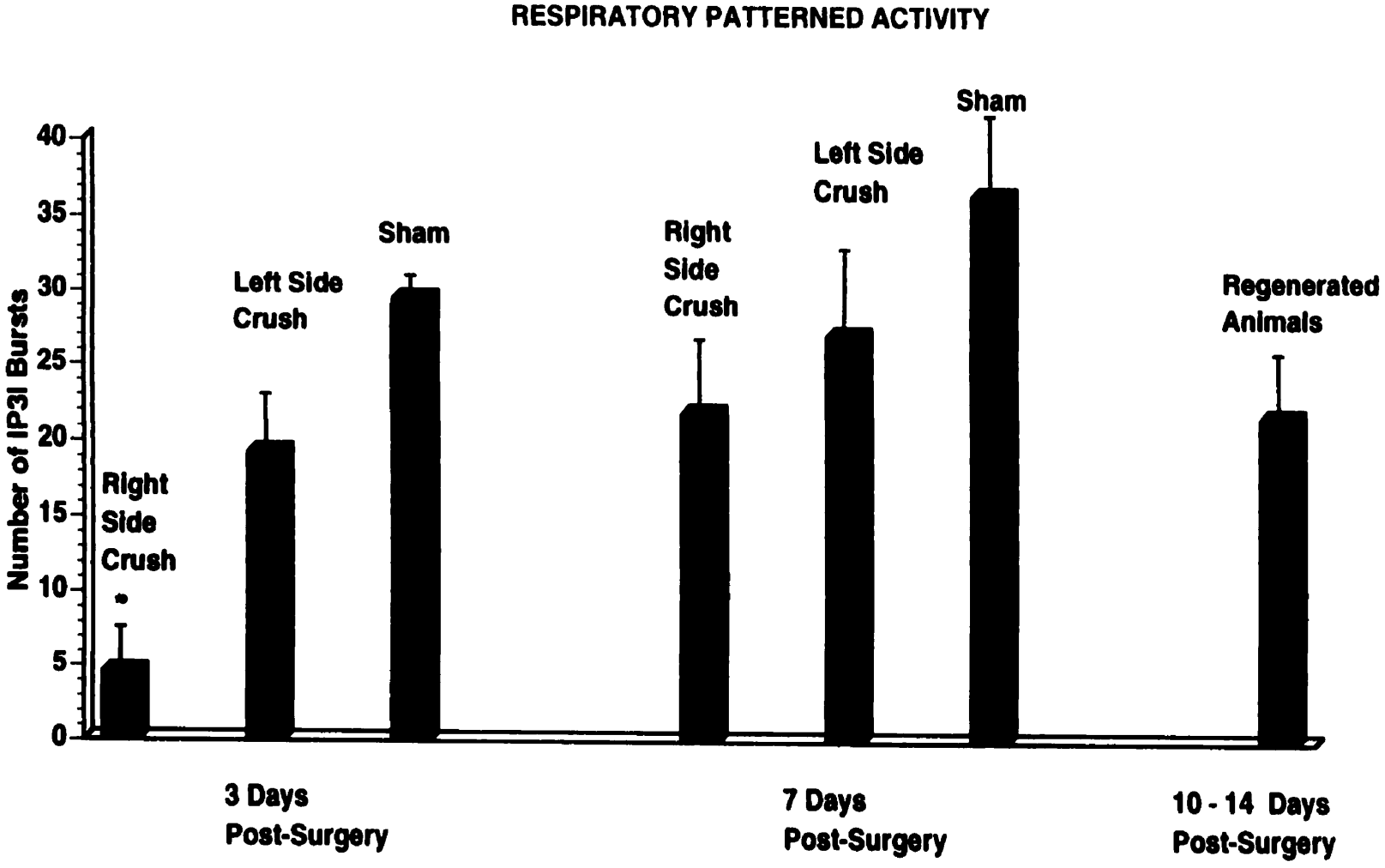
RESPIRATORY PATTERNED ACTIVITY
Number of IP3I Bursts
40
35
30
25
20
15
10
5
0
Right Side Crush
Left Side Crush
Sham
Right Side Crush
Left Side Crush
Sham
Regenerated Animals
3 Days Post-Surgery
7 Days Post-Surgery
10 - 14 Days Post-Surgery

Figure 5.5. IP3I activity in experimental animals resumed after 7 days of post surgery. Raw data trace of intracellular recordings made from RPeD1 and H,I,J,K cells in the control animal (top trace), or from H,I,J,K, and RPA group neurons in experimental animals (middle and bottom traces). IP3I activity was exhibited by both animal groups by day 7.

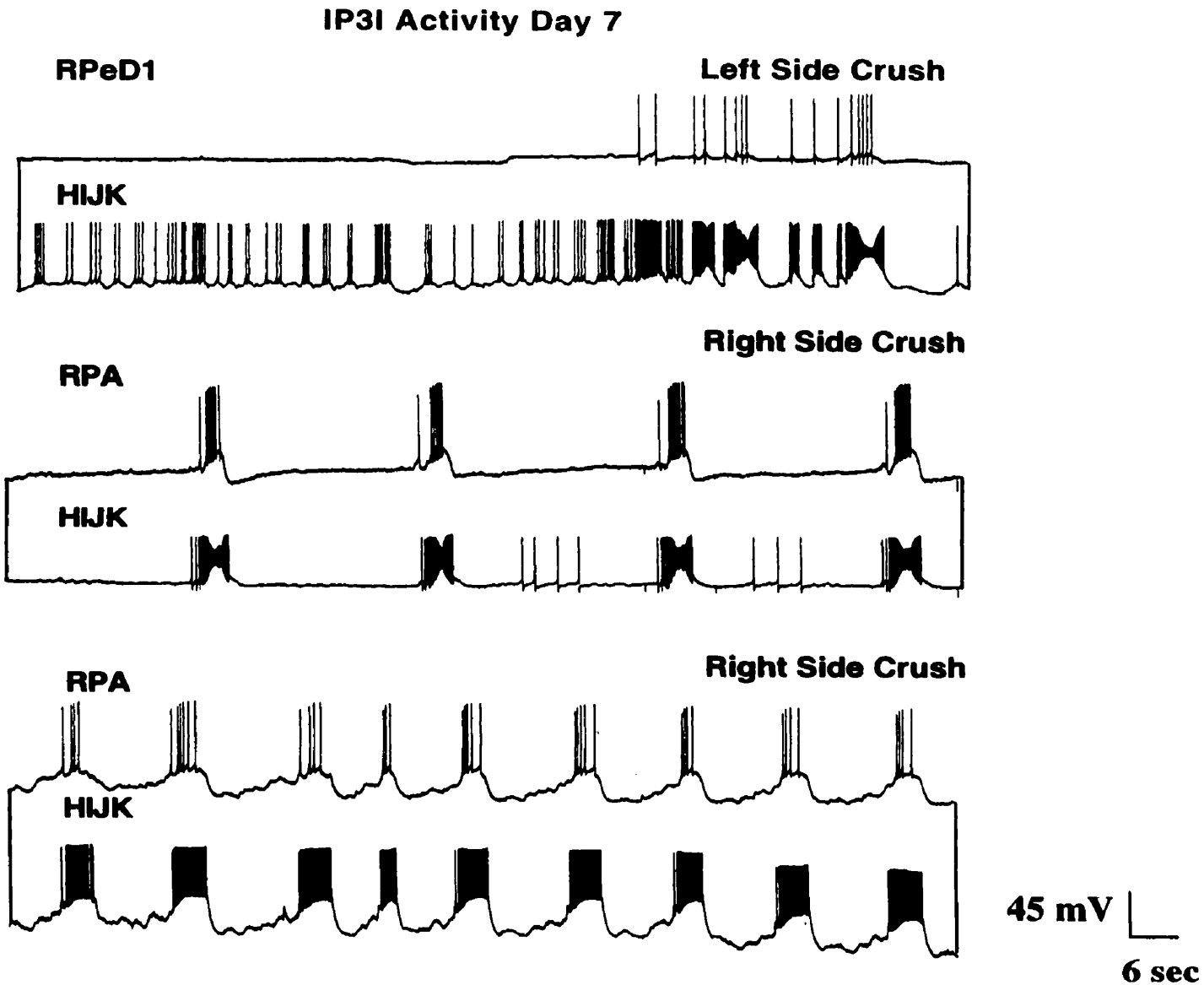
IP3I Activity Day 7
RPeD1
Left Side Crush
HIJK
Right Side Crush
RPA
HIJK
Right Side Crush
RPA
HIJK
45 mV
6 sec

Additional parameters were also examined to gain further insight into the inconsistency between the lack of behavioral recovery and the return of IP3I activity in RPeD1 axotomized animals on day seven. Specifically, the percent time that IP3I was active (30.2 ± 4.5 seconds, experimental; 21.3 ±2.0 seconds, control); duration of IP3I activity (6.9 ± 0.9 seconds, experimental; 11.6 ± 2.9 seconds, control); and the inter-burst intervals between the IP3I discharges (25.3 ± 3.2 seconds, experimental; 21.5 ± 3.0 seconds, control) were analyzed. However, no statistically significant differences were observed, confirming that the respiratory patterned activity exhibited by experimental animals (n = 10) was similar to that of control animals (n = 10) on day seven (Figure 5.6).

The return of IP3 activity on day seven suggested that RPeD1 may have regenerated its axonal and synaptic connections with follower cells located within the CNS. However, the lack of behavioral recovery may indicate that RPeD1 was unable to reestablish connections with the peripheral elements that are known to play an important role in sensory feedback. To demonstrate more clearly the electrical differences exhibited by RPeD1 axotomized animals on day three and day seven, respiratory patterned activity was further analyzed. Percent IP3I activity absent in the experimental animals (87%; n = 16) was significantly higher than control animals (20%; n = 15) on day three ($p < 0.0001$) (Figure 5.7). However, by day seven the differences between experimental (28%) and control (20%) groups were no longer significantly different ($P = 1.000$).

Figure 5.6. Electrophysiological parameters of the IP3I burst activity in right side crush animals were similar to those of the control animals on day 7. To determine both qualitative and quantitative differences in the activity patterns of IP3I discharges, % time during which IP3I was active, duration of IP3I discharges, and the interburst intervals were characterised from both left and right side crush animals. No significant differences in any of the above parameters were observed in either experimental or control groups (t-test). (n = 10)

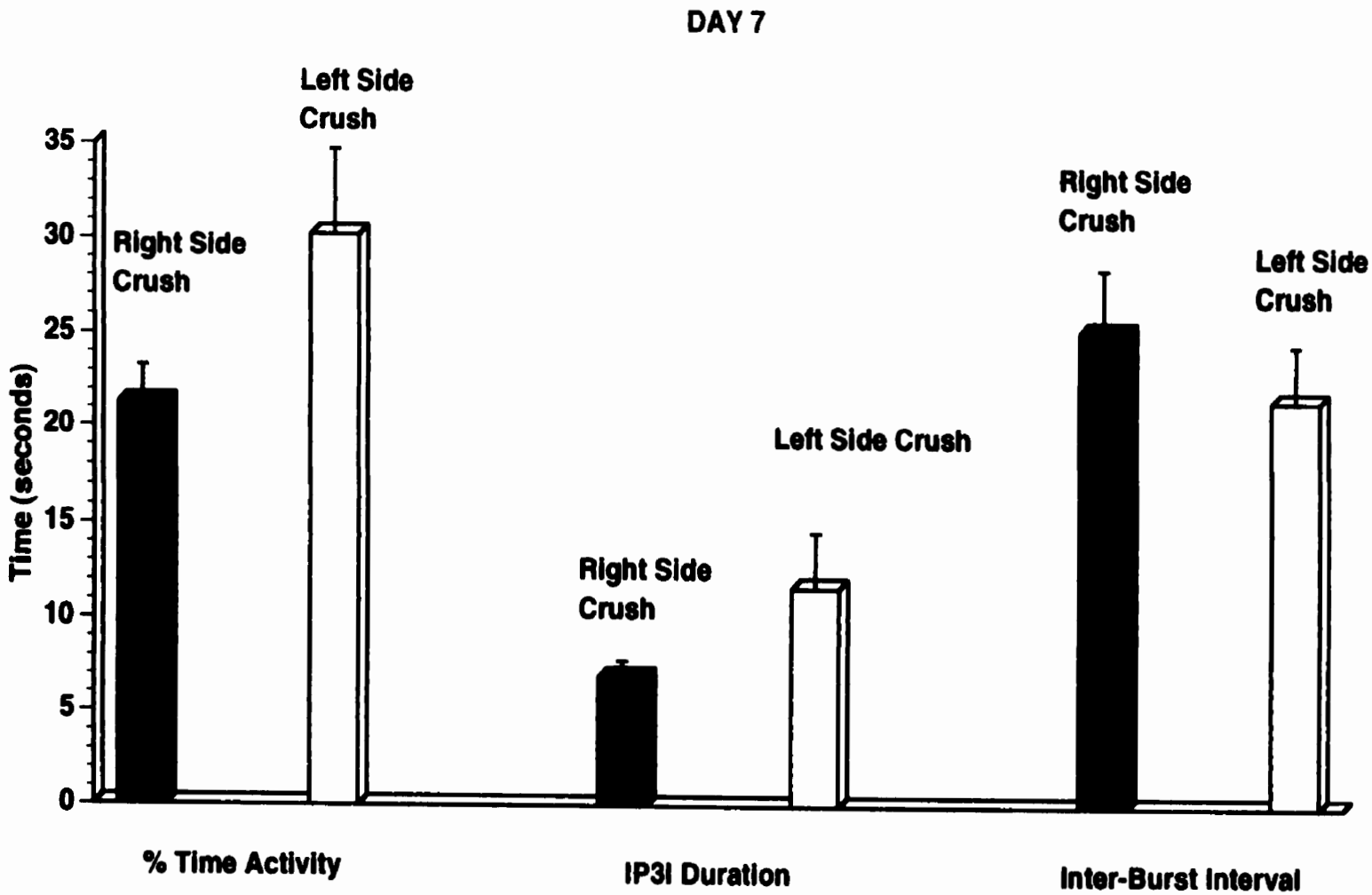
DAY 7
Left Side Crush
Right Side Crush
Right Side Crush
Left Side Crush
Right Side Crush
Left Side Crush
Time (seconds)
35
30
25
20
15
10
5
0
% Time Activity
IP3I Duration
Inter-Burst Interval

Figure 5.7. IP3I activity in right side crush animals was compared to left side crush animals. The percentage of IP3I activity absent in right side crush animals was significantly higher than left side crush animals on day 3 (Fisher's exact test, $p < 0.0001$), but not significantly different on day 7 ($p = 1.000$). (experimental, $n = 16$; control, $n = 15$)

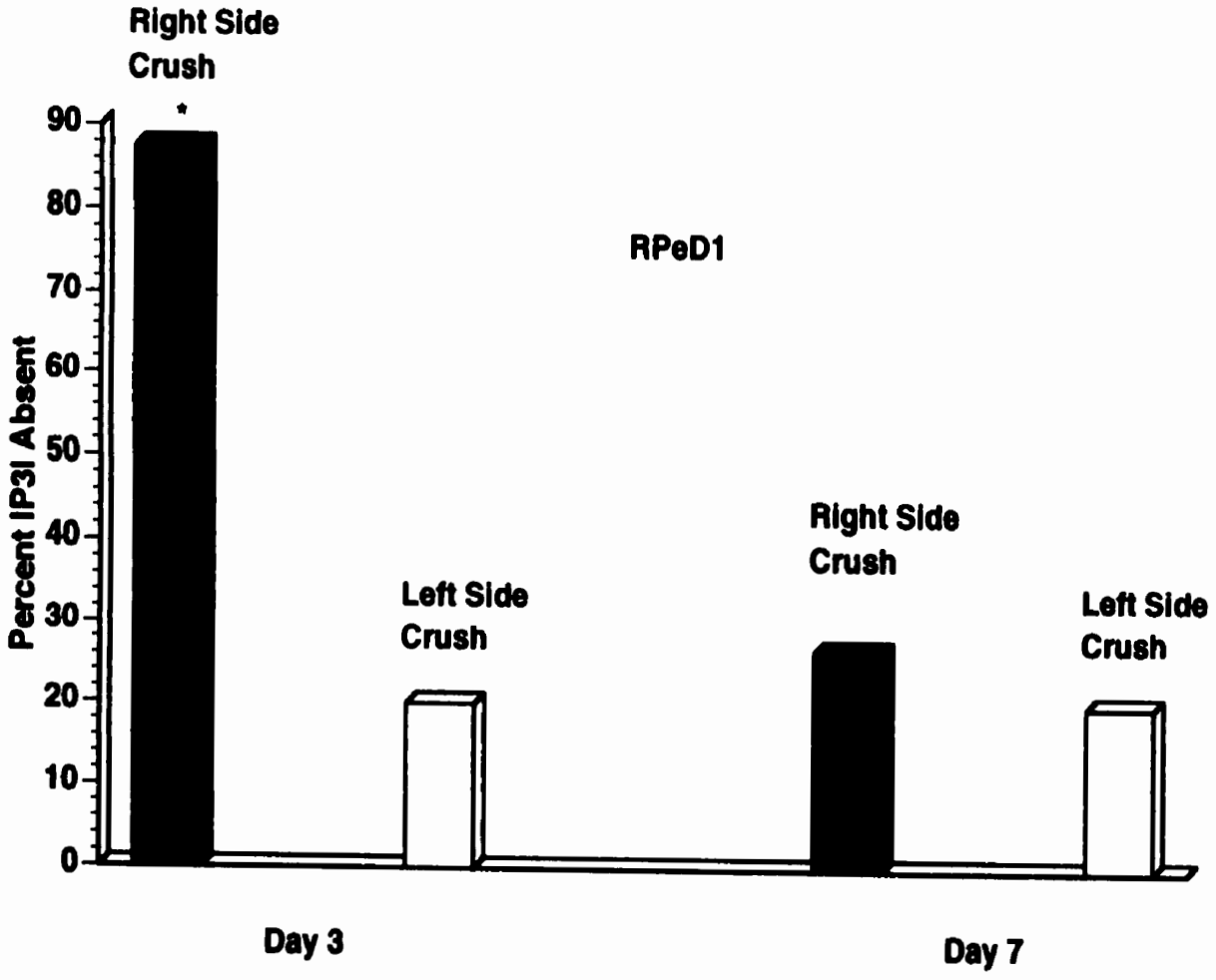
Right Side
Crush
*
90
80
70
60
50
40
30
20
10
0
Percent IP3I Absent
RPeD1
Left Side
Crush
Right Side
Crush
Left Side
Crush
Day 3
Day 7

Additionally, a significantly greater number of RPeD1 cells in the experimental animals (78%; n = 13) did not exhibit spiking activity compared to control animals (8%; n = 12) on day three ($p < 0.001$) (Figure 5.8A). On day seven however, the number of RPeD1 neurons that were silent in experimental animals (20%; n = 10) decreased to a level that was not significantly different from control animals (22%; n = 10) ($p = 1.000$) (Figure 5.8B). Overall, RPeD1 axotomized animals did not exhibit behavioral recovery until 10-14 days following surgery. Consistent with the behavioral analysis, I found that the IP3I activity was absent in experimental animals on day three. On day seven however, IP3I activity was restored in the experimental animals, and these data are therefore inconsistent with the behavioral analysis. Furthermore, the number of IP3I discharges displayed by RPeD1 and the number of dopamine cells that were spiking on day seven, were greater than that on day three. Therefore, the observed incidence of respiratory patterned activity was inconsistent with the lack of behavioral recovery on day seven. These data strongly suggest that RPeD1 regenerated processes may have innervated central but not the peripheral elements on day seven. By day ten however, the normal respiratory behavior returned, suggesting that RPeD1 was now also able to interact with the peripheral components.

5.2.4. RPeD1 regenerated its axonal projections three days after axotomy

Figure 5.8A. The percentage of RPeD1 cells that did not exhibit spiking in right side crush animals was significantly higher than in left side crush animals ($p < 0.001$, Fisher's exact test) 3 days after surgery. (experimental, $n = 13$; control, $n = 12$)

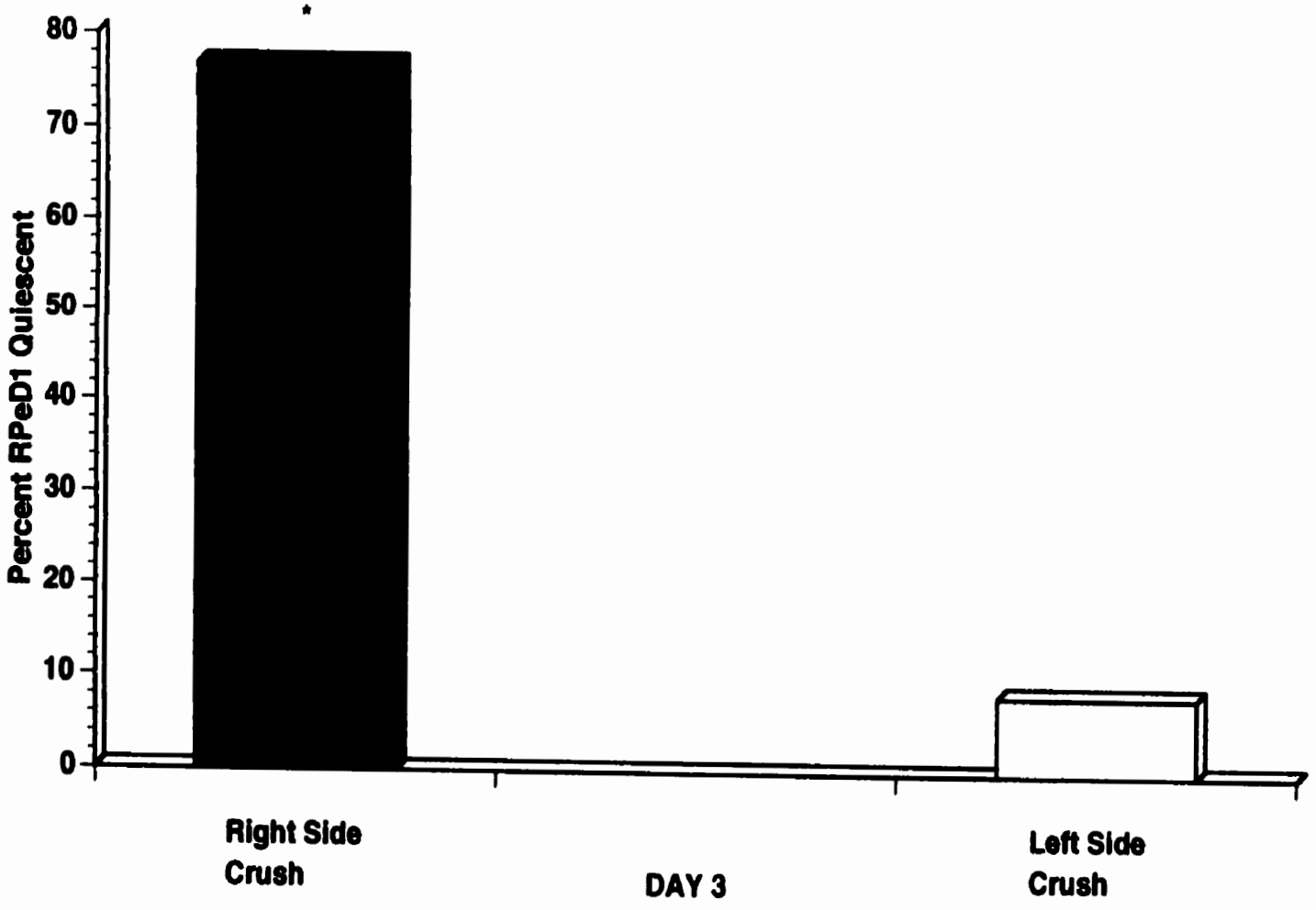
*
80
70
60
50
40
30
20
10
0
Percent RPeD1 Quiescent
Right Side Crush
DAY 3
Left Side Crush

Figure 5.8B. The percentage of RPeD1 cells that were quiescent in right side crush animals was not significantly different than left side crush animals on day 7 ($p = 1.000$, Fisher's exact test). (experimental, $n = 10$; control, $n = 10$)

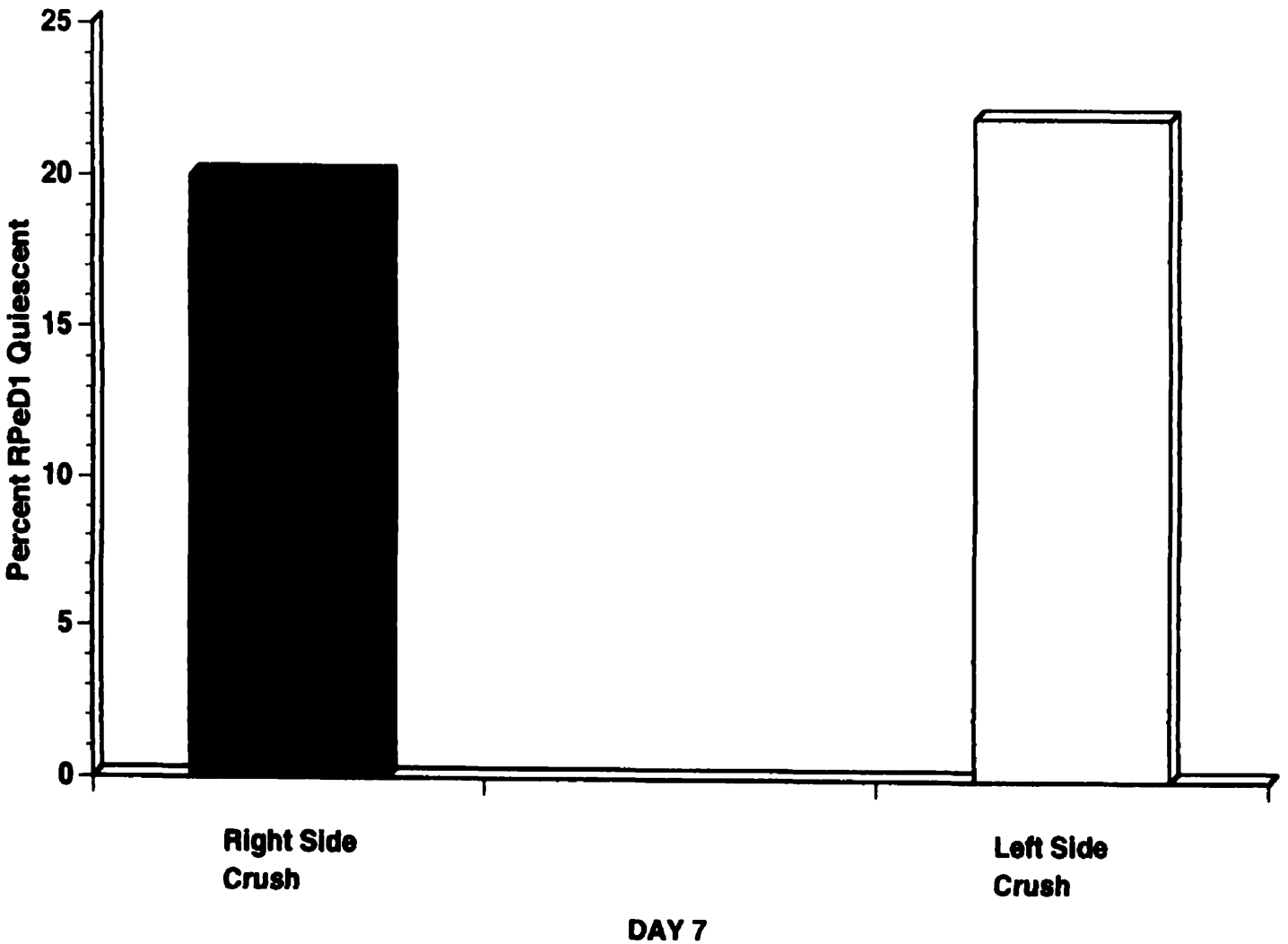
25
20
15
10
5
0
Percent RPeD1 Quiescent
Right Side
Crush
Left Side
Crush
DAY 7

In the next series of experiments, I sought to determine whether the behavior restoration in the experimental animals involved RPeD1 regeneration. Specifically, the central ring ganglia were isolated from animals, which on day three, did not exhibit normal respiratory rhythmogenesis and Lucifer yellow was injected into the RPeD1 somata. These preparations were subsequently processed for fluorescent microscopy. I discovered that in most experimental animals not exhibiting respiratory movements, RPeD1 did indeed regenerate extensive processes into the pleural ganglia (Figure 5.9). These data demonstrates that the restoration of respiratory movements in the experimental animals most likely involved RPeD1 regeneration.

Figure 5.9. Morphology of RPeD1 three days after a right pleural-parietal connective crush. A, B) Following connective crushes (see arrows), RPeD1 was filled with Lucifer yellow. Injection of the dye was used to trace the location of the axon on day three after surgery. Regeneration was displayed on day three. B) Different focal plane of the same cell. Scale bar 100 μm.

Morphology of RPeD1 Three Days After Axotomy

A

B

5.3. DISCUSSION

In this section, I have demonstrated that RPeD1 axotomy disrupts the normal respiratory behavior in intact animals and that the isolated ganglia from these snails do not exhibit IP3I activity on day three. This respiratory behavioral deficit was however, restored in right pleural-parietal crushed animals after 10-14 days of post surgery. It is important to note that although IP3I activity did resume on day seven, the behavioral recovery required up to an additional week. These data suggest that the connectivity pattern between the CPG neurons had to be restored prior to behavioral recovery. Consistent with this electrophysiological analysis is the morphological data, showing that on day 3 the regenerated projections from RPeD1 are indeed discernable in the pleural ganglia. An additional insight gained from these studies is that, during the course of regeneration, both RPeD1 and IP3I were quiescent suggesting that either the incoming excitatory synaptic inputs were absent or that the regenerating neurons maintain lower levels of electrical activity.

This study demonstrates that an axotomized neuron not only regenerates its axonal and synaptic connections in the intact animal but that it also restores the behavioral deficit. In a related study, Benjamin and Allison (1985) and Allison and Benjamin (1985), have shown that when the connectives between the pleural and parietal ganglia are axotomized in the intact animal, RPeD1 regenerates extensive neurites within 3-4 days. Many neurites were shown to extend posteriorly into the

parietal and visceral ganglia where RPeD1 projects, while some neurites extended anteriorly into areas that are not innervated by RPeD1 (Allison and Benjamin, 1985). Growth occurred at a rate of approximately 360-400 $\mu m\ d^{-1}$ (consistent with my data), which allowed the proximal axon segment to reach posterior areas (where connections with follower cells were previously disconnected) as early as 3 to 4 days post axotomy (Allison and Benjamin, 1985).

These works demonstrated that in most instances in which the RPeD1 axon was crushed away from the cell body, the regenerated fibres projected appropriately towards the parietal and pleural ganglion. However, if the axotomy was performed closer to the cell body, RPeD1 exhibited extensive growth, which was directed in the posterior direction. The regenerating axons were shown to reform normal excitatory, inhibitory, and biphasic synaptic connections (Benjamin and Allison, 1985) around the same time (3-4 days after the crush was performed). These postsynaptic responses were initially weaker, but strengthened over time. Some unitary responses (eg. summation properties similar to those seen in normal preparations) were initially observed by day 8, but consistently seen in all preparations on day 33 post surgery. Furthermore, the single action potentials normally observed in RPeD1 were not observed during the first few days after surgery. Instead, spontaneously occurring doublet spikes or bursting activity was recorded consistently after 4-12 days of surgery (note: 0 out of 7 animals exhibited doublet activity the first two days after surgery, and only 3 out of 7

displayed doublet activity on day 3). Normal single spikes returned by day 17.

The data presented in the study are consistent with that of Benjamin and Allison, 1985 and Allison and Benjamin, 1985. Specifically, morphological analysis presented by Allison and Benjamin (1985) revealed growth from RPeD1 into the parietal and visceral ganglia on day 3-4 after surgery, while electrophysiological results showed an altered pattern of firing activity in the RPeD1 cell on day 4 (Benjamin and Allison, 1985; Allison and Benjamin, 1985). Similarly, in this study, Lucifer yellow dye injection into RPeD1 revealed regenerated fibers in the pleural ganglia on day 3 and electrophysiological analysis revealed an altered firing pattern in RPeD1 on day three. However, while 3 out of 7 preparations exhibited doublet activity on day 3 (Benjamin and Allison, 1985), in most of my preparations, RPeD1 was quiescent on day 3. The incidence for the appearance of IP3I activity, concomitant with the presence of regenerated fibers into pleural and parietal ganglion, was however consistent between the two studies. According to Benjamin and Allison (1985), IP3I activity was weaker initially and strengthened significantly by day eight; whereas in my preparations, I did not observe IP3I activity on day 3, but did on day seven after surgery. The reasons for these apparent discrepancies between the two studies are unclear. However, since Benjamin and Allison (1985) did not correlate RPeD1 axotomy with behavior, the effectiveness of their crushes can not be fully deduced, rendering the data comparison difficult.

Since the normal respiratory behavior in RPeD1 axotomized animals resumed after 10-14 days of post surgery, I hypothesized that this behavioral restoration may have involved RPeD1 regeneration. As described above, fine axonal projections from RPeD1 axotomized animals on day three were indeed confined to the central ring ganglia, suggesting that the restoration of its central connections may have been sufficient for the behavioral recovery.

Regarding restoration of behavioral deficit, Syed et al., (1992) had shown earlier that a deficit in normal respiratory behavior resulting from visceral dorsal 4 (VD4) ablation, could be restored by the transplantation of a donor VD4 from the host animal. The transplanted cell not only re-grew its axonal projections but also the normal patterns of synaptic connections were restored. Taken together, with the data presented here, these studies on identified *Lymnaea* neurons demonstrate that both transplanted and regenerated neurons are not only capable of regeneration but that they can also repair behavioral deficit that results from their loss.

Data presented in Figure 5.3 show that the right side crush animals do not exhibit IP3I discharges on day 3 of post-surgery. Following injury, a large number of axotomized neurons have been shown to exhibit hyper-excitability in response to injury (Moffet, 1996) . It is therefore, tempting to attribute the absence of IP3I activity to the injury-induced hyperexcitability in RPeD1. Unfortunately, this argument does not fit well with the data presented in Figure 5.8A, in which RPeD1

was found to be quiescent in most axotomized preparations. These data do not however, rule out the possibility that the severed axon stump may have still exhibited hyper-excitability. This possibility remains to be investigated.

On day 7, normal respiratory behavior resumed in RPeD1 axotomized animals concomitant with the appearance of regenerating processes in the pleural and parietal ganglia on day 3. It is although tempting to attribute these patterns of IP3I activity to the re-establishment of synaptic connections between RPeD1 and its target cells, this possibility however, remains to be tested experimentally. Since on day seven, various parameters of IP3I (duration, inter-burst interval time, and % time activity) were identical in both experimental and control animals, these data do nevertheless, suggest that the normal patterns of respiratory motor activity resumed at this time point during regeneration.

Early during regeneration (day 3), the incidence of IP3I activity can not however, be attributed directly to RPeD1, but rather to its severed axon. An interesting possibility that could be examined in the future is whether following regeneration, IP3I and other target cells of RPeD1 remain doubly innervated, or if newly regenerated fibers out-compete the isolated axon.

In summary, the *Lymnaea* model system provides us with an unparalleled opportunity to determine the functional significance of any of the CPG neurons from a neuronal network to behavioral level. In this

preparation, the individually identified neurons can be selectively removed from the nervous system in an intact animal and their involvement in any given behavior can be determined directly. More importantly, these neurons can either be transplanted from a donor animal or allowed to regenerate in the host ganglion, and their functional significance can thus be tested following behavioral recovery.

BIBLIOGRAPHY

Allison P, Benjamin PR. 1985. Anatomical studies of central regeneration of an identified molluscan interneuron. Proc R Soc Lond Biol Sci. 226:135-157.

Alving BO. 1968. Spontaneous activity in isolated somata of *Aplysia* pacemaker neurones. J Gen Physiol. 51:29-45.

Aminoff MJ, Sears TA. 1971. Spinal cord integration of segemental , cortical, and breathing inputs to thoracic respiratory motoneurons. J Physiol. (London) 215:557-575.

Arshavsky YI, Deliagina, TG, Okshtein IL, Orlovsky GN, Panchin YV, Popova LB. 1994. Defense reaction in the pond snail *Planorbis corneus*. I. Activity of the shell-moving and respiratory systems. J. Neurophysiol. 71, 882-890.

Aritav H, Kitav I, Sakamoto M. 1995. Two distinct descending inputs to the crocothyroid motoneuron in the medulla originating from the amygdala and the lateral hypothalmic area. Adv Exp Med Biol. 393:53-58.

Atwood HL, Dixon D, Wojtowicz JM. 1989. Rapid induction of long-lasting synaptic changes at cruatacean neuromuscular junctions. J Neurobiol. 20:373-385.

Balban PM. 1983. Postsynaptic mechanism of withdrawal reflex sensitization in the snail. J Neurobiol. 14:365-375.

Benjamin PR. 1983. Gastropod feeding: Behavioral and neural analysis of a complex multicomponent system. In: Neural origin of rhythmic movements. (eds.) A Roberts and BL Roberts. Soc Exp Biol Symp. 37:159-193. Cambridge: Cambridge University Press.

Benjamin PR, Allison P. 1985. Regeneration of excitatory, inhibitory, and biphasic synaptic connections made by the snail giant interneuron. Proc R Soc Lond B Biol Sci. 226:159-176.

Berger AJ, Bellinghan MC. 1995. Mechanisms of respiratory motor output. In: Lung Biol Health Dis. 79:79-149.

Benjamin PR, Rose RM. 1985. Intraneuronal circuitry underlying cyclical feeding in gastropod molluscs. In: The motor system in neurobiology.

(eds.) VE Edward, PW Steven, and D Bousfield. pp 67-72. Amsterdam: Elsevier Biomedical Press.

Benjamin PR, Winlow W. 1981. The distribution of three wide-acting synaptic inputs to identified neurones in the isolated brain of *Lymnaea stagnalis* (L.). Comp Biochem Physiol. 70A:293-307.

Bianchi AL, Denavit-Saubie, Champagnat J. 1995. Central control of breathing in mammals: An overview. Lung Biol. Health Dis. 79:39-69.

Bregman BS. 1998. Regeneration in the spinal cord. Curr Opin Neurobiol. 8:800-807.

Bregman BS, McAtee M, Dai HN, Kuhn PL. 1997. Neurotrophic factors increase axonal growth after spinal cord injury and transplantation in the adult rat. 148:475-494.

Brown TG. 1911. The intrinsic factors in the acts of progression in mammal. Proc R Soc B. 84:308-319.

Burleson ML, Smatresk NJ. 1989. The effect of decerebration and anaesthesia on the reflex responses to hypoxia in catfish. Can J Zool. 67:630-635.

Calabrese RL. 1977. The neural control of alternate heart beat coordination states in the leech, *Hirudo medicinalis*. J comp Physiol. 122:111-143.

Cooper JR, Bloom FE, Roth RH (eds.). 1978. The biochemical basis of neuropharmacology. 3rd. edition. Oxford University Press. New York.

Dean J, Cruse H. 1995. Motor pattern generator. In: The handbook of Brain theory and neural networks. Edited by Arbib MA. Cambridge, Massachusetts: MIT Press. pp. 600-605

Delcomyn F. 1980. Neural basis of rhythmic behavior in animals. Science. 210:492-498.

Dobbins EG, Feldman JL. 1994. Brainstem network controlling descending drive to phrenic and medial gastrocnemius motoneurons in the cat spinal cord. Exp Neurol. 86:559-575.

DuffinJ, Ezure K, Lipski J. 1995. Breathing rhythm generation: Focus on the rostral ventrolateral medulla. New Physiol Sci. 10:133-140.

Eldridge FL, Millhorn DE, Waldrop TG. 1981. Exercise hypernea and locomotion: Parallel activation from the hypothalmus. Science. 211:844-846.

Erlichman JS, Leiter JC. 1993. Response of the pneumostome to CO_2 and sites of CO_2 chemoreception in the pulmonate snail, *Helix aspersa*. Resp Physiol. 93:347-363.

Erlichman JS, Leiter JC. 1994. Central chemoreceptor stimulus in the terrestrial, pulmonate snail, *Helix aspersa*. Resp Physiol. 95:209-226.

Erlichman JS, Coates EL, Leiter JC. 1994. Carbonic anhydraze and CO_2 and chemoreception in the pulmonate snail, *Helix aspersa*. Resp Physiol. 98:27-41.

Euler von C. 1985. Central pattern generation during breathing. In: the motor system in neurobiology. (eds.) VE Edward, PW Steven, and B David. Amsterdam: Elsevier Biomedical Press.

Euler von C. 1986. Brainstem mechanisms for the generation and control of breathing. In: The handbook of physiology. The respiratory system (II). Control of breathing (part I). Am Physiol Soc. Bethesda, MD. USA. pp.1-67.

Ezyr K. 1990. Synaptic connections between medullary respiratory neurons and considerations on the genesis of respiratory rhythm. Prog. Neurobiol. 35:429-450.

Fedorko L, Connelly CA, Remmers JE. 1987. Neurotransmitters mediating synaptic inhibition of phrenic motoneurons. In: respiratory Muscles and their neuromotor control (GC Sieck, SC Gandevia, WE Cameron eds.,).pp.167-173. Liss, New York.

Feldman JL. 1986. Neurophysiology of breathing in mammals. In: Handbook of Physiol (FE Bloom, ed.), Sect. 1, Vol. IV, pp. 463-524.

Felman JL, McCrimmon DR. 1999. Neural control of breathing: In Fundamental neuroscience. (ML Zigmond, FE Bloom, SC Landis, JL Roberts, LR Squire, eds.), pp. 1063-1090. San Diego, California

Feldman JL, Smith JC. 1989. Cellular mechanisms underlying modulation of breathing pattern in mammals. In: Modulation of defined vertebrate neural circuits. Ann NY Acad Sci. 563:114-130.

Fitch MT, Silver J. 1997. Glial cell extracellular matrix: boundaries for axon growth in development and regeneration. Cell Tissue Res. 290::371-377.

Funk GD, Feldman JL. 1995. Generation of respiratory rhythm and pattern in mammals: insights from developmental studies. Curr Opin in Neurobiol. 5:778-785.

Furshpan EJ, Potter DD. 1957. Mechanism of nerve-impulse transmission at a crayfish synapse. Nature (London). 180:342-343.

Getting PA.1983. Neural control of swimming in *Tritonia*. Symp Soc Exp Biol. 37:89-128.

Getting PA. 1986. Understanding central pattern generators. Insights gained from the study of invertebrate locomotion. (eds.) S Grillner, PSG Stein, DG Stuart, H Forsberg, and R Herman. Pp. 231-244. London: The MacMillan Press Ltd.

Getting PA. 1988. Comparative analysis of invertebrate central pattern generators. In: Neural control of rhythmic movements. (eds.) AH Cohan, S Rossignol, and S Grillner. New York: Wiley.

Getting PA, Dekin MS. 1985. *Tritonia* swimming: a model sysyem for integration within rhythmic motor systems, In: Model neural networks and behavior, AI Selverston, ed. Plenum Press, New York, pp. 3-20.

Gonzalez_Lima F, Frystak RJ. 1991. Functional mapping of the rat brain during vocalizations: A 2-deoxyglucose study. Neurosci. Lett. 124:74-78.

Goshgarian HG, Rafols JA. 1984. Brainstem network controlling descending drive to phrenic motoneurons in rat. J Comp Neurol. 347:64-86.

Grillner S, Wallen P. 1977. Is there a peripheral control of the central pattern generators for swimming in dogfish?. Brain Res. 127:291.

Grillner S, Wallen P. 1982. On peripheral control mechanism acting on the central pattern generators for swimming in the dogfish. J Exp Biol. 98:1-22.

Grillner S, Wallen P, Brodin A, Lanser A., 1991. Neuronal network generating locomotor behavior in lamprey: circuitry, transmitters, membrane properties, and stimulation. Ann Rev Neurosci. 14:169.

Grossfeld RM, McKinnon E, Hargittai PT, Lieberman EM. 1994. Glutamine cycle enzymes in the crayfish medial giant nerve fiber: implications for axon-to-glia signaling. Soc Neurosci Abs 20:914.

Harada Y, Kuno M, wang YZ. 1985. Differential effects of carbon dioxide and pH on central chemoreceptors in the rat *in vitro*. J physiol. (London) 3368:679-693.

Harris-Warrick RM. 1988. Chemical modulation of central pattern generators. In: Neural control of rhythmic movements in vertebrates, edited by AH Cohen, S Rossignol, and S Grillner. New York: Wiley. pp. 285-331.

Harris-Warrick RM, Marder E. 1991. Modulation of neural networks for behavior. Annu Rev Neurosci. 14:39-57.

Holstege G. 1989. Anatomical study of the final common pathway for vocalization in the cat. J Comp Neurol. 284:242-252.

Hoy RR, Bittner GD, Kennedy D. 1967. Regeneration in crustacean neurons: evidence for axonal fusion. Science. 15:251-252.

Inoue T, Takasaki M, Lukowiak K, Syed NI. 1996a. Inhibition of the respiratory pattern-generating neurons by an identified whole-body withdrawal interneuron of *Lymnaea stagnalis*. J Exp Biol. 199:1887-1898.

Inoue T, Haque Z, Takasaki M, Lukowiak K, Syed NI. 1996b. Hypoxia induced respiratory patterned activity in *Lymnaea* originates at the periphery: role of the dopamine cell. Soc Neurosci Abstr. 22:1142.

Inoue T, Takasaki M, Lukowiak K, Syed NI. 1996c. Identification of a putative mechanosensory neuron in *Lymnaea*: characterization of its synaptic and functional connections with the whole-body withdrawal interneuron. J Neurophysiol. 76:3230-3238.

Jones HD. 1961. Aspects of respiration in *Planorbis corneus* (L). (Gastropoda: Pulmonata). Comp Biochem Physiol. 4:1-29.

Kristan WB Jr. 1980. Generation of rhythmic motor patterns. In: Information processing in the nervous system. (eds.) HM Pinsker, WD Willis Jr., pp. 241-261. New York. Raven Press.

Kupfermann I, Weiss KR. 1978. The command neuron concept. The behavioral and brain sciences. 1:3-39.

Lissmann HW. J. Exp. Biol. 1946. 23:162.

Lukowiak K., Cotter R., Westly J., Ringeis E., Spencer G., Syed N. I. (1998). Long term memory of an operantly conditioned respiratory behavior in *Lymnaea stagnalis*. J Exp Biol 201:877-882.

Lukowiak K, Ringseis E, Spencer G, Wildering W, Syed NI. 1996. Operant conditioning of aerial respiratory behavior in *Lymnaea stagnalis*. J Exp Biol 199:683-691.

Marder E, Calabrese RL. 1996. Principles of rhythmic motor pattern generation. Physiol Rev. 76(3):687-717.

McLean H. 1992. Endogenous respiratory rhythm in isolated brainstem preparations. Phd thesis, University of Calgary.

Meech RW. 1979. Membrane potential oscillators in molluscan "burster" neurons. J Exp. Biol. 81:93-112.

Meryrand P, Simmers J, Moulins M. 1991. Dynamic construction of a neural pattern generating circuit with neurons of different networks. Nature Lond. 351:60-63.

Milsom WK. 1990a. Control and co-ordination of gas exchanged in air breathers. In: Comparative and environmental physiology. (vol 6): Vertebrate Gas Exchange. (ed.) R.G. Boutilier. Springer-Verlag, New York, USA. Pp. 347-401.

Milsom WK. 1990b. Mechanoreceptor modulation of endogenous respiratory rhythms in vertebrates. Am J Physiol. R898-R910.

Milsom WK, Brill R. 1986. Oxygen sensitive afferent information arising from the first gill arch of yellowfin tuna. Resp Physiol. 66:193-203.

Mitchell GS. 1993. Modulation and plasticioty of the exercise ventilatory response. Funkis Biol Syst. 23:269-277.

Moffet S. 1995. Neural regeneration in gastropod molluscs. Progress in Neurobiology. 46:289-330.

Moffet S. 1996. Zoophysiology: Nervous system regeneration in the invertebrates. (eds.) SD Bradshaw, W Burggren, HC Heller, S Ishii, H Langer, G Neuweiler, and DJ Randall. Springer-Verlag, New York. Volume 34.

Monteau R, Hilaire G. 1991. Spinal respiratory motoneurons. Prog. Neurobiol. 37:83-144.

Nusbaum MP, Friesen WO, Kristan WB Jr., Pearce RA. Neural mechanisms generating the leech swimming rhythm: swim-initiator neurons excite the network of swim oscillator neurons. 1987. J Comp Physiol. A Sens. Neural Behav. Physiol. 161:355-366.

Nusbaum MP, Weinmann JM, Golowasch J, Marder E. 1992. Presynaptic control of modulatory fibres by their neural network targets. J Neurosci. 12:2706-2714.

Onimaru H. 1995. Studies of the respiratory center using isolated brainstem-spinal cord preparations. Neurosci res. 21:183-190.

Pearson KG, Duysens J. 1976. Function of segmental reflexes in the control of stepping in cockroaches and cats. In: Neural control of locomotion. (eds.) RM Herman, S Grillner, PSG Stein, and DG Stuart. pp. 519-537. New York: Plenum Press.

Pearson KG, Reye DN, Robertson RM. 1983. Phase-dependent influences of wing stretch receptors on flight rhythm in the locust. J Neurophys. 49:1168-1181.

Ramirez J, Richter DW. 1996. The neuronal mechanisms of respiratory rhythm generation. Curr Opin in Neurobiol. 6:817-825.

Richter DW, Ballanyi K, Schwarzacher S. 1992. Mechanisms of respiratory rhythm generation. Curr Opin. Neurobiol. 2:788-793.

Ridgeway RL, Syed NI, Bulloch AG. 1993. *In vitro* evidence for multiple neuritogenic factors in the central nervous system of pulmonate molluscs. Acta Biol Hungarica. 44(1):109-13.

Ross TL, Govind CK, Kirk MD. 1994. Neuromuscular regeneration of buccal motoneuron B15 after peripheral nerve crush in *Aplysia californica*. J Neurophysiol. 72:1897-1910.

Sakhorov DA, S-Rozsa K. 1989. Defensive behavior in the pond snail, *Lymnaea stagnalis*. The whole body withdrawal associated with exsanguination. Acta Biol Hing. 40:329-341.

Schwarzacher SW, Smith JC, Richter DW. 1995. Pre-Botzinger complex in the cat. J Neurophysiol. 73:1452-1461.

Selverston AI. 1980. Are central pattern generators understandable? Behav Brain Sci. 3:535-571.

Selverston AI, Miller JP, Wadepuhl M. 1983. Cooperative mechanisms for the production of rhythmic movements. in: neural origin of rhythmic movements. (eds.) A Roberts and BL Cambridge: Cambridge University Press.

Shelton G, Jones DR, Milsom WK. 1986. Control of breathing in ectothermic vertebrates. In: The handbook of physiology. The respiratory system (II). Control of breathing (part II). Am Physiol Soc. Bethesda, MD. USA. pp.857-909.

Smith TG Jr. 1980. Ionic conductances in bursting pacemaker cells and their hormonal modulation. In: cold Spring harbor reports in the neuroscinces. 1. Molluscan nerve cells: From biophysics to behavior (eds.) J Koester and JH Byrne. Pp.135-143. USA: Cold spring harbour laboratory.

Smith JC, Ellenberger HH, Ballanyi K, Richter DW, Feldman JL. 1991. Pre-Botzinger complex: A brainstem region that may generate respiratory rhythm in mammals. Science. 254:726-729.

Smith JC, Funk GD, Johnson SM, Feldman JL. Cellular and synaptic mechanisms generating respiratory rhythm: insights from *in vitro* and computational studies. In: Ventral brainstem mechanisms and control of respiration and blood pressure. Edited by CO Trouth, R Millis, H Kiwull_Schone. New York: M Dekker: 463-496.

Spencer GE, Syed NI, Lukowiak K. 1999. Neural changes after operant conditioning of the aerial repiratory behavior in *Lymnaea* stagnalis. J Neurosci. 19(5):1836-1843.

Stenhouwer DJ, Farel PB. 1980. Central and peripheral controls of swimming in anuran larvae. Brain Res. 195:323-335.

Syed NI. 1988. The Neural control of locomotion in *Lymnaea*. PhD thesis. University of Leeds

Syed NI, Bulloch AGM, Lukowiak K, 1990. *In vitro* reconstruction of the respiratory central pattern generator (CPG) of the mollusc *Lymnaea*. Science. 250.:282-285.

Syed NI, Ridgway RL, Lukowiak K, Bulloch AGM. Transplantation and functional integration of an identified respiratory interneuron in *Lymnaea stagnalis*. Neuron. 8:767-774.

Syed NI, Winlow W. 1991a. Respiratory behavior in the pond snail *Lymnaea stagnalis*. J Comp Physiol. 169:557-568.

Syed NI, Winlow W. 1991b. respiratory behavior in the pond snail *Lymnaea stagnalis*. II. Neural elements of the central pattern generator (CPG). J Comp Physiol. A 169:557-568.

Tenney SM, Ou LC. 1977. Ventilatory response of decorticate and decerebrate cats to hypoxia and carbon dioxide. Respir Physiol. 29:81-92.

Tuszynski MH, Gabriel K, Gage FH, Suhr S, Meyer S, Rosetti A. 1996. Nerve growth factor delivery by gene transfer induces differential outgrowth of sensory, motor, and noradrenergic neurites after adult spinal cord injury. Exp Neurol. 137:157-173.

Van Minnen J, Bergman JJ, Van Kesteren ER, Smit AB, Geraerts WP, Lukowiak K, Hasan SU, Syed NI. 1997. De Novo protein synthesis in isolated axons of identified neurons. Neuroscience. 80(1):1-7.

Vehovszky A, Kemenes G, S-Rozsa K. 1989. Central and peripheral connections of an identified pedal neurone modifying pneumostome movements in Helix. Comp Biochem Physiol. A 94:735-741.

Viancour TA, Bittner GD, Seshan Ks, Sheller RA. 1988. Protein transport between crayfish lateral giant axons. Brain Res. 439:211-221.

Vitalis TZ, Milsom WK. 1986. Pulmonary mechanics and the work of breathing in the semi-aquatic turtle, *Pseudemys scripta*. J Exp Biol. 125:137-155.

Waldrop TG, Porter JP. 1995. Hypothalamic involvement in respiratory and cardiovascular regulation. Lung Biol Health Dis. 79:315-364.

Wendler G. 1978. The possible role of fast wing reflexes in locust flight. Naturwissenschaften 65:65.

White DP. 1990. Ventilation and the control of respiration during sleep: Normal mechanisms, pathologic nocturnal hypo-ventilation, and central sleep apnea. In: Cardiorespiratory disorders during sleep. (RJ Martin, ed.), pp. 53-108. Futura Publ. Co., Mount Kisco, NY.

Xu XM, Guenard V, Kleitman N, Bunge MB. 1995. Axonal regeneration into Schwann cell-seeded guidance channels grafted into transected adult rat spinal cord. J Comp Neurol. 351:145-160.

Xue Z, Grossfeld RM. 1993. Stess protein synthesis and accumulation after traumatic injury of crayfish CNS. Neurochem Res. 18:209-218.

Ye JH, Houle JD. 1997. Treatment of the chronically injured spinal cord with neurotrophic factors can promote axonal regeneration from supraspinal neurons. Exp Neurol. 143:70-81.